NGU REPORT 2020.025

Processing and interpretation of water column data from the Polarrev High, Barents Sea

GEOLOGY FOR SOCIETY

SINCE 1858

GEOLOGICAL SURVEY OF NORWAY

- NGU -

NORGES GEOLOGISKE UNDERSØKELSE
- NGU -

REPORT

Geological Survey of Norway
P.O.Box 6315 Torgarden
NO-7491 TRONDHEIM
Tel.: 47 73 90 40 00

Report no.: 2020.025

ISSN: 0800-3416 (print)
ISSN: 2387-3515 (online)

Grading: Open

Title:
Processing and interpretation of water column data from the Polarrev High, Barents Sea

Authors:
Shyam Chand, Terje Thorsnes

Client:
Norwegian Petroleum Directorate (NPD)

County:

Commune:
Trondheim

Map-sheet name (M=1:250.000)

Map-sheet no. and -name (M=1:50.000)

Deposit name and grid-reference:

Number of pages: 116 **Price (NOK):** 530
Map enclosures:

Fieldwork carried out:

Date of report:
26.06.2020

Project no.:
311758

Person responsible:
Reidulv Bøe

Summary:

This study was carried out using multibeam echo sounder data collected during Mareano surveys in 2013. The data from the surveys have been processed and interpreted to identify natural gas seeps, visible as gas flares, in the water column data. The data is also used for extracting bathymetry and backscatter.

The study area lies on the Bjarmeland platform area in the southern Barents Sea, mainly over the Polarrev High with a small part lying in the Kong Karl Platform and Bjarmeland Platform. The water depth is shallow and ranges from 150 to 225 m.

The following results were obtained:

- Processing and interpretation of water column data from 2275 km^2 area on the Polarrev High and nearby areas, Barents Sea (FOSAE-2013-D19, D21, D23 and D26) using Fledermaus Midwater and/or Qimera softwares.
- Flares are categorized according to the standard methods used in Mareano and other projects.
- Details of water column acoustic gas flares found including both certain and uncertain gas flares indicate a total of 98 flares.
- 38 flares were identified, with a confidence level higher than 50% thus representing 40% of total flares.

Keywords: Water Column	Gas Flare	Acoustic
Multibeam	Barents Sea	Polarrev High
Bjarmeland Platform		

INNHOLD

1. Introduction 4
2. Study area 4
3. Methods 6
   3.1 Multibeam 6
   3.2 Fledermaus Software 6
4. Results 7
   4.1 Bathymetry 7
   4.2 Backscatter 9
   4.3 Sediment Classification 11
   4.4 Water Column 12
      4.4.1 D19 17
      4.4.2 D21 42
      4.4.3 D23 66
      4.4.4 D26 109
5. Summary 115
6. References 116

1. INTRODUCTION

Marine methane vents and cold seeps are widespread on continental margins, including the Barents Sea (Skarke et al., 2014). Active seepage on the continental shelf is commonly associated with underlying oil and gas reservoirs, trapped gas under gas hydrates, and dissociation of gas hydrate (Milkov and Sassen, 2003). Detection of gas flares from marine methane vents and cold seeps can be efficiently detected using multibeam echosounders (Urban et al., 2017).

This study is carried out using multibeam echo sounder data collected during the Mareano surveys in 2013. The data from the surveys have been processed and interpreted in order to identify natural gas seeps, visible as gas flares, in the water column data. The data is also used for extracting bathymetry and backscatter.

2. STUDY AREA

The study area lies in the Bjarmeland platform area of the southern Barents Sea (Fig. 1). The study area is mainly located over the Polarrev High with a small part lying in Kong Karl Platform and Bjarmeland platform (Fig. 1). The water depth is shallow and ranges from 150 to 225m.

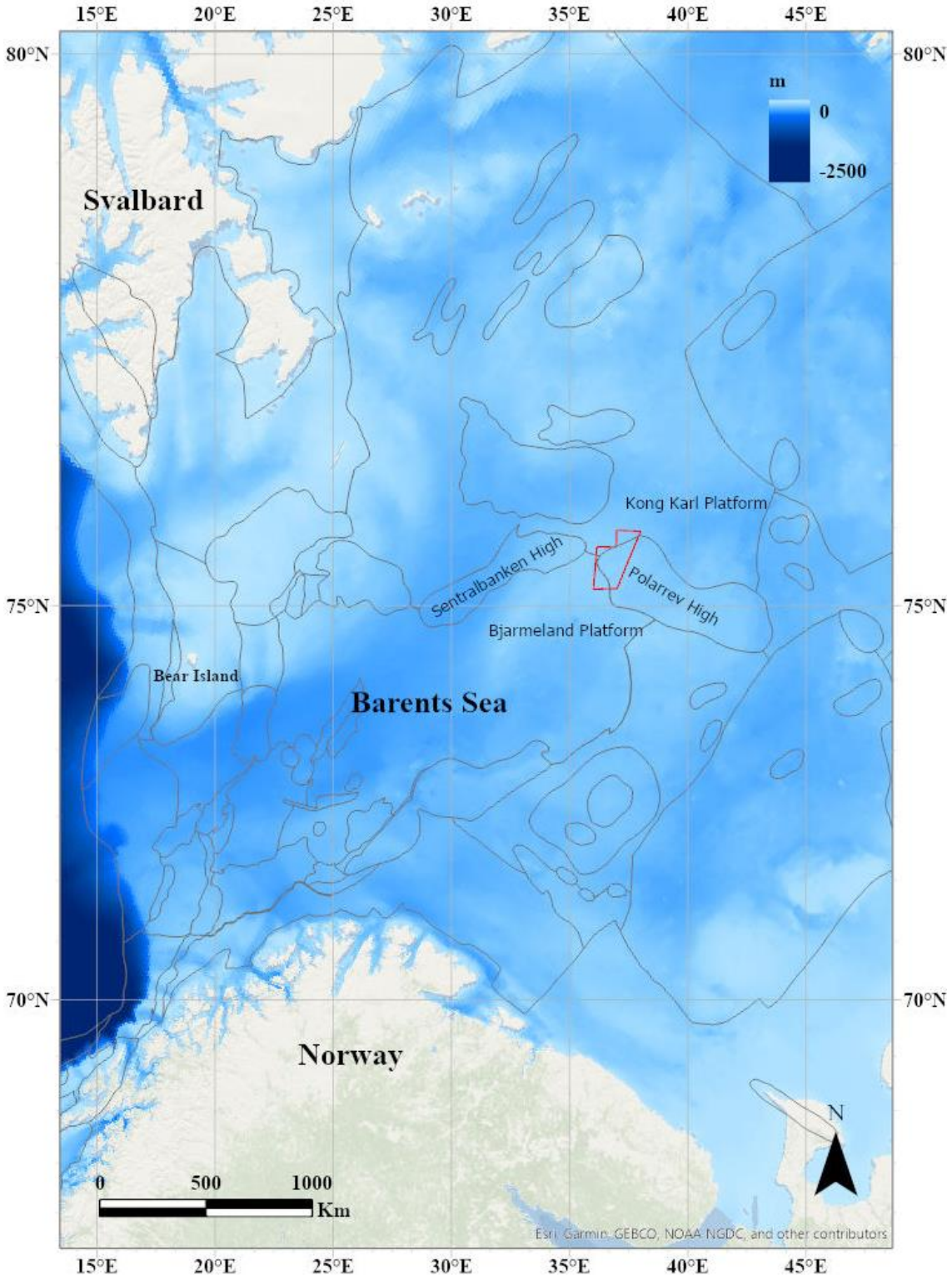

Figure 1. Regional bathymetry map of the Barents Sea showing the major structural boundaries (grey lines) and the study area (red polygon).

3. METHODS

3.1 Multibeam

Kongsberg EM710 multibeam system onboard ship Karoline was used by Fugro to acquire data from the study area. An important feature of the EM710 multibeam echosounder system is that it can record water column data also. The operating frequency used by EM710 (70-100 kHz) is also advantageous for the intermediate water depths, between 200 m and 1000 m, where other systems usually need a change in frequency. The operating frequency of 70-100 kHz and water depths of ca. 120 m give a Fresnel zone diameter (foot print) of around 4 m thus mapping 16 m2 by each beam. As a general rule, features smaller than the size of one fourth the wavelength cannot be resolved (Sheriff, 1980). Hence, features larger than 1 meter in diameter can be theoretically detected using the system. The water column data recorded by the system can be used for detection of active gas seeps and also detection of fauna. The presence of fish schools (air in bladder) can be easily identified and is hence useful to estimate the energy loss in the water column during detailed backscatter processing. More diffuse clouds in the water column are assigned to plankton. Indications of mammals are seen as fairly large, single reflections, often associated with hyperbolic reflections.

3.2 Fledermaus Software

FlederMaus (FM) Midwater package was used to process water column data for detecting and analysing gas anomalies. The data was loaded in FM Midwater along with navigation (*.all) and converted to GWC files. During conversion, it was observed that there was fewer *.all files present. This resulted in no navigation for some lines when converted to *.gwc format for analysis. The *.all file from the previous line are used to convert these *.wcd files for possible navigation loading as a test and found that few lines have navigation located in them. The data was analysed for possible discrepancies, but some lines were converted still without any navigation, but the relative location is known from the line numbers. All the lines were hence converted with this method and interpreted. Special care was taken to go through the noisy lines to avoid any missing flares and overall, it is concluded that only weak flares might have been missed through this process.

Similar water column anomalies collected in other areas have been ground truthed confirming the feasibility of this method (Chand et al 2012a, 2012b, 2016). During interpretation, the following procedure was used:

1. The depth range was adjusted to maximise the vertical display of the line (FMM)
2. The display was adjusted to 1:1 horizontal display (FMM)
3. The colour range was adjusted to the dynamic range of signals in the water column, optimizing the display of water column features (FMM). Here we used a range between 0 and 90dB.
4. The data were inspected using the R-stack water column view, and the stacked fan water column view.

The water column data were evaluated in parallel (along-track) and perpendicular (across-track) directions to the track lines for identifying anomalies. The coordinates of potential gas

flares were recorded, along with the survey name and line ID. A subjective assessment of the apparent magnitude has been assigned (table 1). A confidence estimate is provided for codes 2-6. The maximum confidence for visual classification is 90%. A confidence of 100% is reserved for gas flares where gas bubbles have been observed by video/photo inspection or measured using gas sniffers, or where authigenic carbonate crusts have been observed. Very uncertain, but still possible gas flares have been assigned 10% confidence.

Table 1. Codes used for assessment of magnitude, and confidence intervals.

Code	Description	Confidence %
2	Weak gas flare	10 - 100
3	Medium strong gas flare	10 - 100
4	Strong gas flare	10 - 100
5	Very strong gas flare	10 - 100
6	Giant gas flare	10 - 100

Generally, the recognition of gas flares is based on two criteria – the bubbles have higher backscatter strength than the ambient noise in the water column data, and the objects with higher backscatter strength form characteristic patterns in the water column. Under ideal conditions, gas plumes may be observed as flare-shaped objects which start at the seabed and become narrower until they disappear at least 50-100 m above the seabed. If currents are sufficiently strong, the flares will be deflected. The identification of gas flares may be complicated due to several factors, such as high ambient (periodic or random) noise, fish schools, high density of plankton, strong and/or irregular currents, and sub-optimal intersection of the multibeam swath with the gas flare (i.e. covering only part of the flare). The MBE data can also be used to derive the seafloor reflection (i.e., backscatter) properties which will indirectly give an indication of sediment type/grain size and/or hardness of the sea bottom. The FM Geocoder package was used to process the MBE data for backscatter.

4. **RESULTS**

4.1 **Bathymetry**

The bathymetry of the study area shows a rugged seafloor eroded during last glaciation (Fig.2a). Many iceberg plough marks can be clearly seen criss-crossing the seafloor. Some pockmark-like depressions (Fig. 2b) are observed along the small basins probably indicating soft sediment deposition in these areas during and after deglaciation.

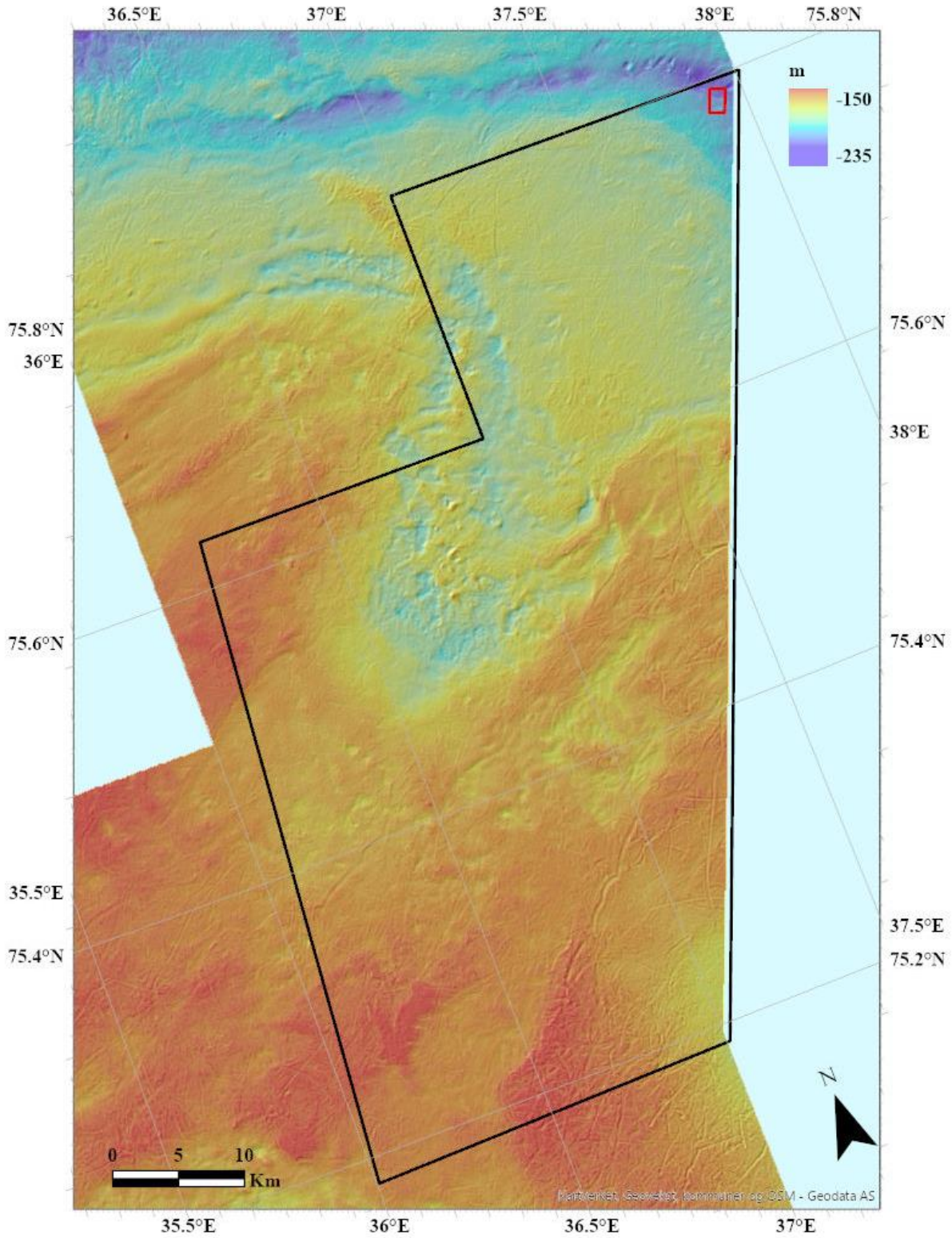

Figure 2a. Bathymetry of the study area (black polygon) and surrounding showing the detailed morphology of the seafloor. The location of Fig. 2b is also shown (red rectangle).

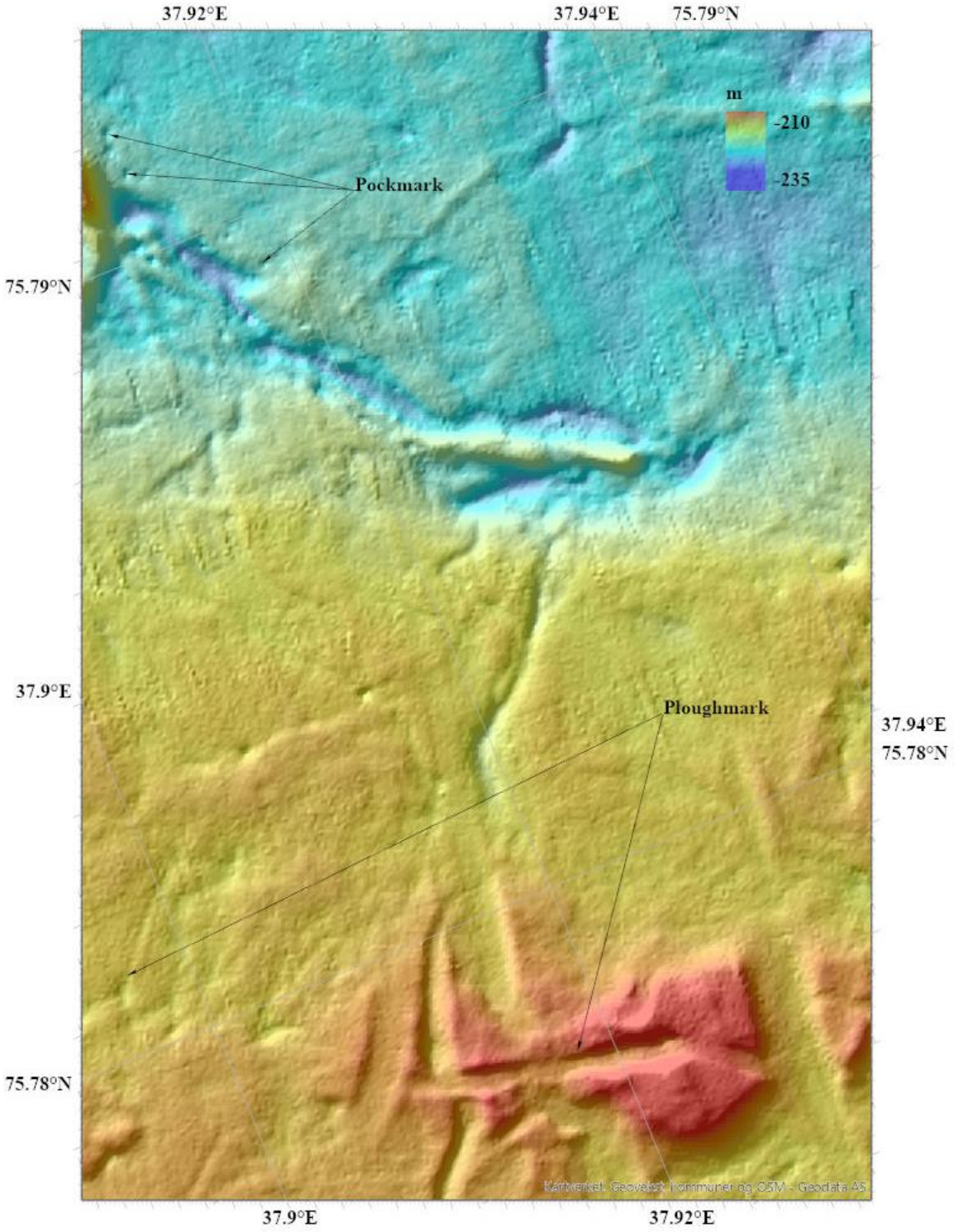

Figure 2b. Bathymetry from pockmark area showing their sparse distribution even in deep areas of the study area.

4.2 **Backscatter**

The backscatter (Fig. 3) from the study area shows low values in depressions related to possible soft sediment deposition during and after deglaciation. In addition, low backscatter values are observed outside the depressions along the south-western part of the study area.

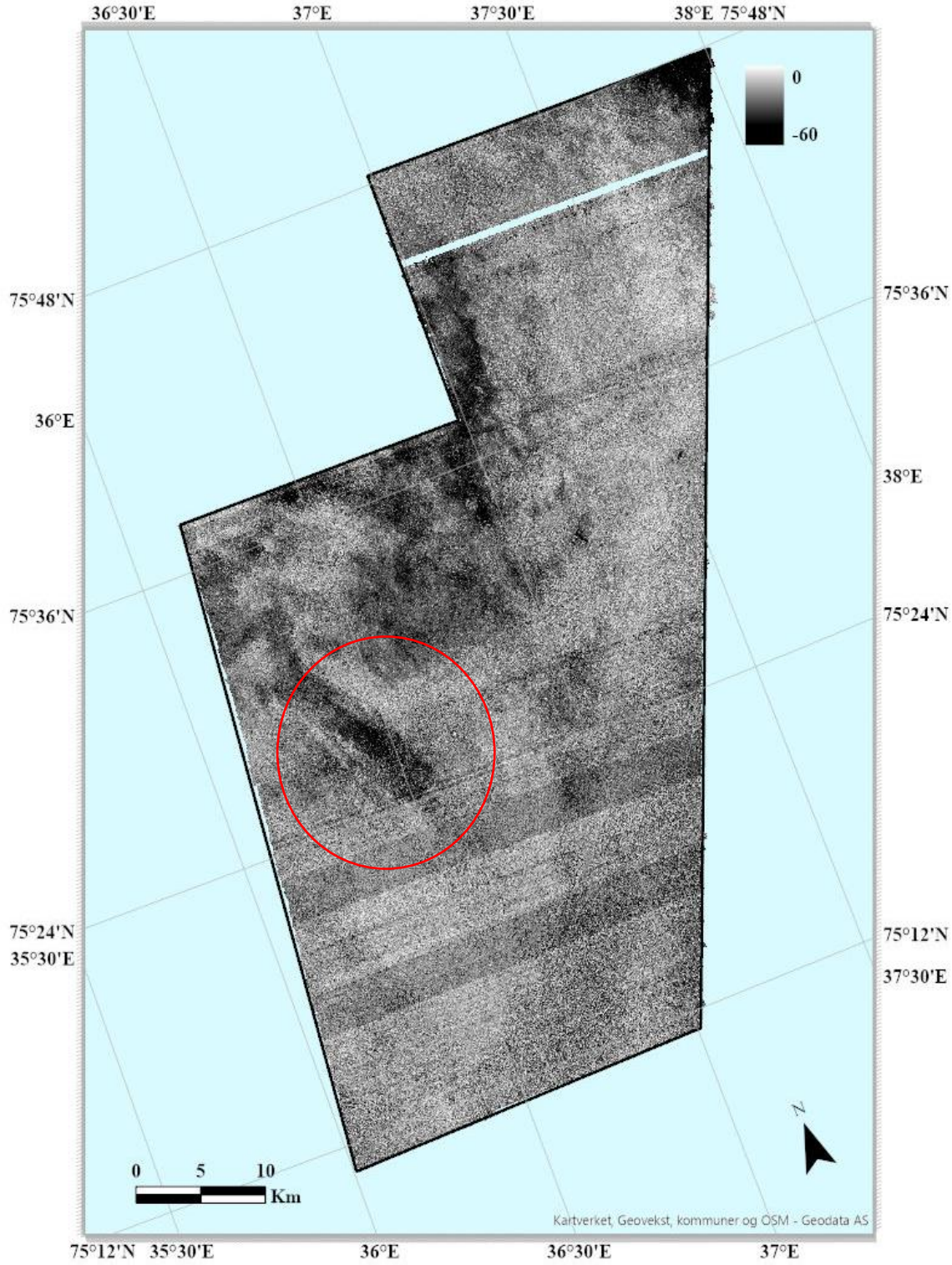

Figure 3. Backscatter of the study area showing the locations of low backscatter concentrated mainly along depressions. Low backscatter outside depressions are indicated by red circle. The interpretation of sediment types based on various datasets along with backscatter is given in Figure 4.

4.3 **Sediment Classification**

The sediments at the seafloor of the study area has been classified using multibeam bathymetry and backscatter together with ground truthing samples from gravity/multicore and video observations. The sediment map shows clay to sands present in the area (Fig. 4).

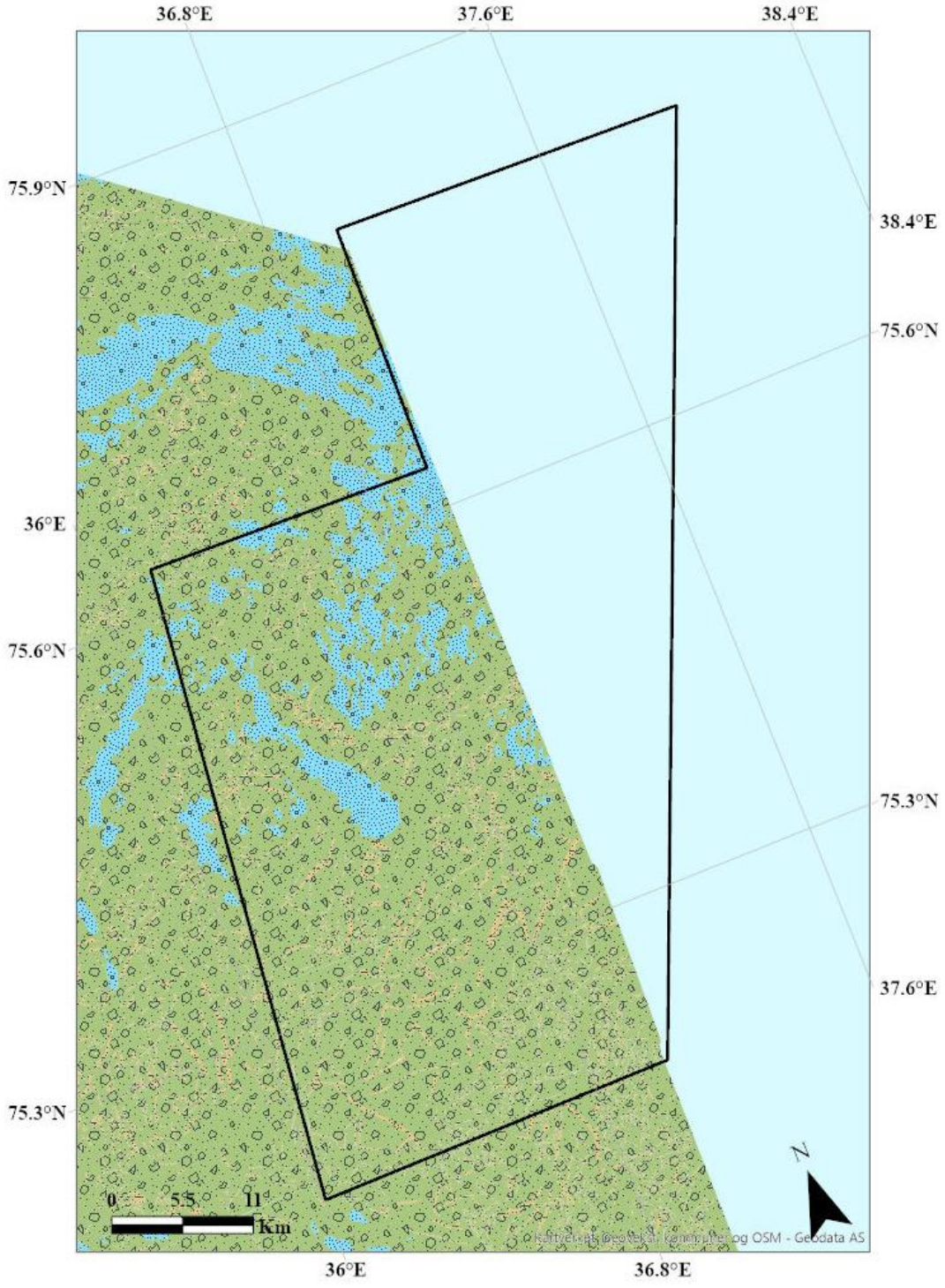

Figure 4. Detailed sediment grain size map from Mareano interpretation based on various datasets covering a part of the study area.

4.4 **Water Column**

Several gas flares have been reported earlier from the Sentralbanken area of Barents Sea (Nixon et al., 2019). The flares are suggested to occur close to seafloor depressions formed during deglaciation (Nixon et al., 2019). The subsurface of the area indicates eroded old sedimentary rocks pinching out close to the seafloor. The present study area lies east of the Sentralbanken and mainly located along the Polarrev High (Figs. 1 & 5). The study area is covered by four Fugro surveys named as D19, D21, D23 and D26. The data includes EM710 water column measurements and the results are divided based on the survey names. The combined results from the water column data analysis of all the four survey areas are shown in Figs. 5 and 6.

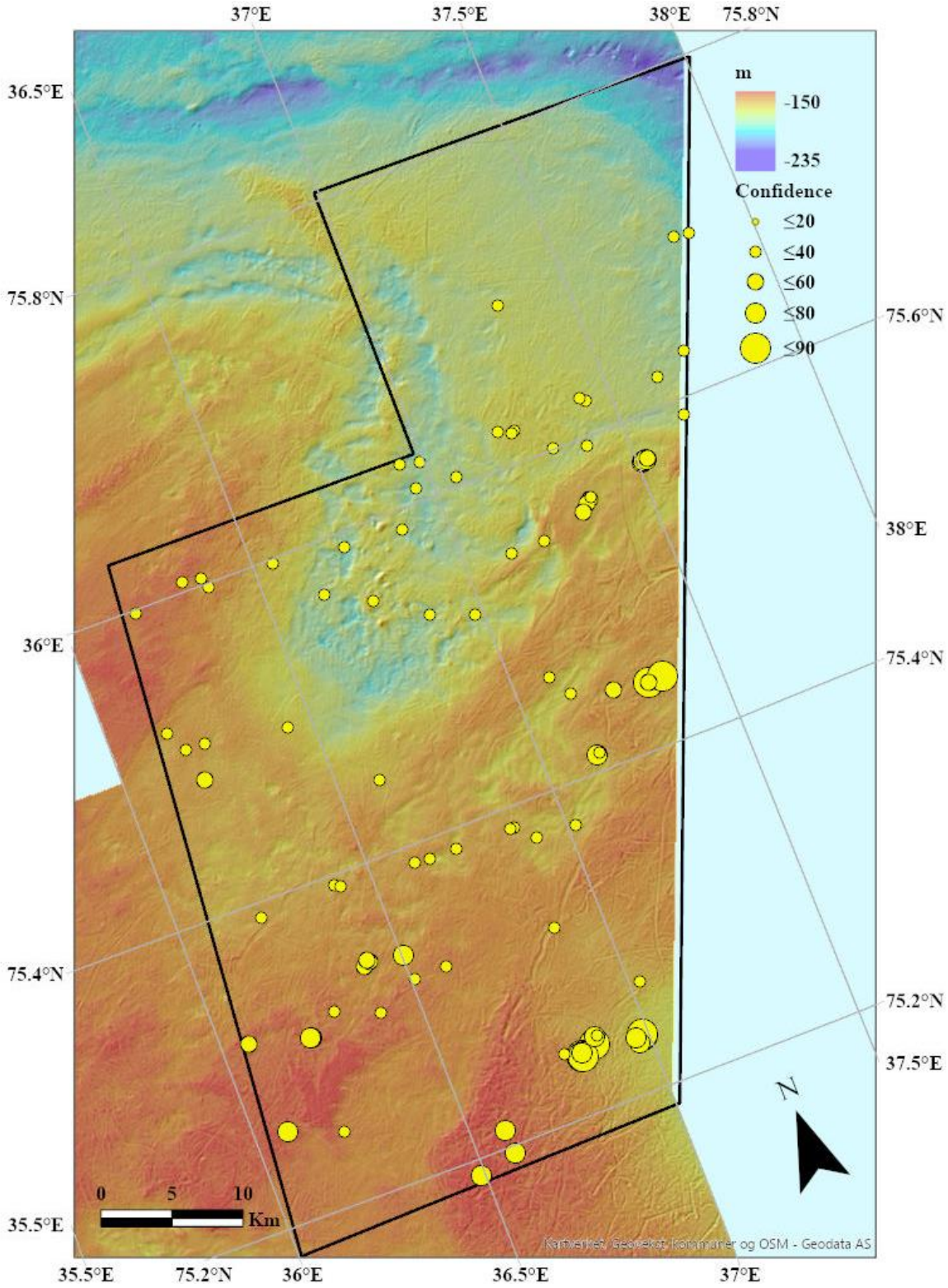

Figure 5a. Locations of flares identified from the study area and their confidence level is shown on bathymetry map of the study area.

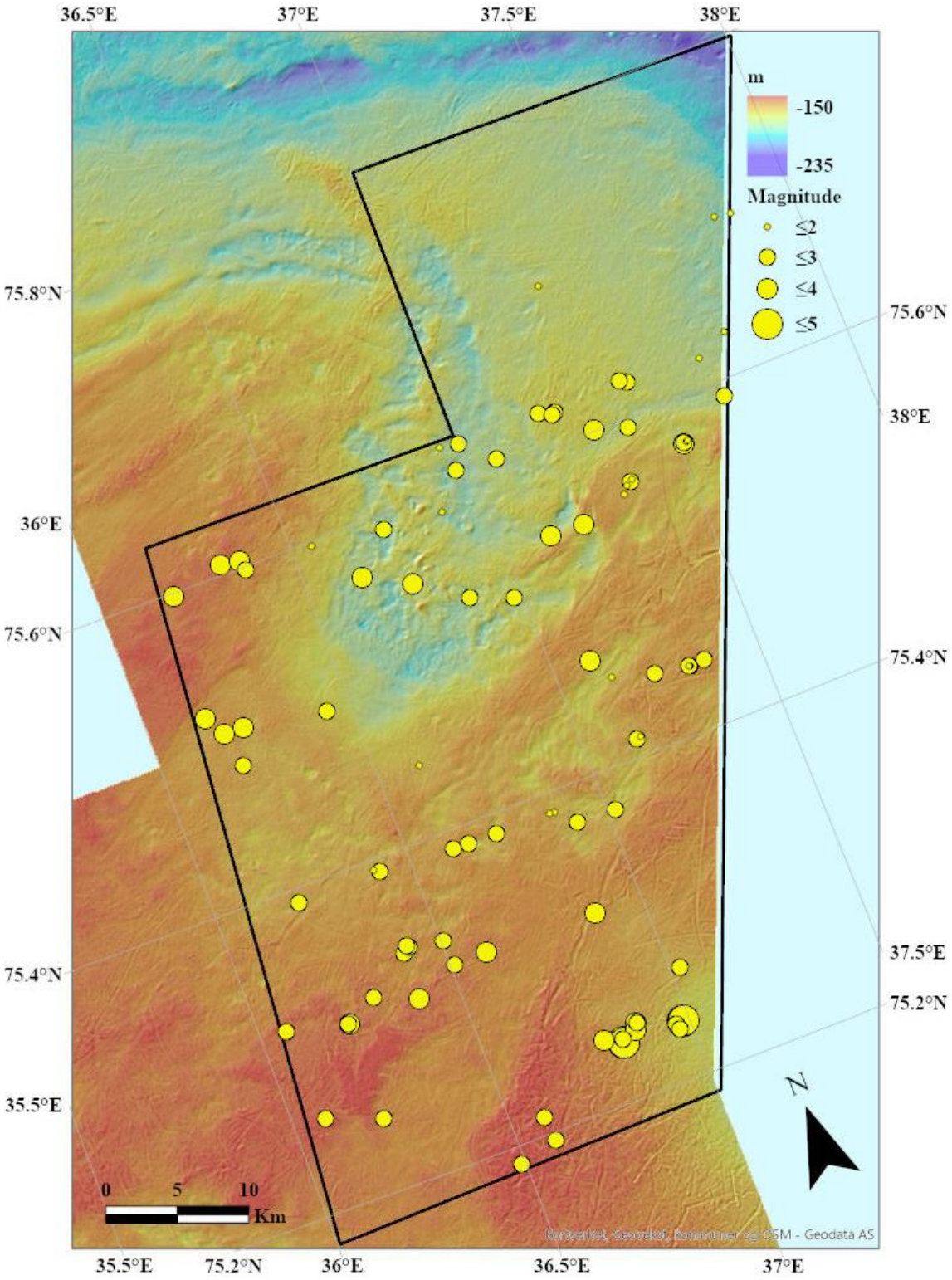

Figure 5b. Locations of flares identified from the study area and their magnitude is shown on bathymetry map of the study area.

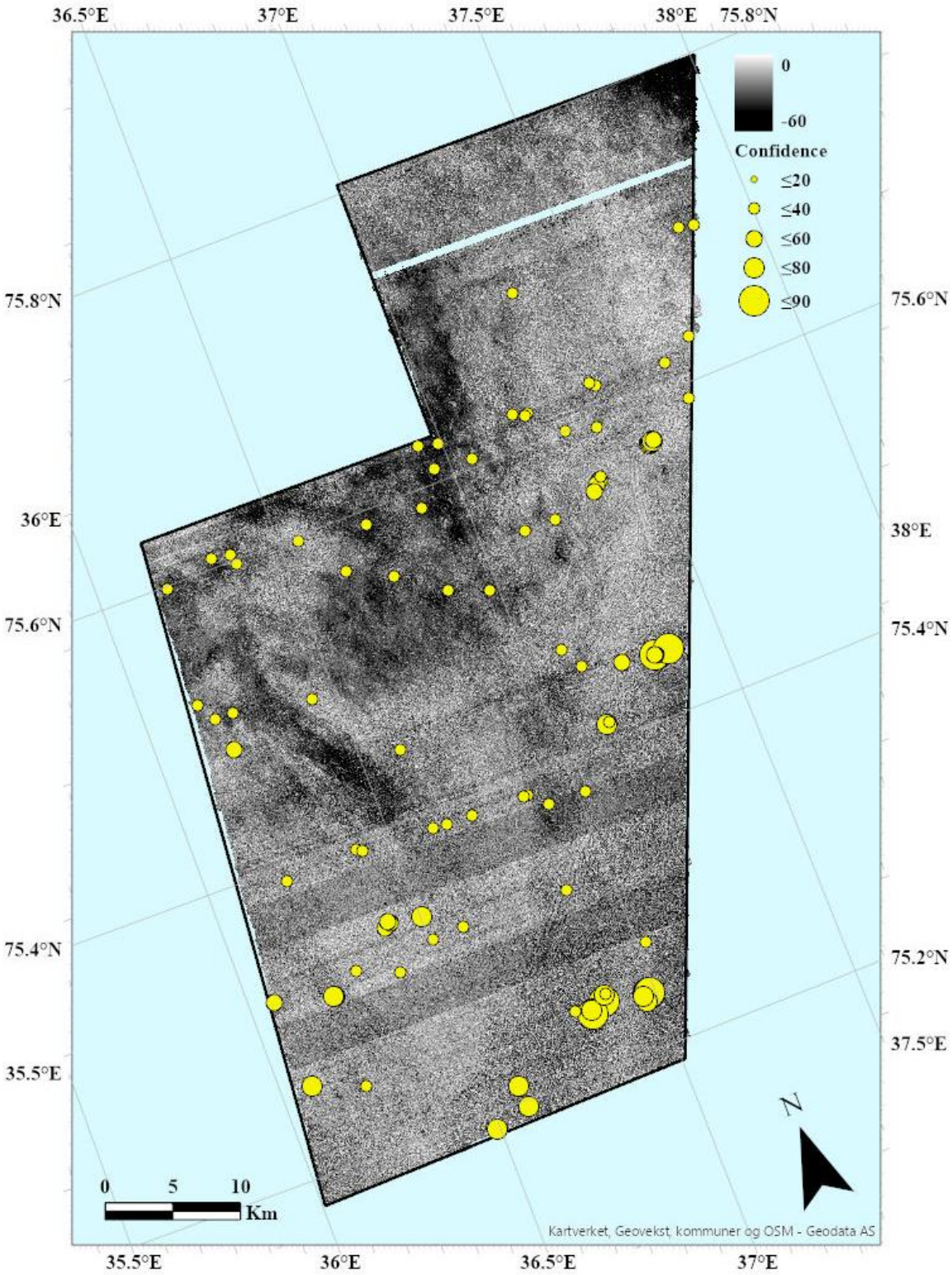

Figure 6a. Locations of flares identified from the study area and their confidence level is shown on backscatter map of the study area.

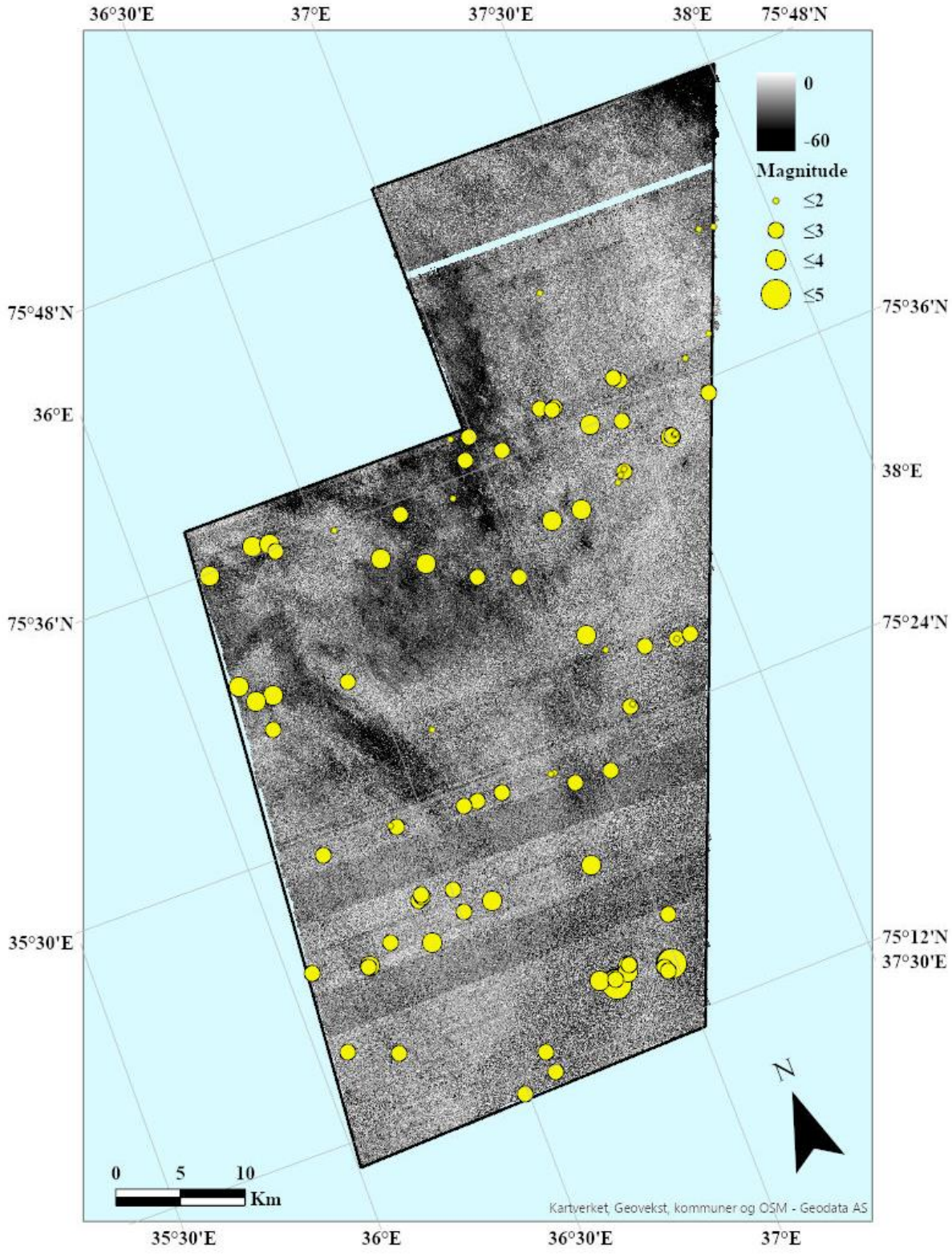

Figure 6b. Locations of flares identified from the study area and their magnitudes are shown on backscatter map of the study area.

4.4.1 D19

The FOSAE-2013-D19 survey consists of 519 water column (*.wcd) survey lines. The data was loaded in Fledermaus Midwater along with navigation (*.all) and converted to GWC files. During conversion, it was observed that there was only 466 *.all files present. This resulted in no navigation for the 53 lines when converted to *.gwc format for analysis. The *.all file from the previous line are used to convert these *.wcd files for possible navigation loading. But only few lines were found to have navigation located in these lines. There was no flare found in the lines with missing navigation. 29 flares of varying confidence level were found in the data. The flares found are listed in Table 2. 77 lines were noisy and would have resulted in some weak flares missing. The flares identified are shown in Figures. 7 – 29.

Table 2. Details of flares identified from Survey Area D19.

Survey	LineId	Latitude	Longitude	Depth	Height	Time	Magnitude	Confidence
FOSAE-2013-D19	6359	75.31872900	36.06598100	-151.23	55.00	02/25/2014 7:45:36.1	3	50
FOSAE-2013-D19	6359	75.31947200	36.29384600	-159.01	40.00	02/25/2014 8:09:15.0	3	30
FOSAE-2013-D19	6360	75.32074100	36.51023600	-158.55	35.00	02/25/2014 8:31:39.6	3	30
FOSAE-2013-D19	6360	75.32124100	36.59346100	-159.85	35.00	02/25/2014 8:40:22.2	4	40
FOSAE-2013-D19	6361	75.31924200	36.87843000	-167.46	100.00	02/25/2014 9:09:45.8	4	40
FOSAE-2013-D19	6397	75.30893700	36.21727400	-154.84	100.00	02/27/2014 8:59:28.3	4	80
FOSAE-2013-D19	6397	75.30909	36.21410	-155.00	100.00	02/27/2014 8:59:13.3	3	70
FOSAE-2013-D19	6403	75.30869600	36.40001100	-156.88	50.00	02/27/2014 12:28:00.5	4	40
FOSAE-2013-D19	6571	75.26847400	37.02439400	-170.80	50.00	03/18/2014 15:28:34.7	3	40
FOSAE-2013-D19	6593	75.25899400	36.08083700	-150.06	90.00	03/19/2014 1:29:13.8	3	70
FOSAE-2013-D19	6619	75.24595100	36.87171300	-171.46	75.00	03/19/2014 12:39:49.0	4	70
FOSAE-2013-D19	6619	75.24621300	36.87739700	-164.06	60.00	03/19/2014 12:39:04.6	3	40
FOSAE-2013-D19	6622	75.24610900	36.21163800	-157.26	50.00	03/19/2014 14:07:07.4	3	40
FOSAE-2013-D19	6627	75.24310900	36.78692500	-155.66	35.00	03/19/2014 16:12:19.4	4	30
FOSAE-2013-D19	6637	75.23599200	36.96512300	-174.58	70.00	03/19/2014 21:22:43.3	3	70
FOSAE-2013-D19	6637	75.23664400	36.98387100	-178.74	90.00	03/19/2014 21:25:02.2	5	90
FOSAE-2013-D19	6637	75.23728700	36.82636500	-167.44	50.00	03/19/2014 21:05:22.8	5	90
FOSAE-2013-D19	6637	75.23631100	36.98270000	-180.95	70.00	03/19/2014 21:24:53.2	5	90
FOSAE-2013-D19	6637	75.23669400	36.98262778	-180.35	70.00	03/19/2014 21:24:53.2	5	90
FOSAE-2013-D19	6637	75.23665278	36.98418611	-179.50	70.00	03/19/2014 21:25:04.5	5	90
FOSAE-2013-D19	6639	75.23217800	36.96909600	-174.25	65.00	03/19/2014 22:09:40.7	3	80
FOSAE-2013-D19	6664	75.24194200	36.86724700	-171.07	80.00	03/20/2014 8:34:15.5	4	90
FOSAE-2013-D19	6689	75.23730900	36.82743500	-166.87	65.00	03/20/2014 15:16:47.4	5	90
FOSAE-2013-D19	6689	75.23982200	36.82903100	-165.81	65.00	03/20/2014 15:15:52.4	3	80
FOSAE-2013-D19	6689	75.23770800	36.82725278	-166.80	140.00	03/20/2014 15:16:38.5	5	90
FOSAE-2013-D19	6689	75.23694167	36.82768330	-166.30	150.00	03/20/2014 15:16:54.9	5	90
FOSAE-2013-D19	6713	75.21102800	36.58187100	-152.55	60.00	03/21/2014 5:30:39.4	3	70
FOSAE-2013-D19	6739	75.19591400	36.58695800	-154.52	80.00	03/21/2014 16:40:50.4	3	70
FOSAE-2013-D19	6749	75.18954700	36.48938800	-154.00	80.00	03/21/2014 21:27:35.4	3	70

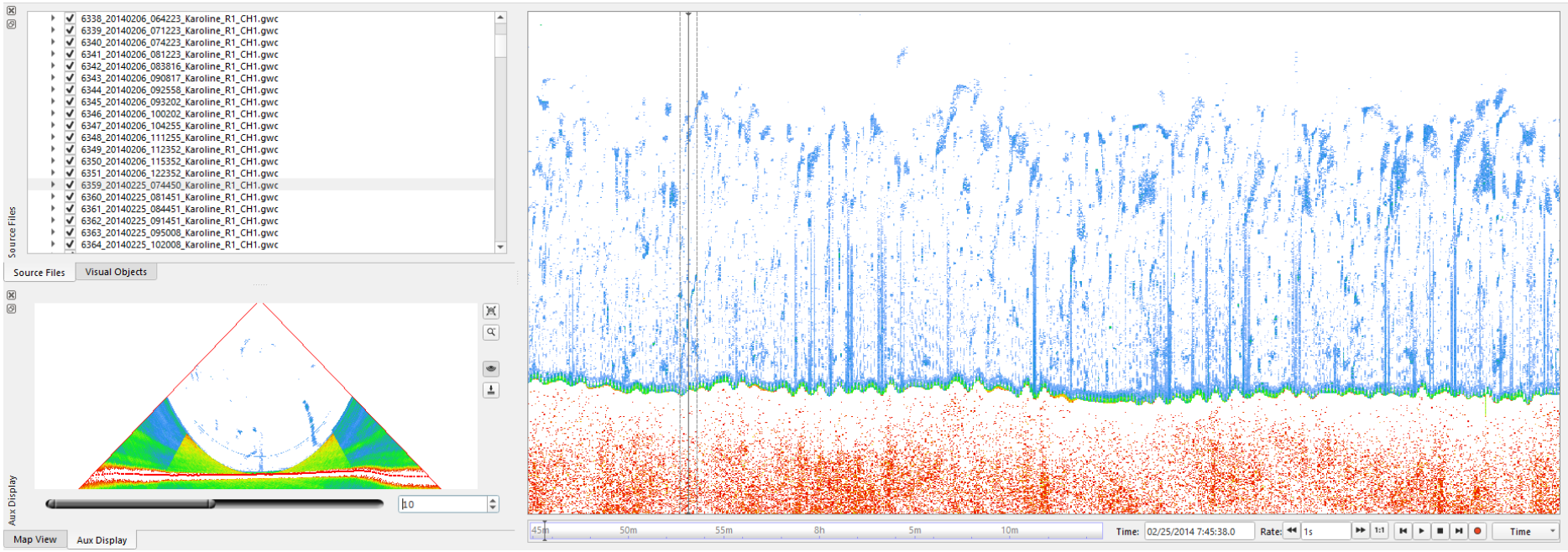

Figure 7. Gas flare from line 6359 showed on Fan view and stack view. Magnitude 3, Confidence 50%.

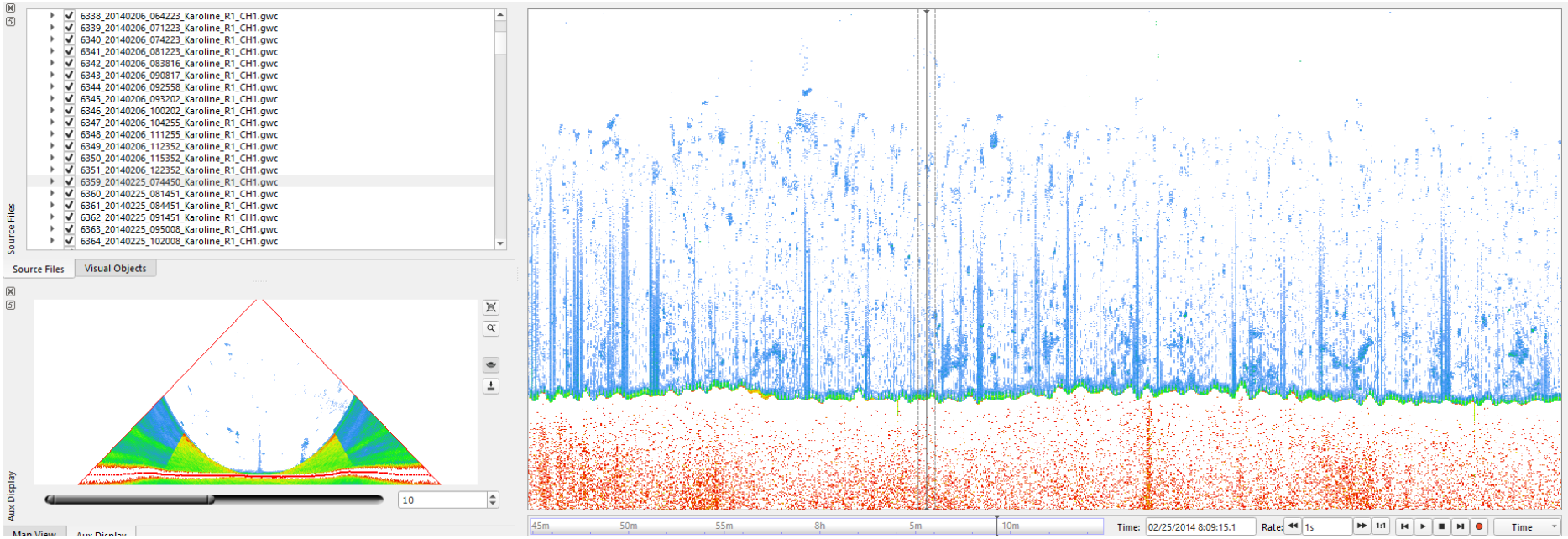

Figure 8. Possible gas flare from line 6359 showed on Fan view and stack view. Magnitude 3, Confidence 30%.

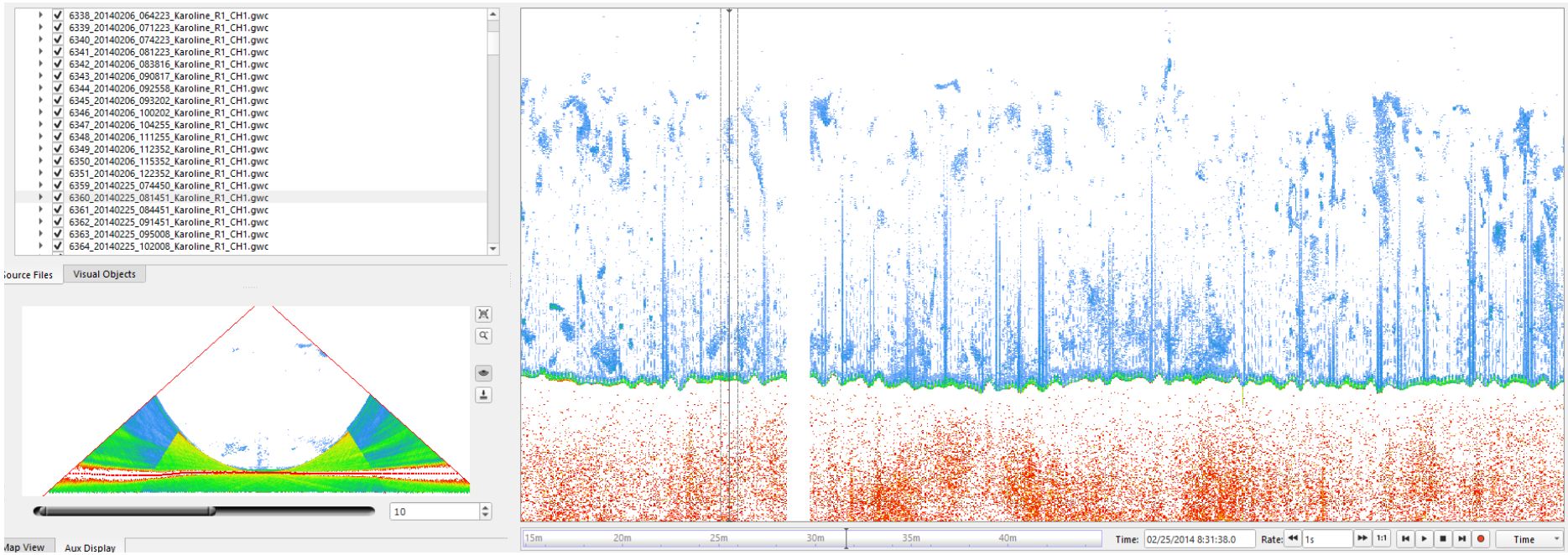

Figure 9. Possible gas flare from line 6360 showed on Fan view and stack view. Magnitude 3, Confidence 30%.

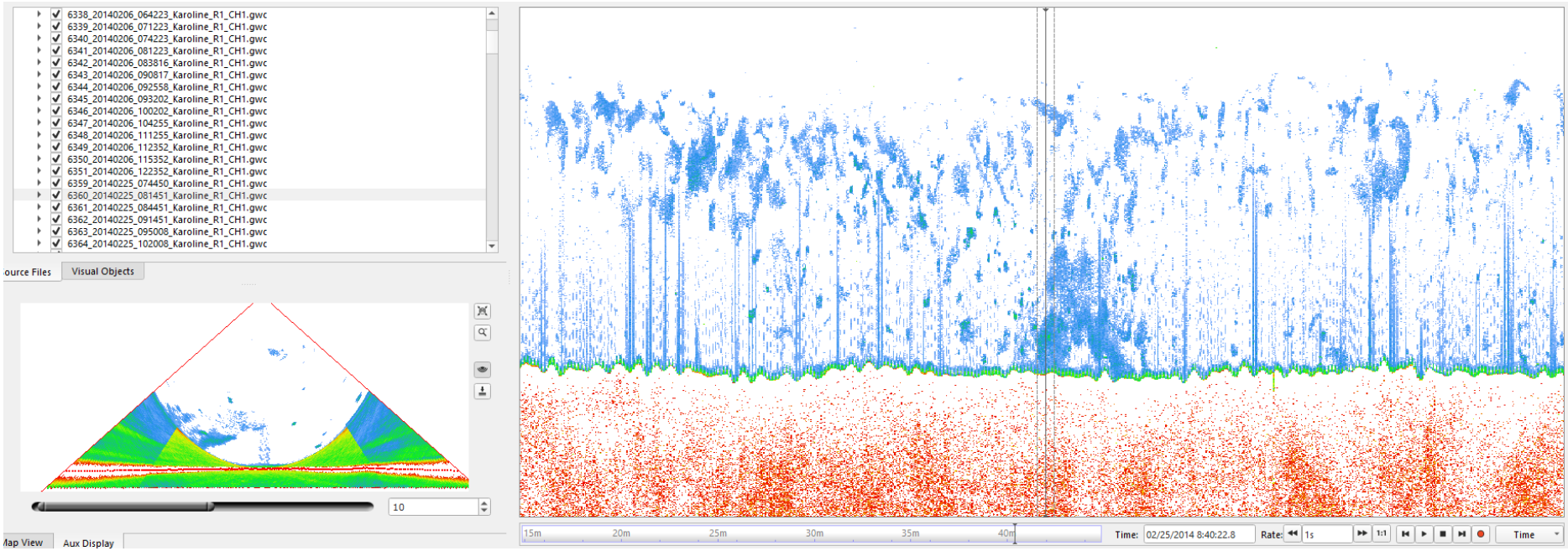

Figure 10. Possible gas flare from line 6360 showed on Fan view and stack view. Magnitude 4, Confidence 40%.

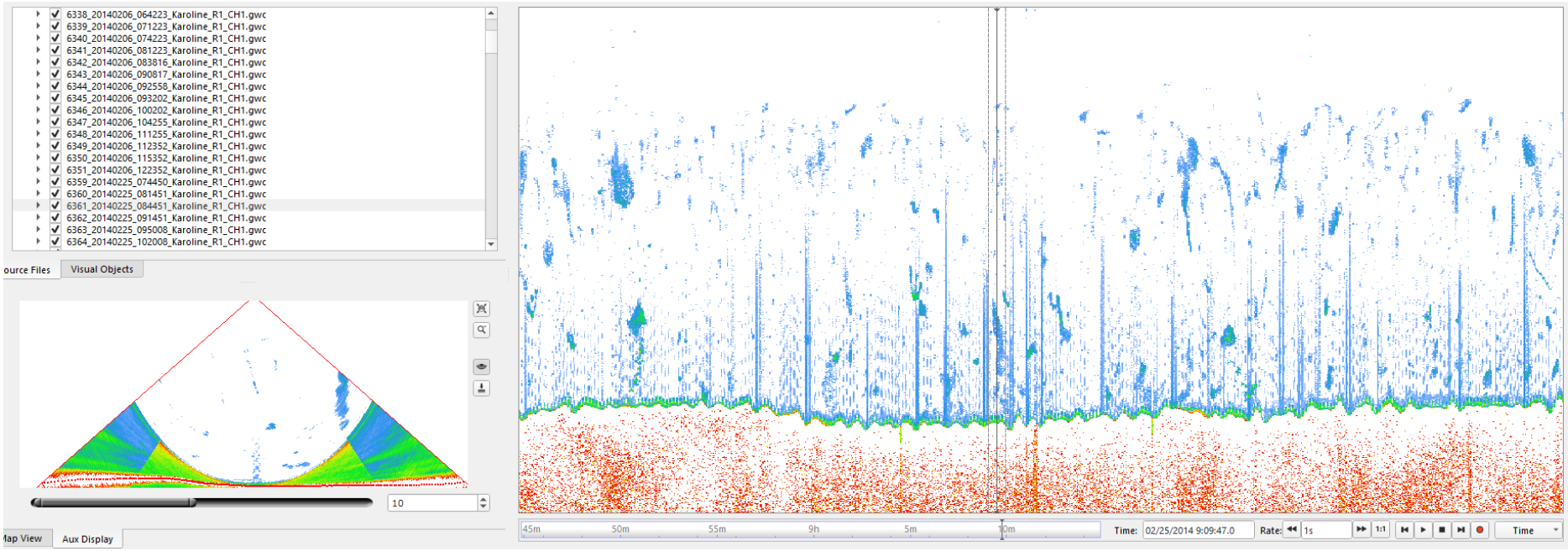

Figure 11. Possible gas flare from line 6361 showed on Fan view and stack view. Magnitude 4, Confidence 40%.

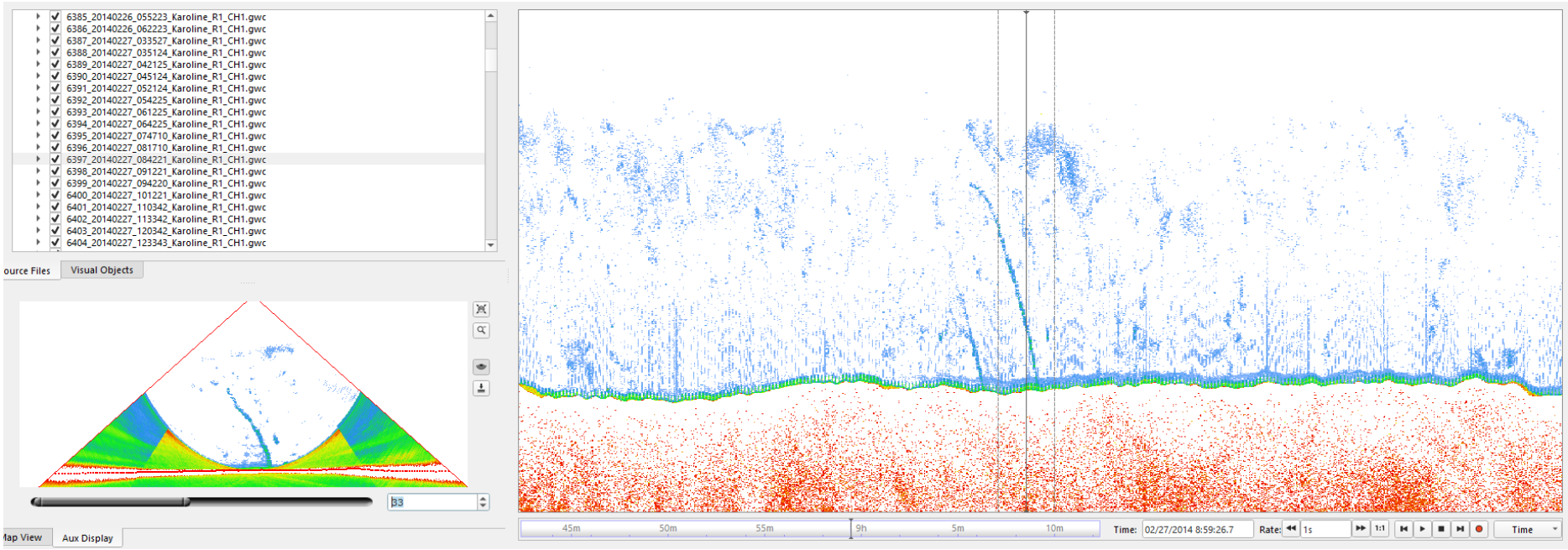

Figure 12. Gas flare from line 6397 showed on Fan view and stack view. Magnitude 4, Confidence 80%.

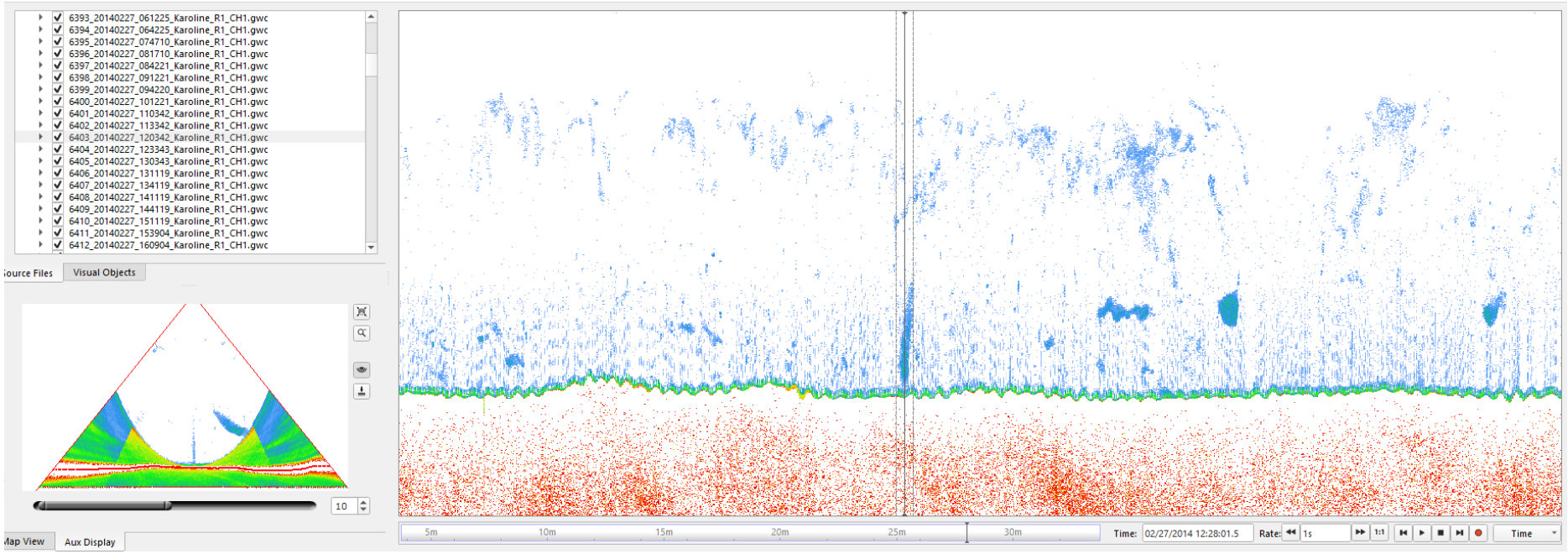

Figure 13. Possible gas flare from line 6403 showed on Fan view and stack view. Magnitude 4, Confidence 40%.

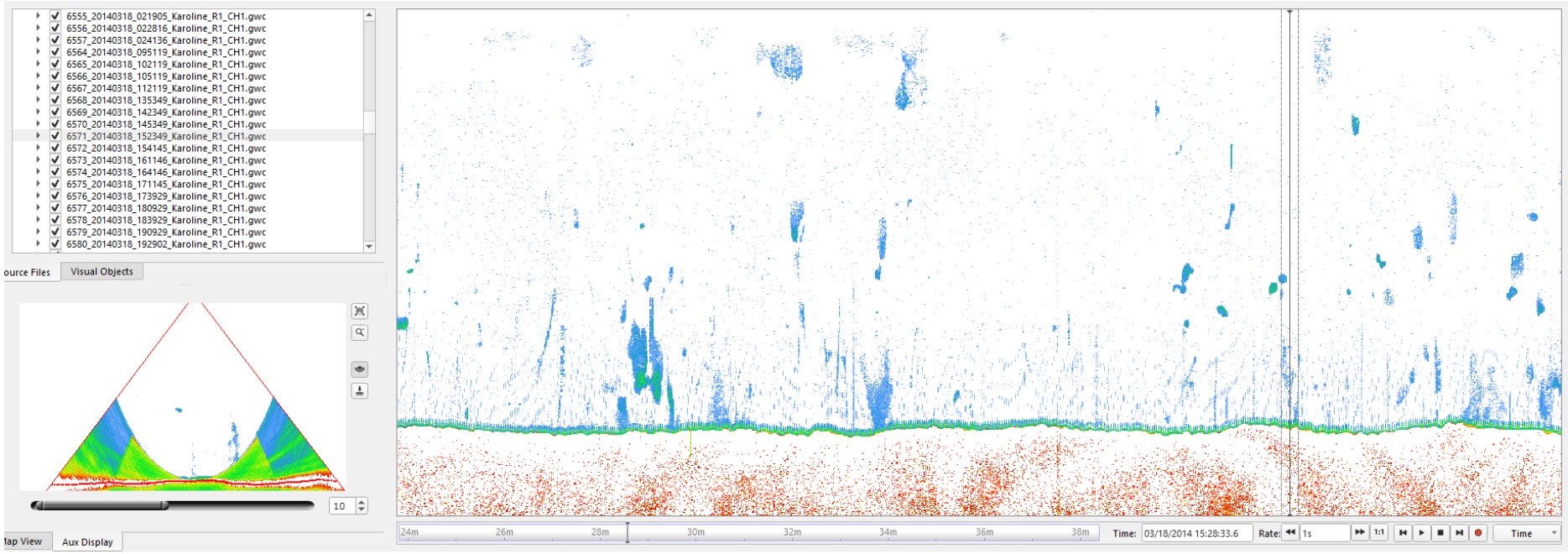

Figure 14. Possible gas flare from line 6571 showed on Fan view and stack view. Magnitude 3, Confidence 40%.

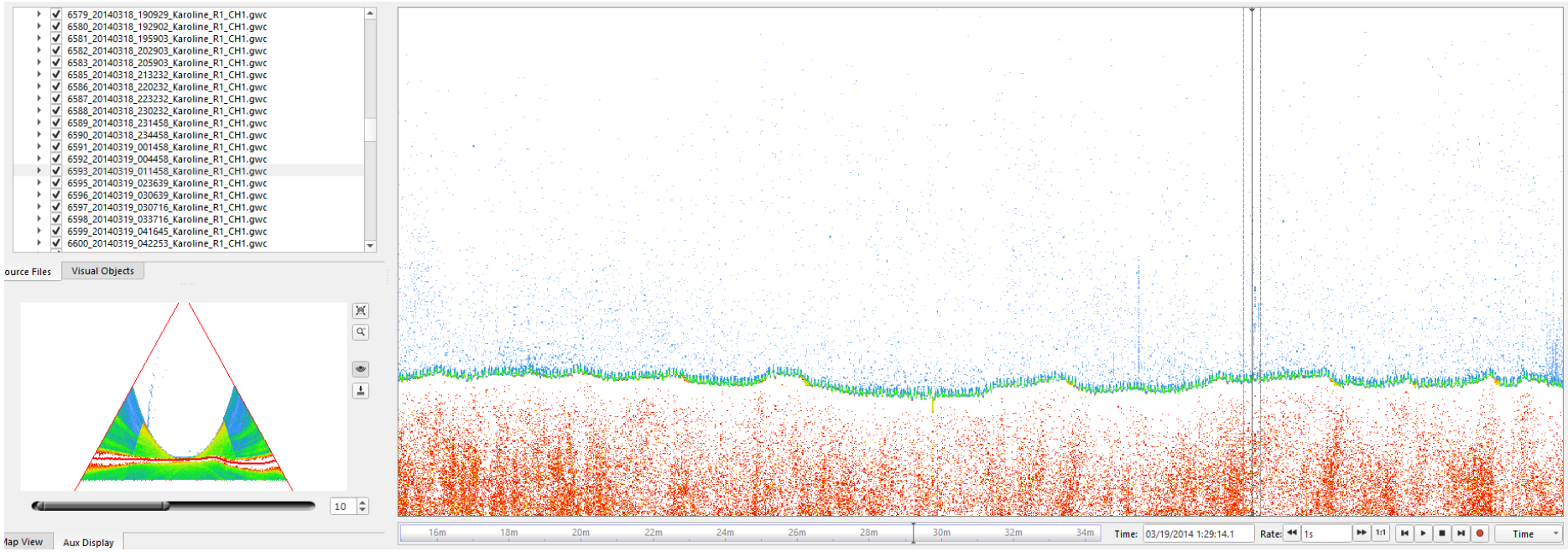

Figure 15. Gas flare from line 6593 showed on Fan view and stack view. Magnitude 3, Confidence 70%.

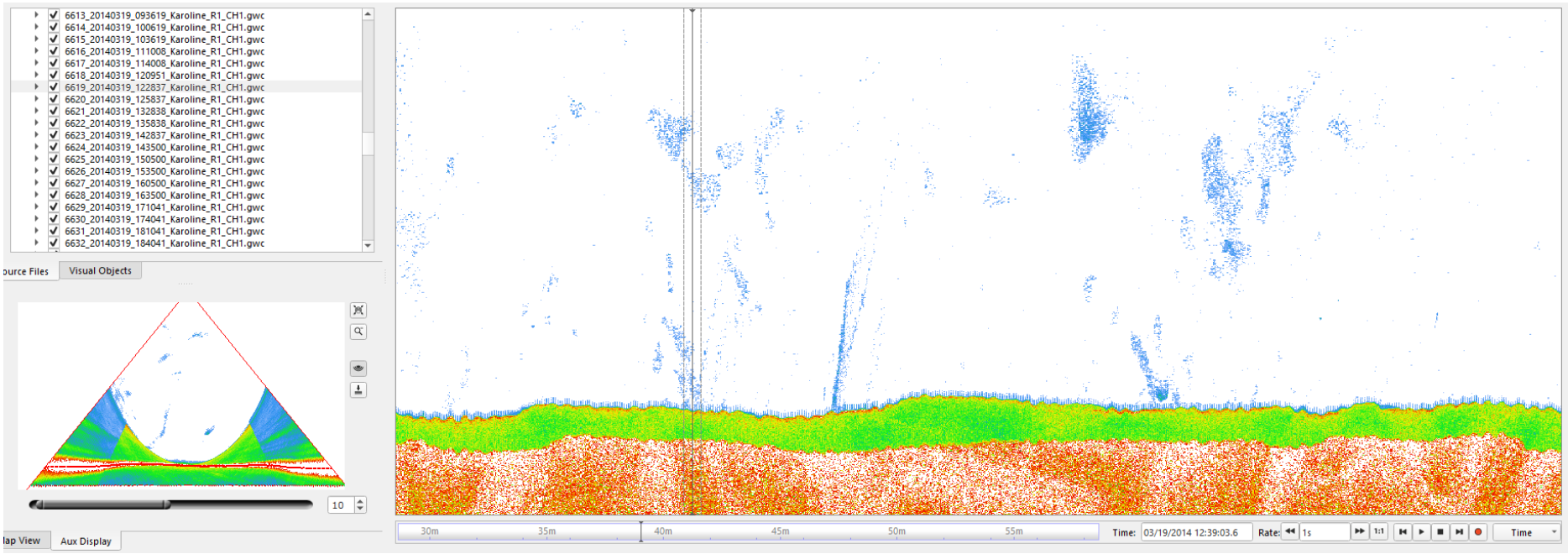

Figure 16. Gas flare from line 6619 showed on Fan view and stack view. Magnitude 3, Confidence 40%.

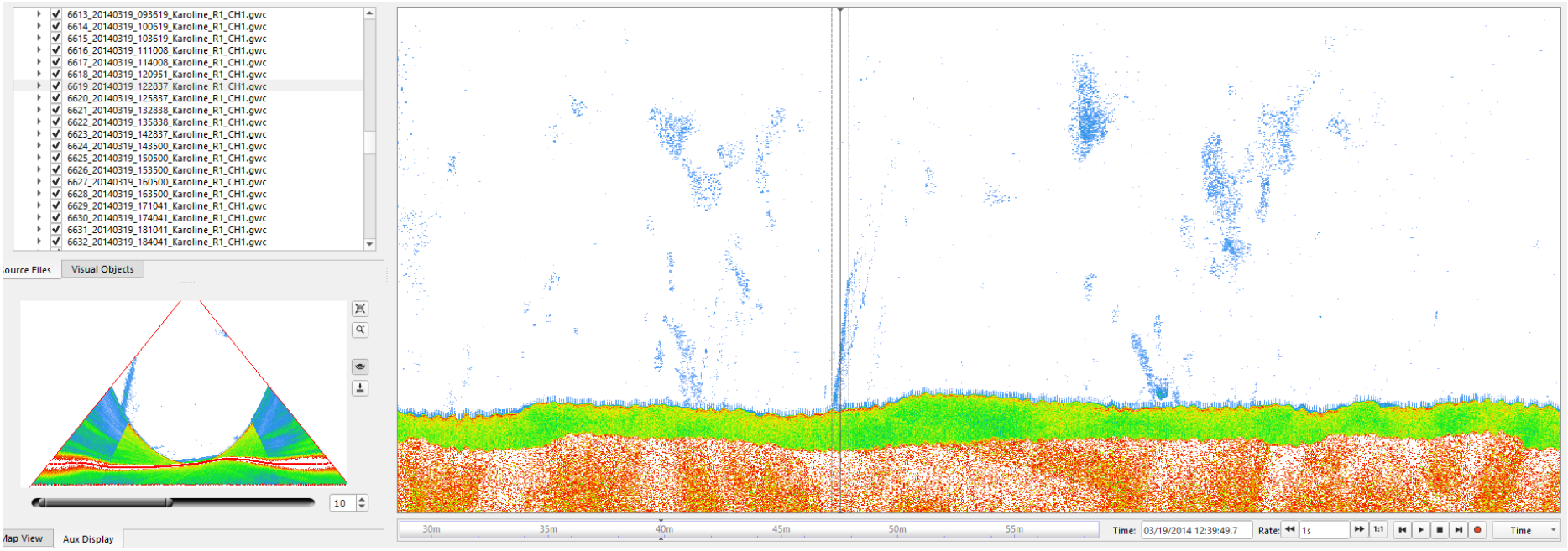

Figure 17. Possible gas flare from line 6619 showed on Fan view and stack view. Magnitude 4, Confidence 70%.

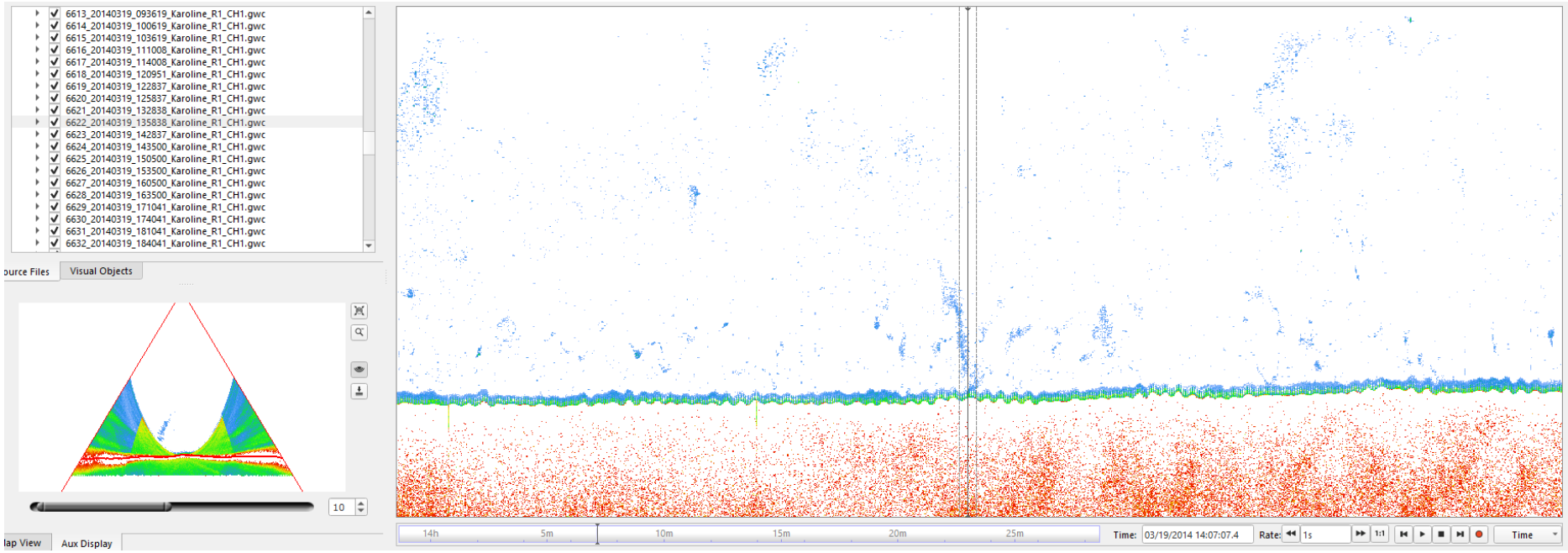

Figure 18. Possible gas flare from line 6622 showed on Fan view and stack view. Magnitude 3, Confidence 40%.

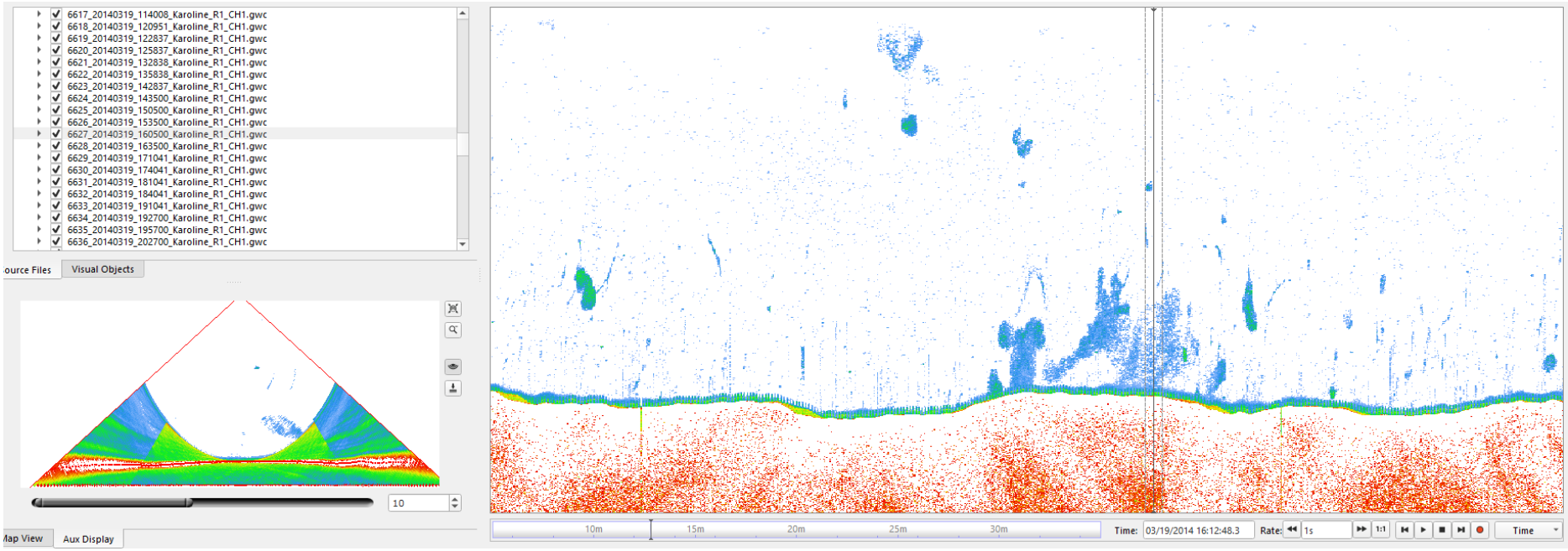

Figure 19. Possible gas flare from line 6627 showed on Fan view and stack view. Magnitude 4, Confidence 30%.

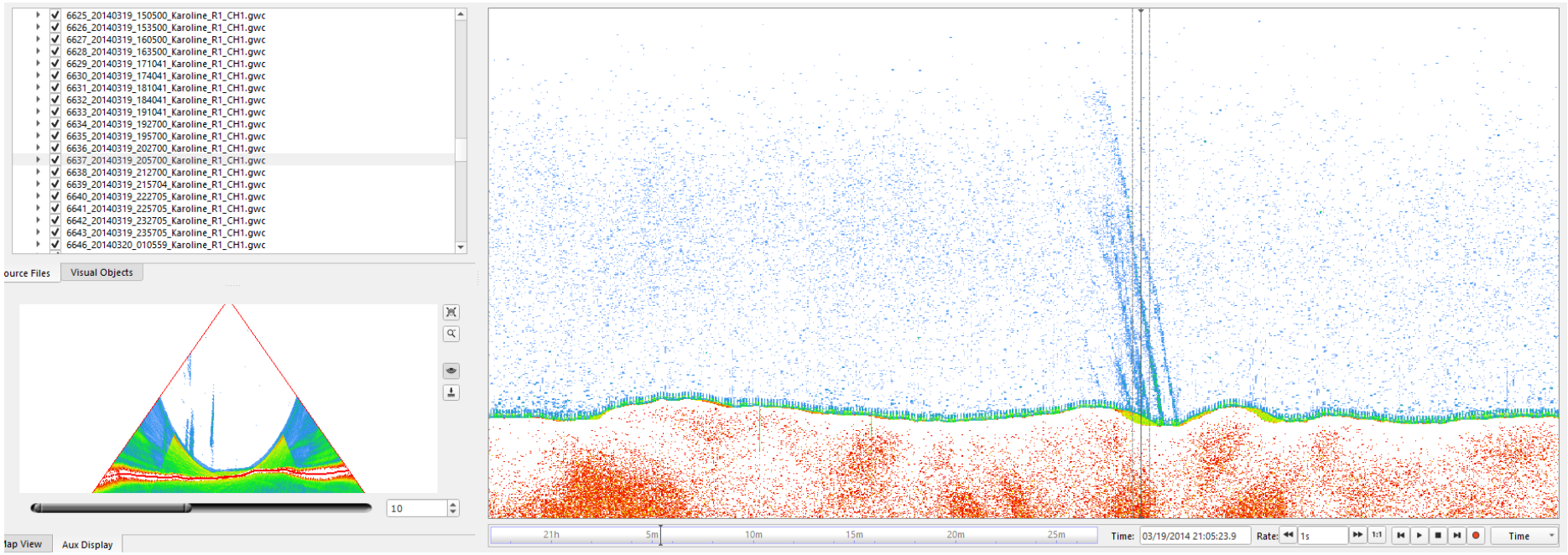

Figure 20. Gas flare from line 6637 showed on Fan view and stack view. Magnitude 5, Confidence 90%.

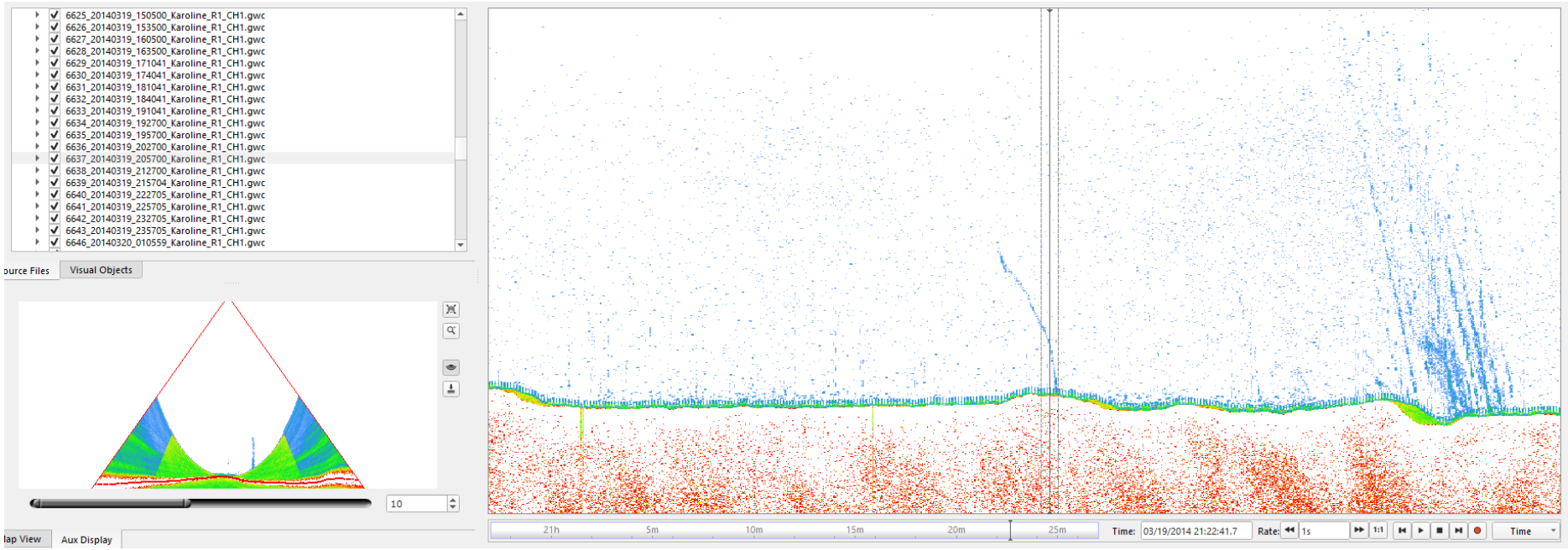

Figure 21. Gas flare from line 6637 showed on Fan view and stack view. Magnitude 3, Confidence 70%.

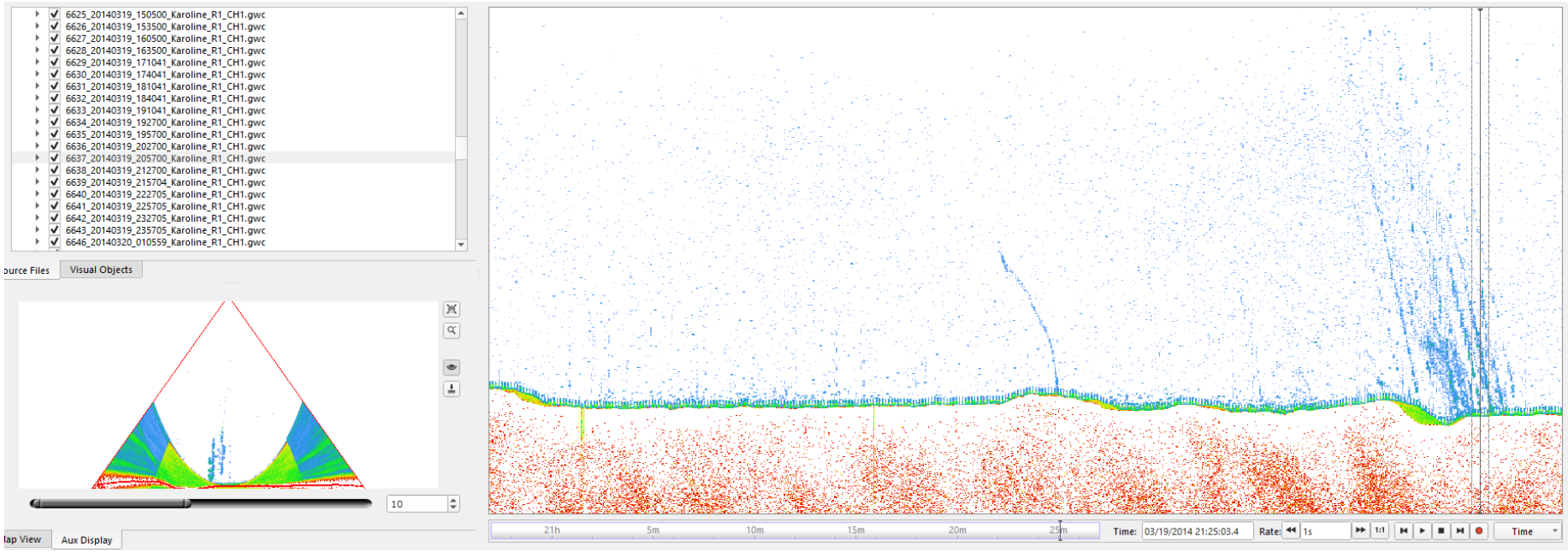

Figure 22. Gas flare from line 6637 showed on Fan view and stack view. Magnitude 5, Confidence 90%.

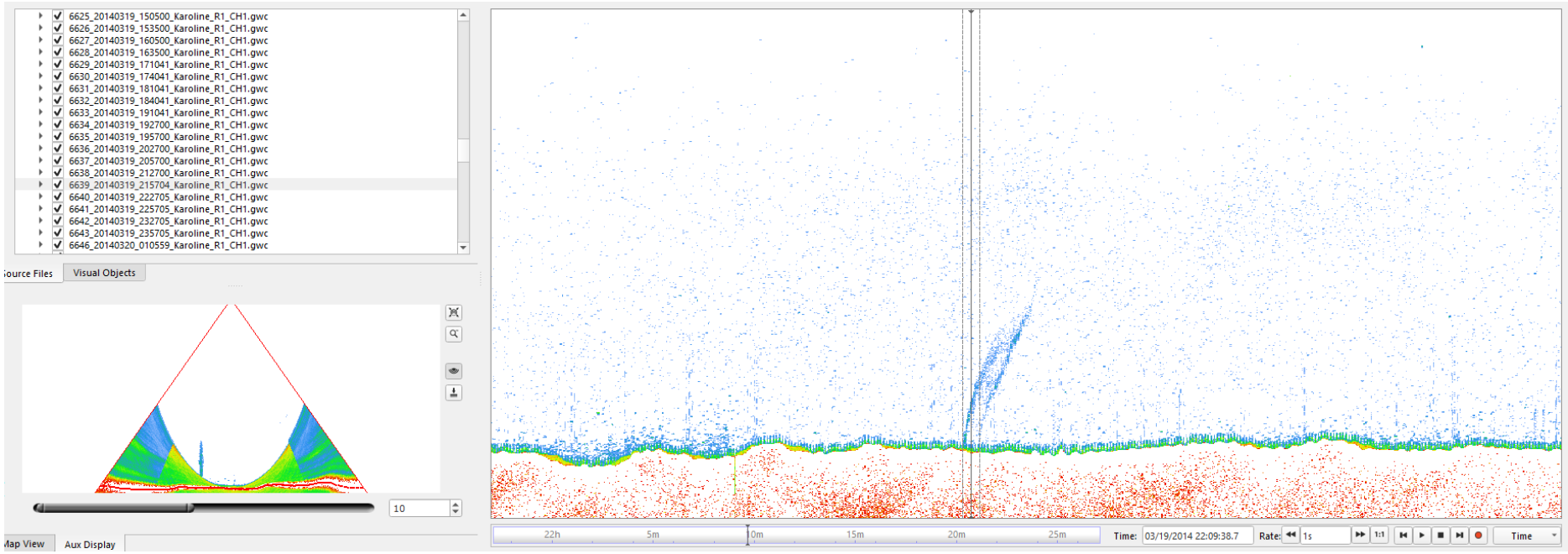

Figure 23. Gas flare from line 6639 showed on Fan view and stack view. Magnitude 3, Confidence 80%.

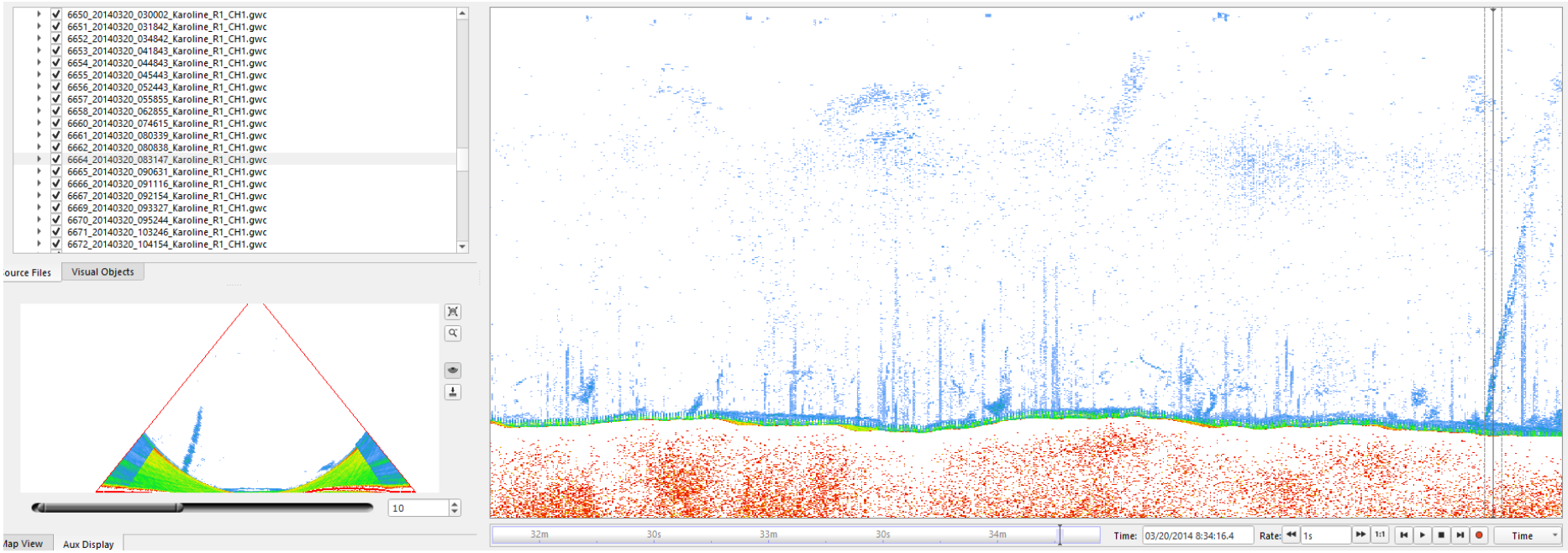

Figure 24. Gas flare from line 6664 showed on Fan view and stack view. 1:1 display not possible. Magnitude 4, Confidence 90%.

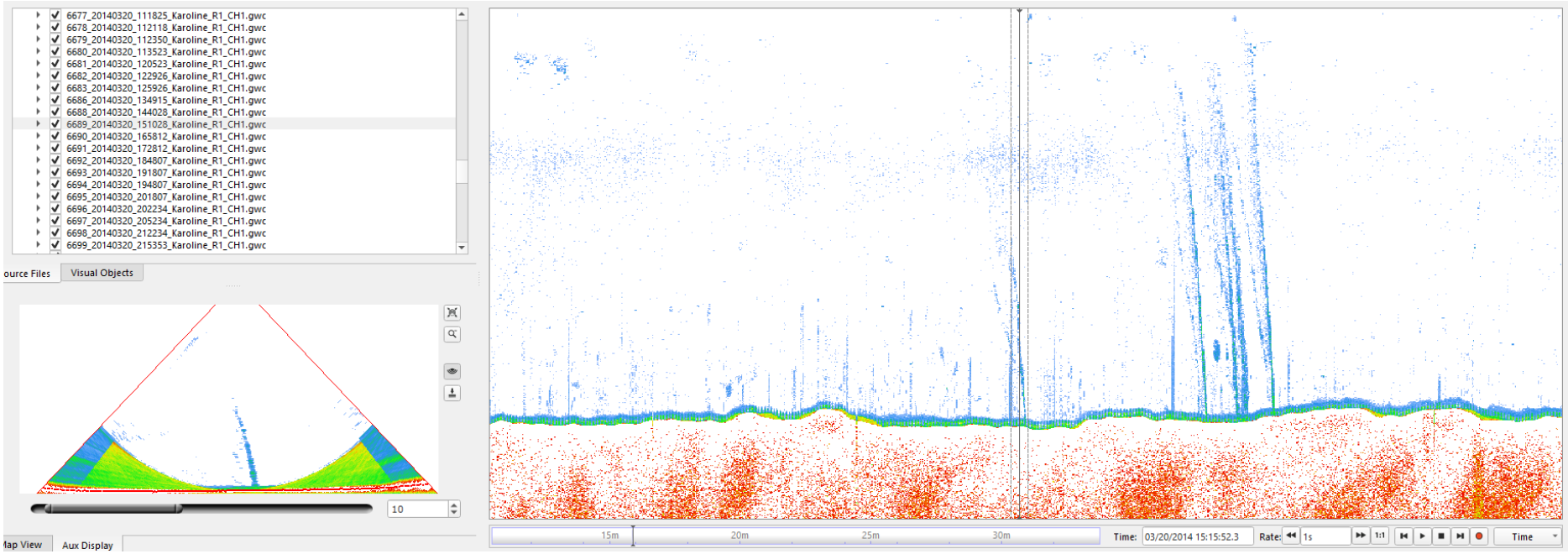

Figure 25. Gas flare from line 6689 showed on Fan view and stack view. Magnitude 3, Confidence 80%.

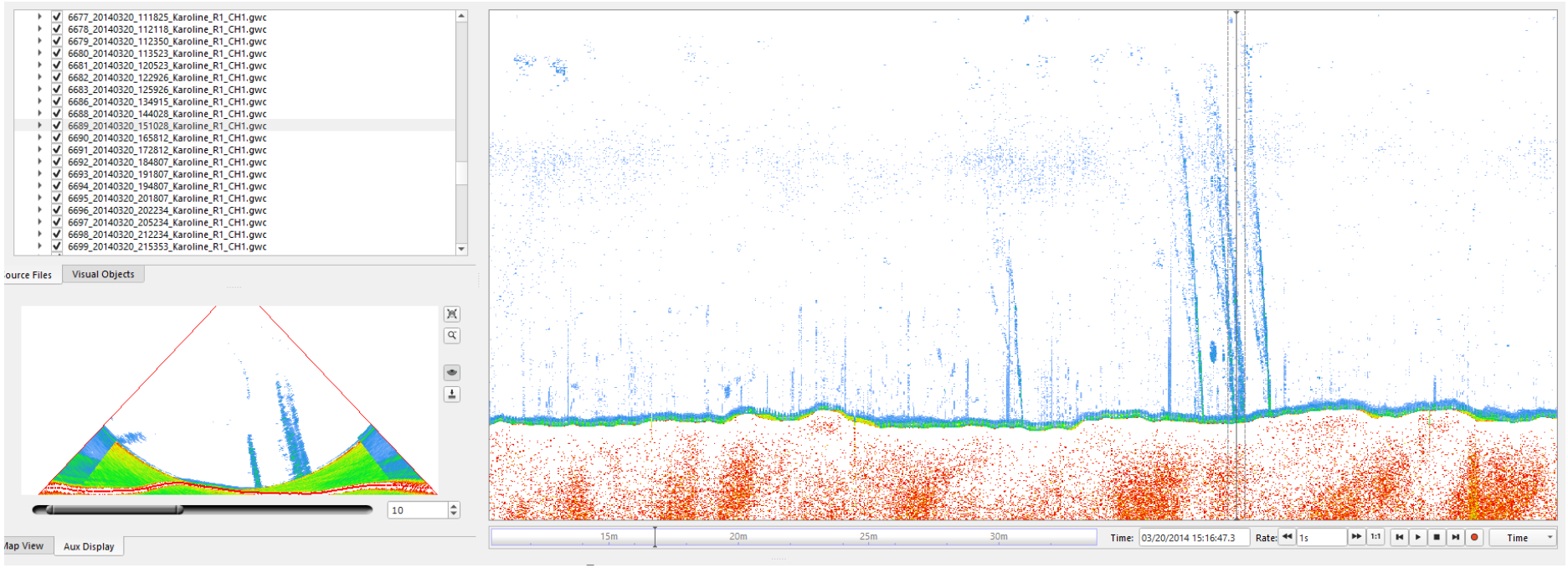

Figure 26. Gas flare from line 6689 showed on Fan view and stack view. Magnitude 5, Confidence 90%.

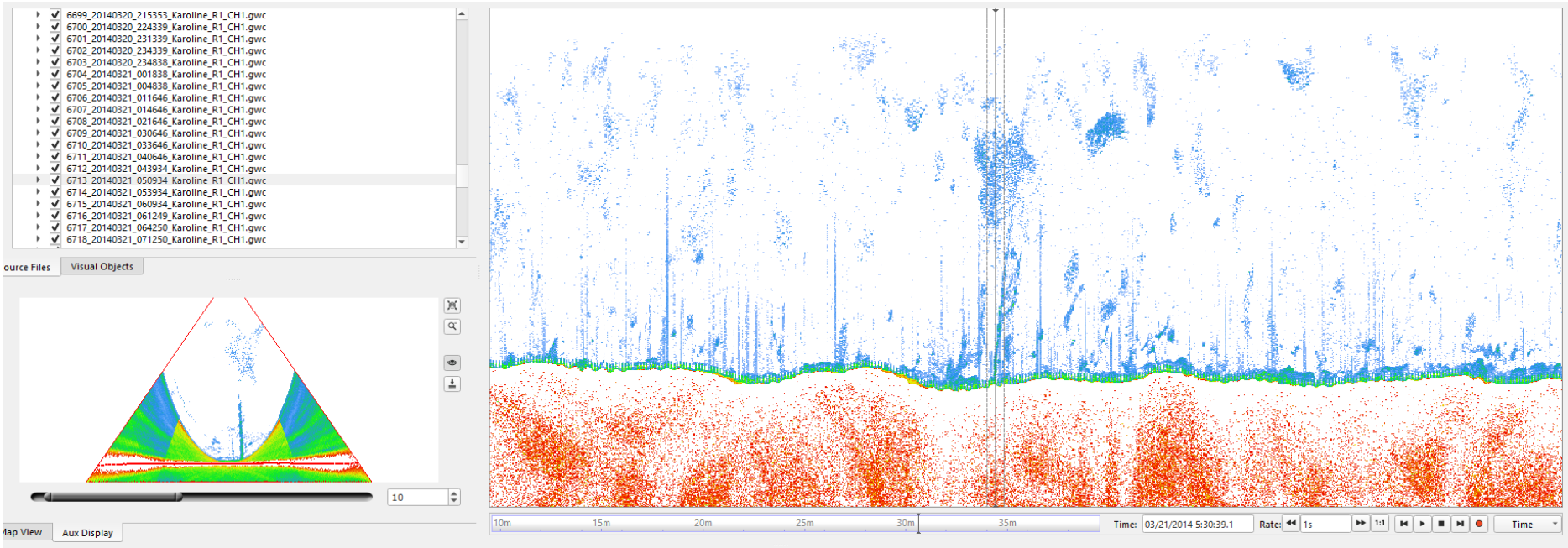

Figure 27. Gas flare from line 6713 showed on Fan view and stack view. Magnitude 3, Confidence 70%.

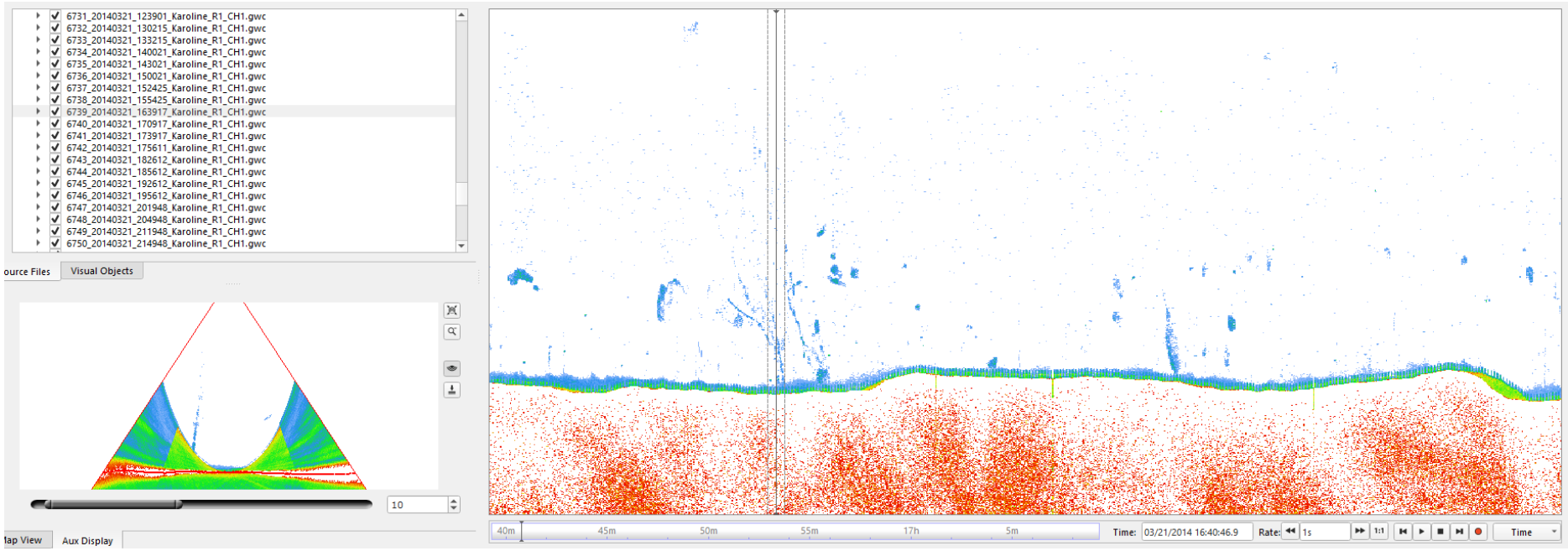

Figure 28. Gas flare from line 6739 showed on Fan view and stack view. Magnitude 3, Confidence 70%.

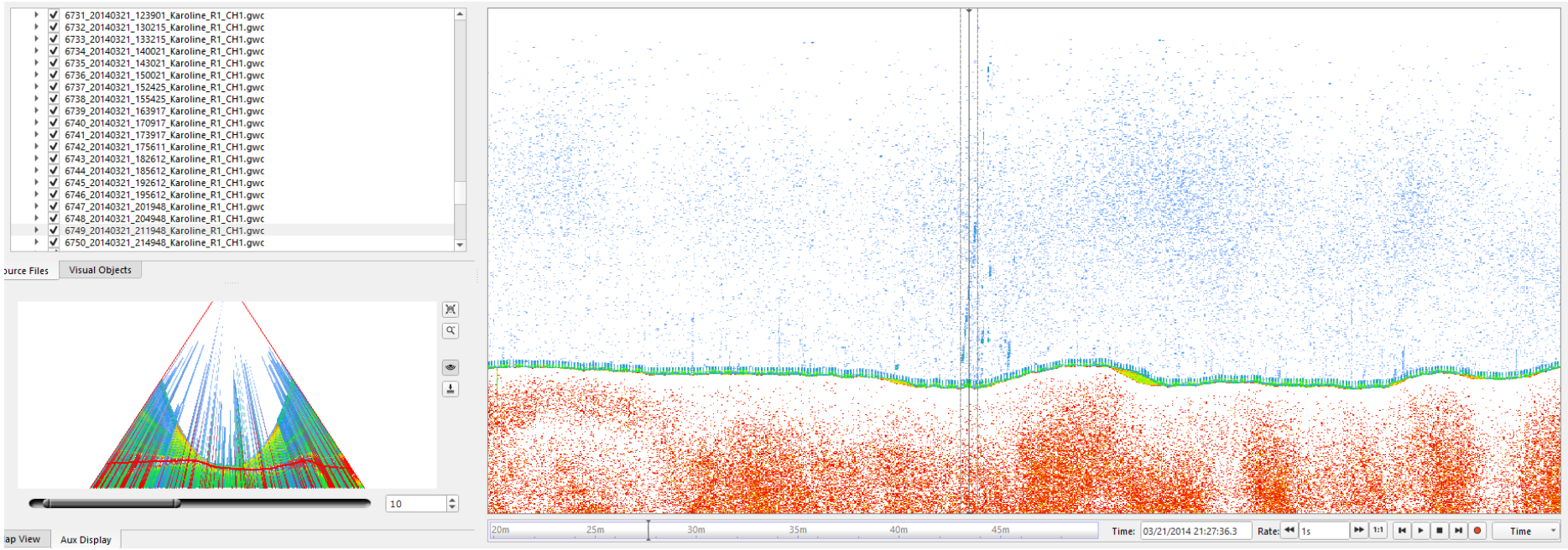

Figure 29. Gas flare from line 6749 showed on Fan view and stack view. Magnitude 3, Confidence 70%.

4.4.2 D21

The FOSAE-2013-D21 survey consists of 500 water column (*.wcd) survey lines. The data was loaded in Fledermaus Midwater along with navigation (*.all) and converted to GWC files. During conversion, it was observed that there was only 456 *.all files present. This resulted in no navigation for the 44 lines when converted to *.gwc format for analysis. The *.all file from the previous line are used to convert these *.wcd files for possible navigation loading. But only few lines were found to have navigation located in these lines. There was no flare found in the lines with missing navigation. 25 flares were found in the data of varying confidence level. The flares found are listed in Table 3. 36 lines were noisy and would have resulted in some weak flares missing. The flares identified are shown in Figures 30 – 51.

Table 3. Details of flares identified from Survey Area D21.

Survey	LineId	Latitude	Longitude	Depth	Height	Time	Magnitude	Confidence
FOSAE-2013-D21	5807	75.33887500	36.40383800	-162.00	80.00	01/20/2014 17:15:30.706	3	60
FOSAE-2013-D21	5808	75.39406400	36.40581600	-162.62	80.00	01/20/2014 17:39:31.605	2	30
FOSAE-2013-D21	5843	75.45289000	37.12747000	-175.65	75.00	01/21/2014 19:10:50.586	2	30
FOSAE-2013-D21	5860	75.44541300	37.23084600	-162.70	80.00	01/22/2014 6:27:10.128	3	50
FOSAE-2013-D21	5877	75.44186200	37.31967700	-165.07	70.00	01/22/2014 14:04:49.201	3	90
FOSAE-2013-D21	5877	75.44204000	37.31844400	-166.48	90.00	01/22/2014 14:04:42.844	3	90
FOSAE-2013-D21	5877	75.44231000	37.35852000	-165.33	55.00	01/22/2014 14:09:22.560	3	90
FOSAE-2013-D21	5877	75.44238400	37.35809500	-166.40	55.00	01/22/2014 14:09:19.381	3	90
FOSAE-2013-D21	5884	75.44539700	36.60533900	-171.14	30.00	01/22/2014 18:00:03.594	2	30
FOSAE-2013-D21	5904	75.44195100	37.31972400	-164.77	30.00	01/23/2014 3:01:31.320	2	60
FOSAE-2013-D21	5904	75.44207500	37.31860900	-166.09	120.00	01/23/2014 3:01:22.101	2	60
FOSAE-2013-D21	6002	75.41137200	37.13306700	-168.77	100.00	01/25/2014 5:15:32.456	3	70
FOSAE-2013-D21	6002	75.41195600	37.14176300	-168.83	50.00	01/25/2014 5:16:28.694	2	40
FOSAE-2013-D21	6090	75.38709900	36.87536500	-166.46	80.00	01/30/2014 9:24:55.989	2	30
FOSAE-2013-D21	6090	75.38740300	36.86353500	-165.14	80.00	01/30/2014 9:26:01.584	2	30
FOSAE-2013-D21	6090	75.38789000	36.72179600	-163.92	90.00	01/30/2014 9:40:29.589	3	30
FOSAE-2013-D21	6090	75.38849900	36.65057700	-165.31	100.00	01/30/2014 9:46:41.626	3	30
FOSAE-2013-D21	6091	75.38904500	36.61101300	-165.67	80.00	01/30/2014 9:51:43.600	3	30
FOSAE-2013-D21	6092	75.39217000	36.41909700	-161.91	100.00	01/30/2014 10:16:00.867	3	30
FOSAE-2013-D21	6093	75.39117200	36.20612700	-167.79	80.00	01/30/2014 11:12:54.384	3	30
FOSAE-2013-D21	6140	75.37627000	36.91898100	-170.55	110.00	01/31/2014 9:59:30.1	3	30
FOSAE-2013-D21	6141	75.37520700	37.01960500	-170.06	95.00	01/31/2014 10:13:13.7	3	30
FOSAE-2013-D21	6284	75.34083700	36.41897900	-160.09	90.00	39:04.5	3	60
FOSAE-2013-D21	6284	75.34244300	36.41601800	-158.48	120.00	38:45.8	3	60
FOSAE-2013-D21	6298	75.33759200	36.50392800	-162.57	80.00	20:18.1	3	70

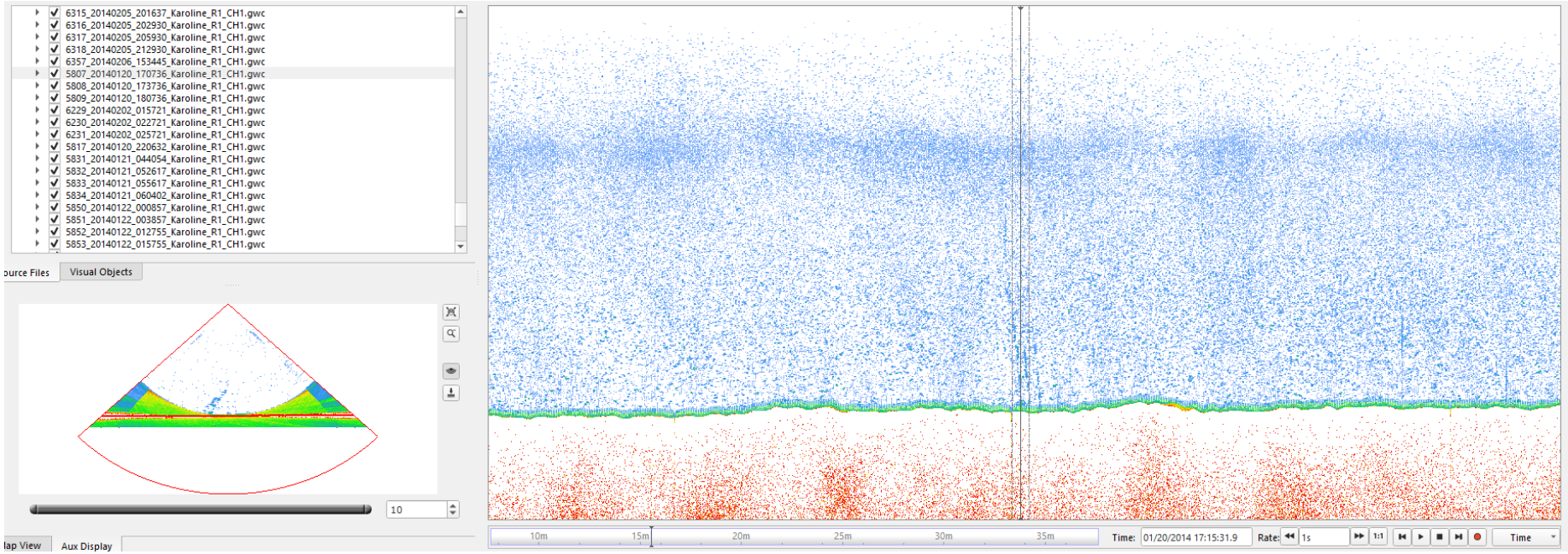

Figure 30. Gas flare from line 5807 showed on Fan view and stack view. Magnitude 3, Confidence 60%.

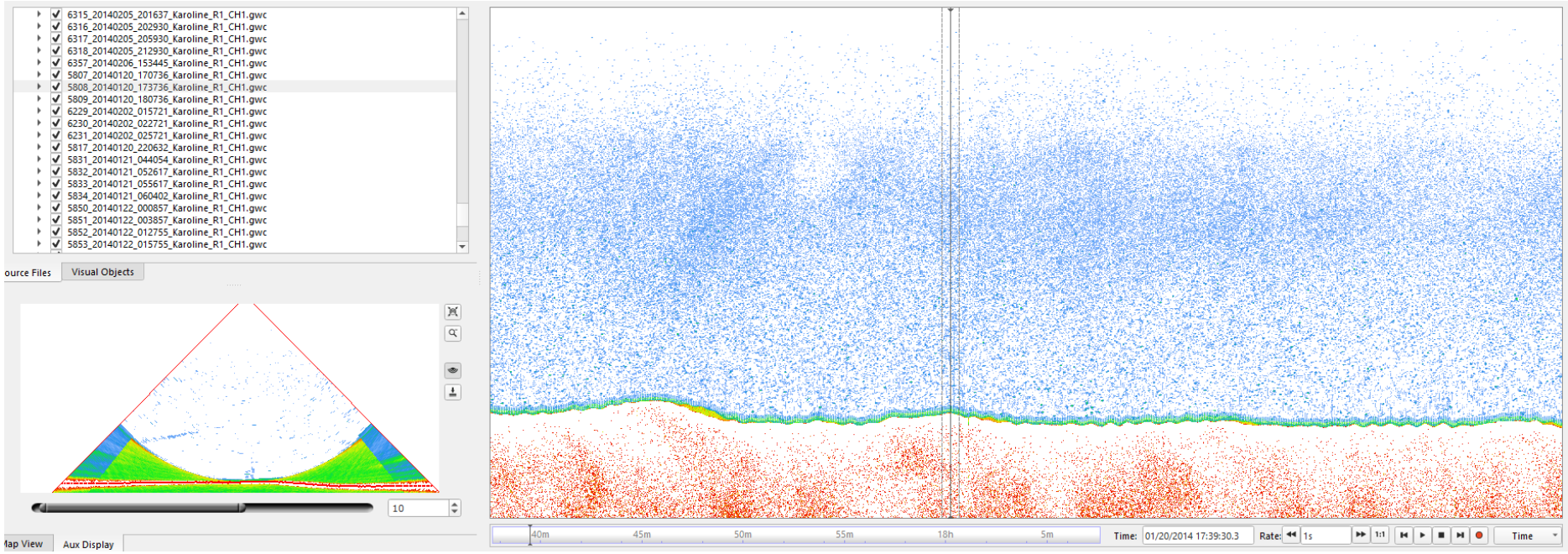

Figure 31. Possible gas flare from line 5808 showed on Fan view and stack view. Magnitude 2, Confidence 30%.

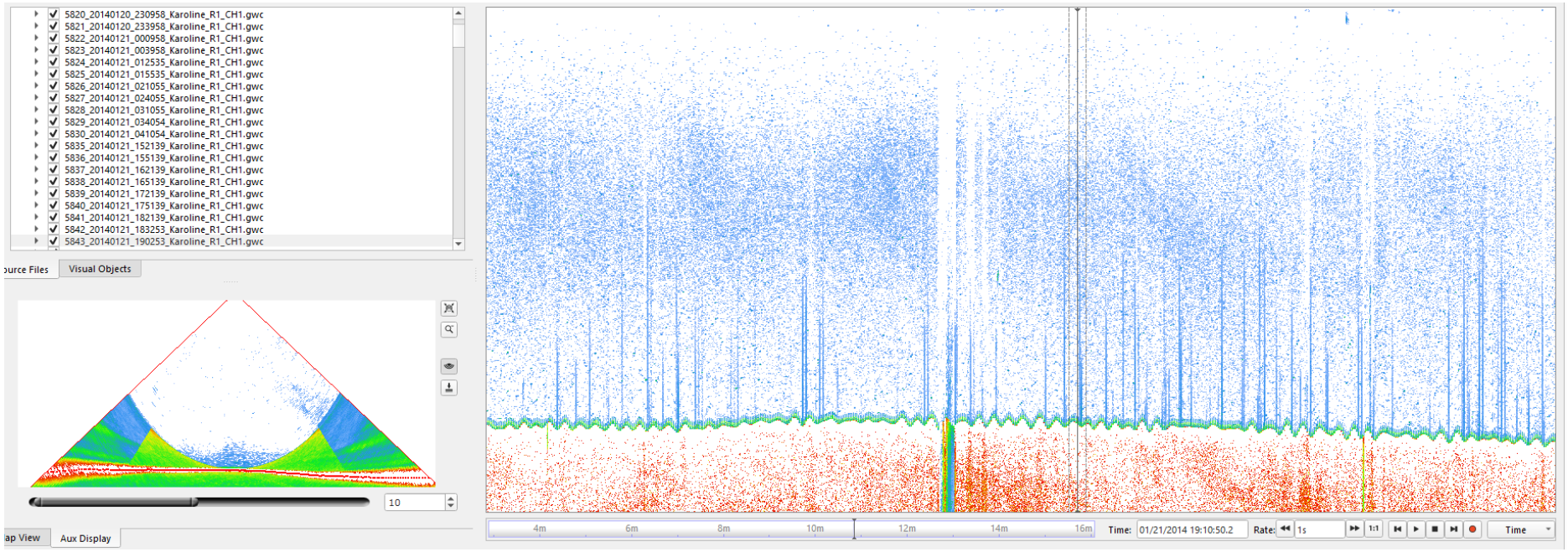

Figure 32. Possible gas flare from line 5843 showed on Fan view and stack view. Magnitude 2, Confidence 30%.

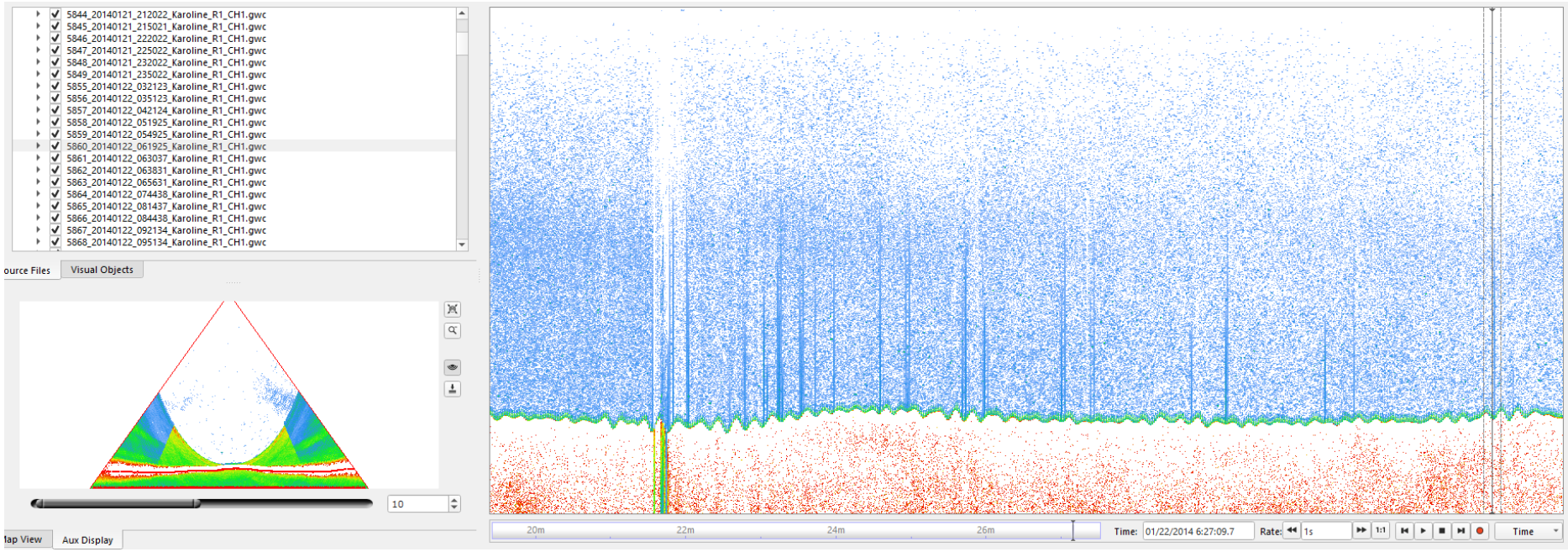

Figure 33. Gas flare from line 5860 showed on Fan view and stack view. Magnitude 3, Confidence 50%.

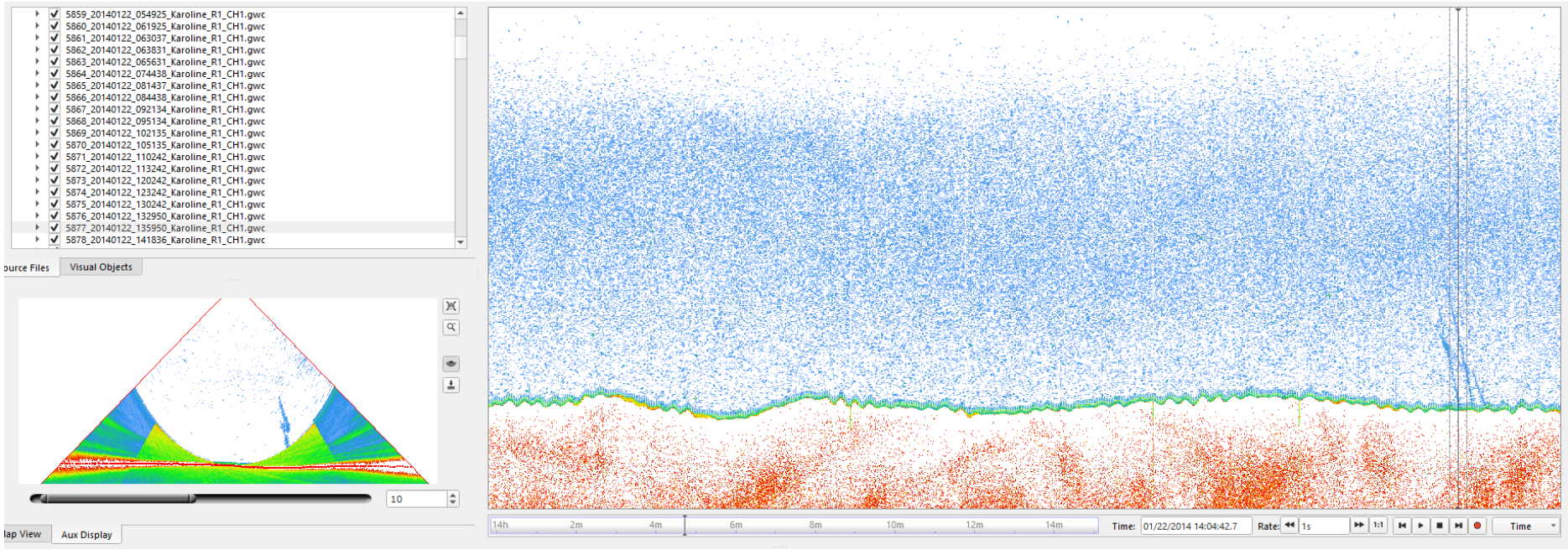

Figure 34. Gas flare from line 5877 showed on Fan view and stack view. Magnitude 3, Confidence 90%.

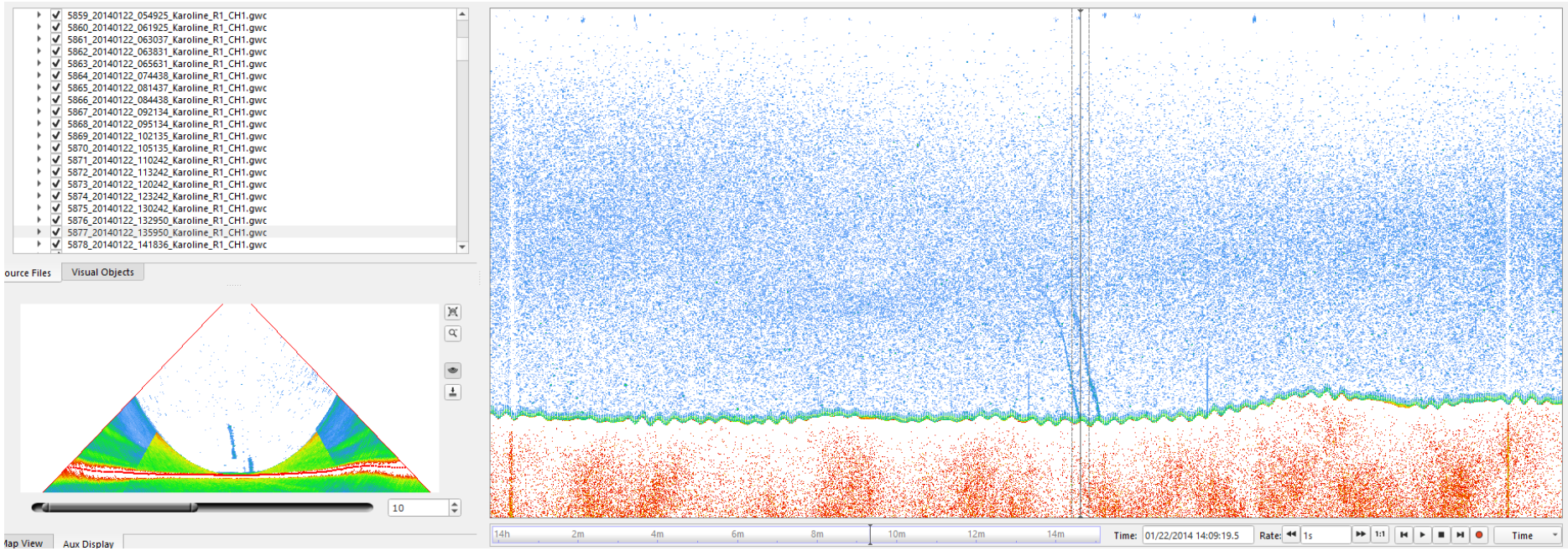

Figure 35. Gas flare from line 5877 showed on Fan view and stack view. Magnitude 3, Confidence 90%.

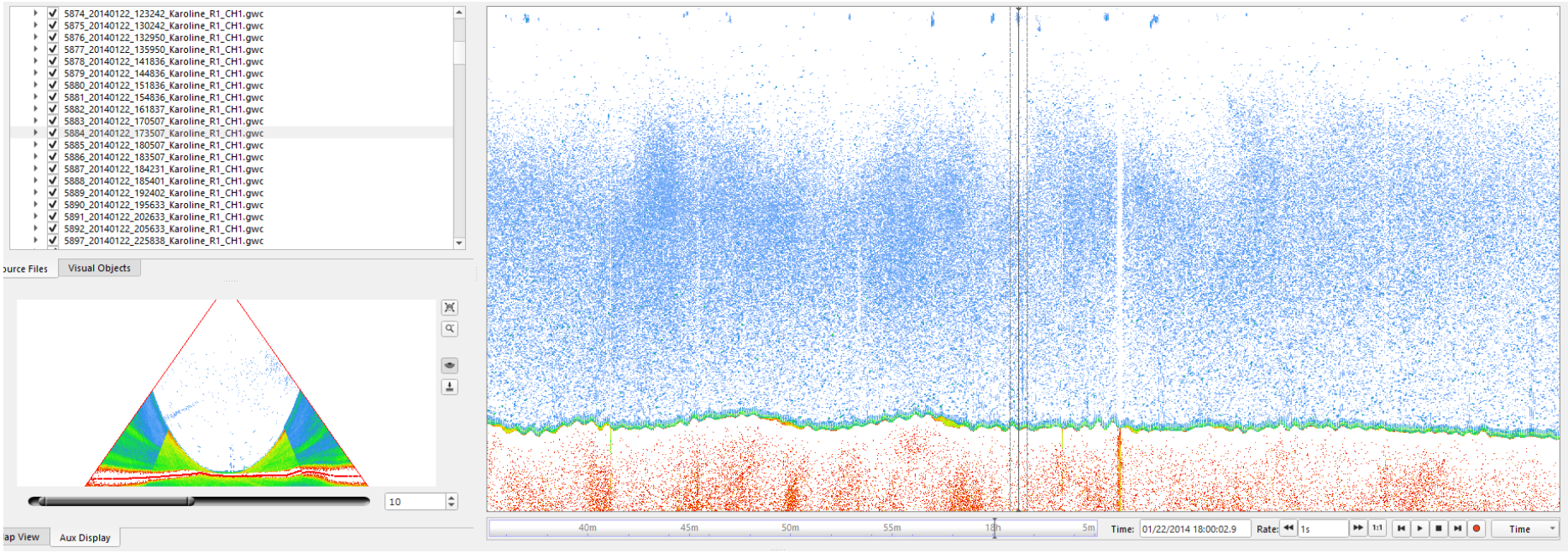

Figure 36. Possible gas flare from line 5884 showed on Fan view and stack view. Magnitude 2, Confidence 30%.

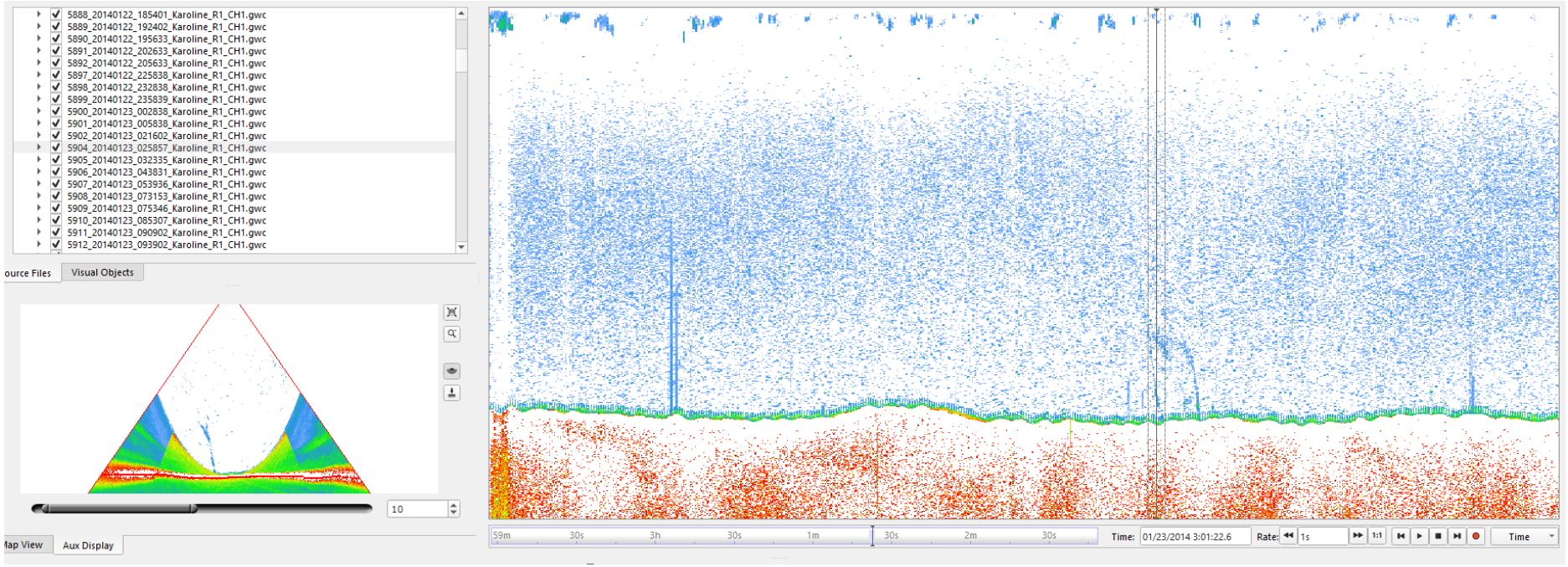

Figure 37. Gas flare from line 5904 showed on Fan view and stack view. 1:1 display not possible. Magnitude 2, Confidence 60%.

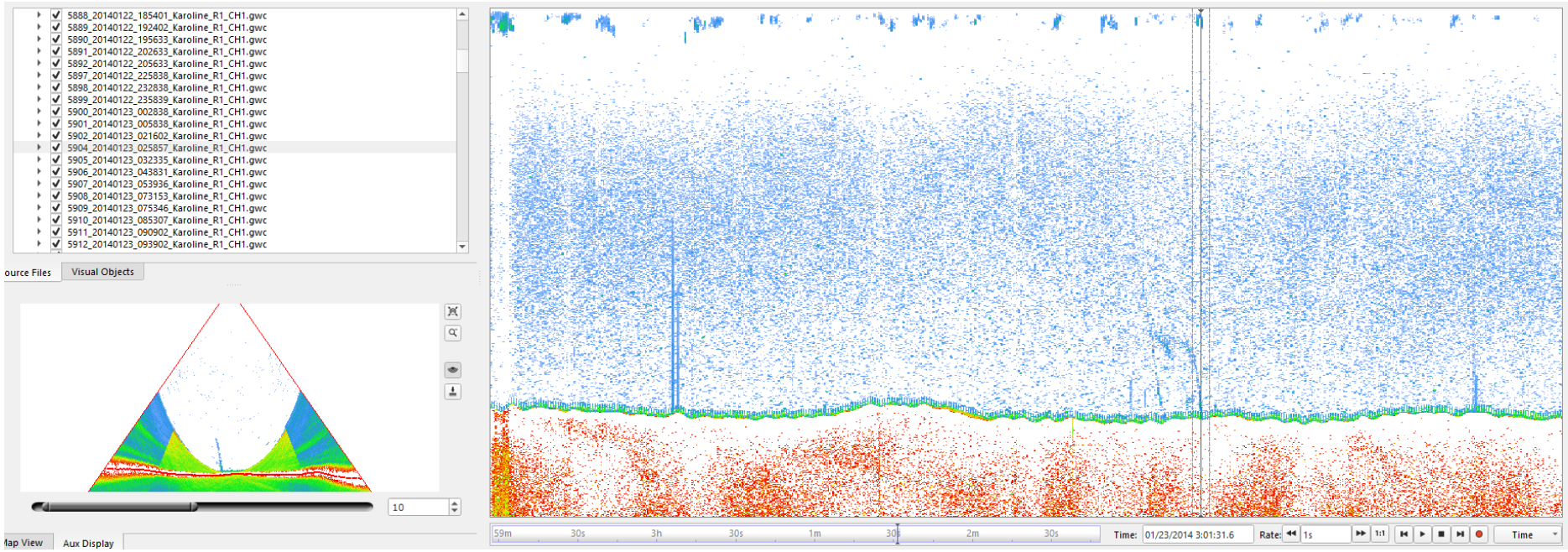

Figure 38. Gas flare from line 5904 showed on Fan view and stack view. Magnitude 2, Confidence 60%.

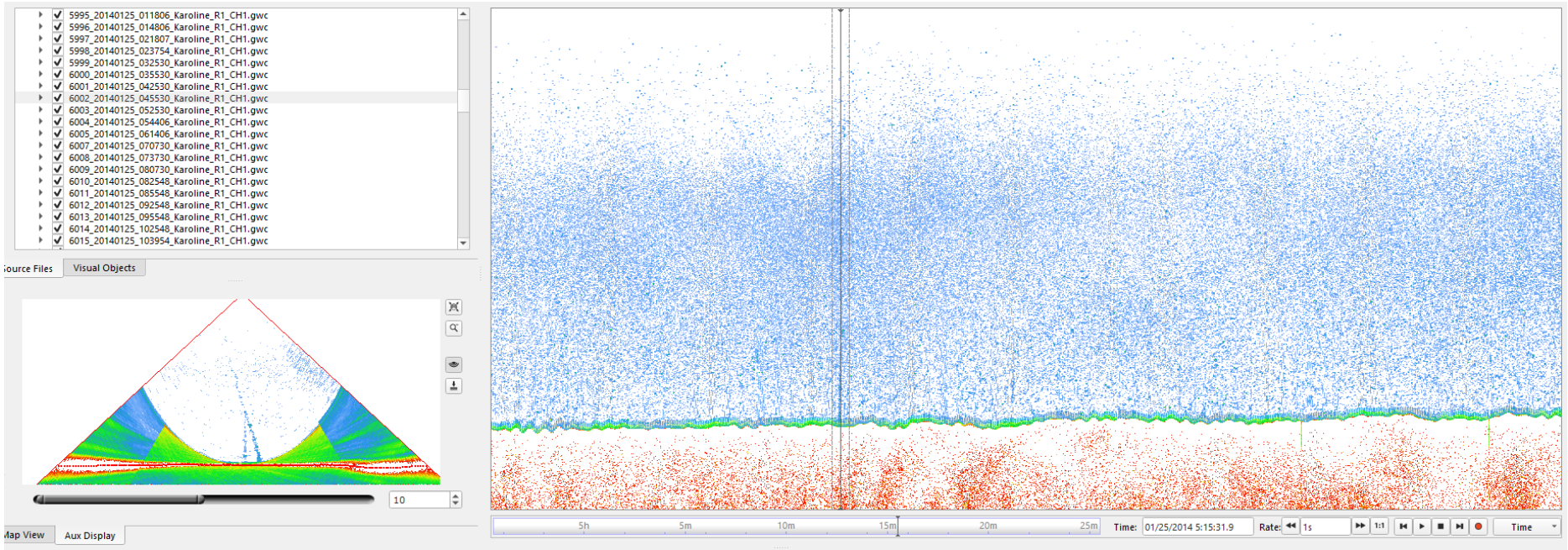

Figure 39. Gas flare from line 6002 showed on Fan view and stack view. Magnitude 3, Confidence 70%.

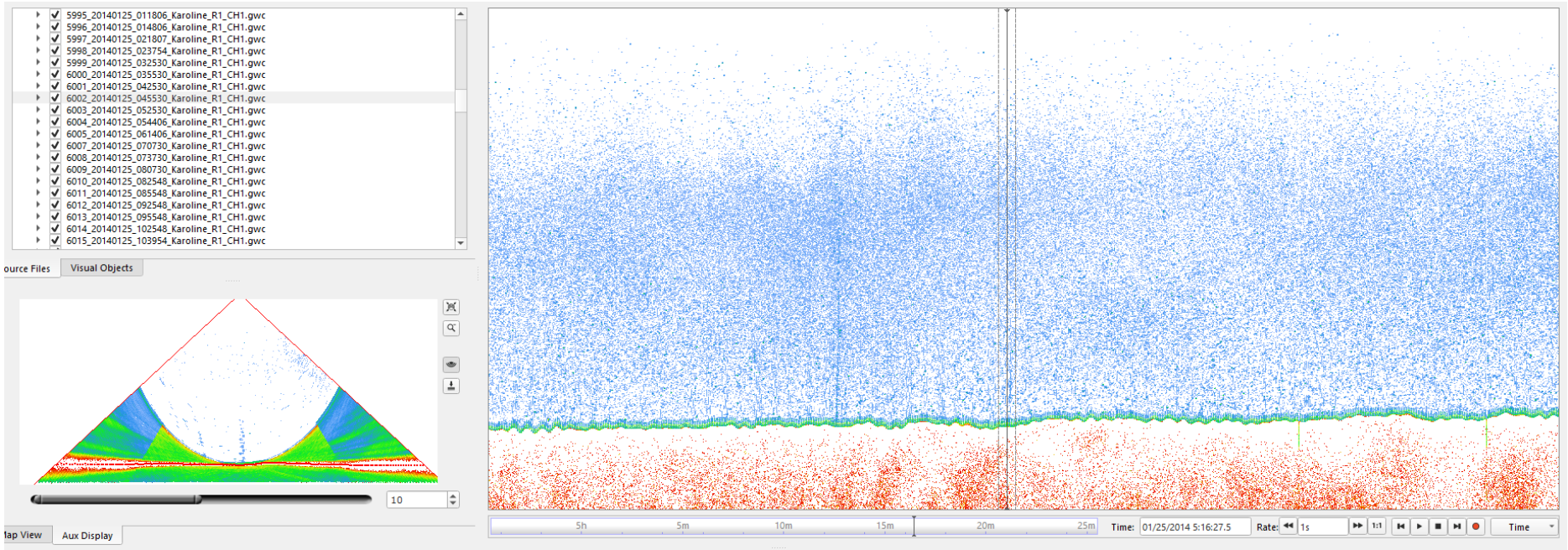

Figure 40. Possible gas flare from line 6002 showed on Fan view and stack view. Magnitude 2, Confidence 40%.

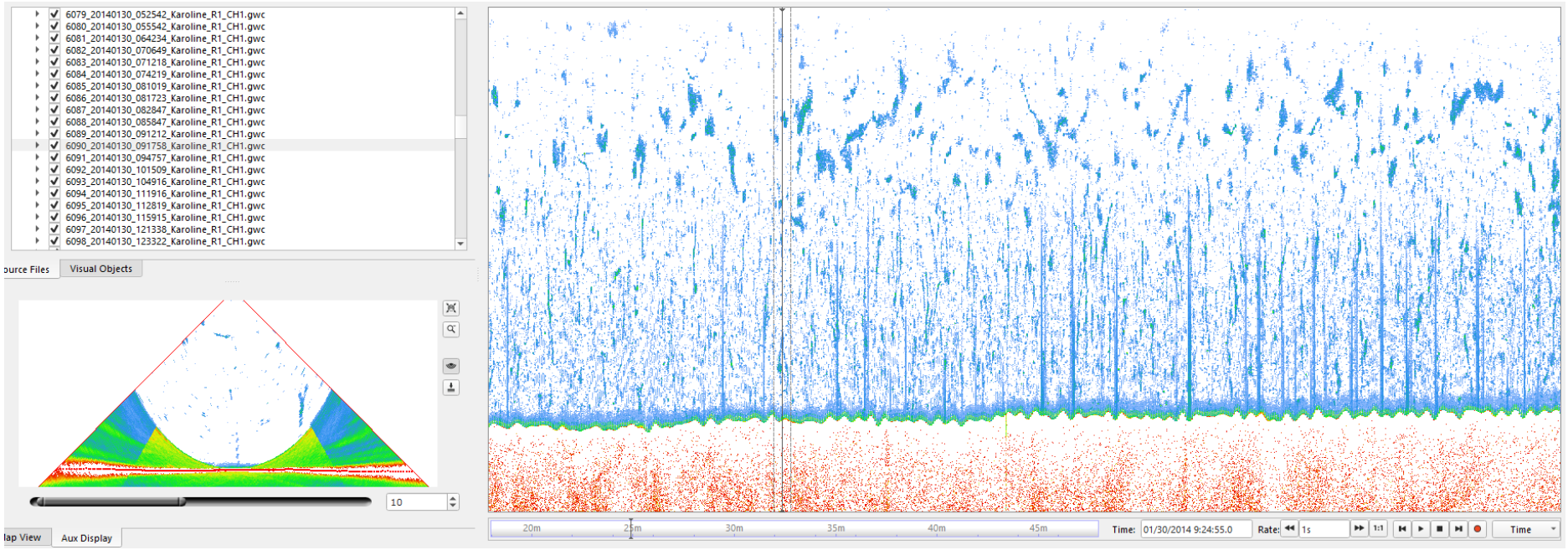

Figure 41. Possible gas flare from line 6090 showed on Fan view and stack view. Magnitude 2, Confidence 30%.

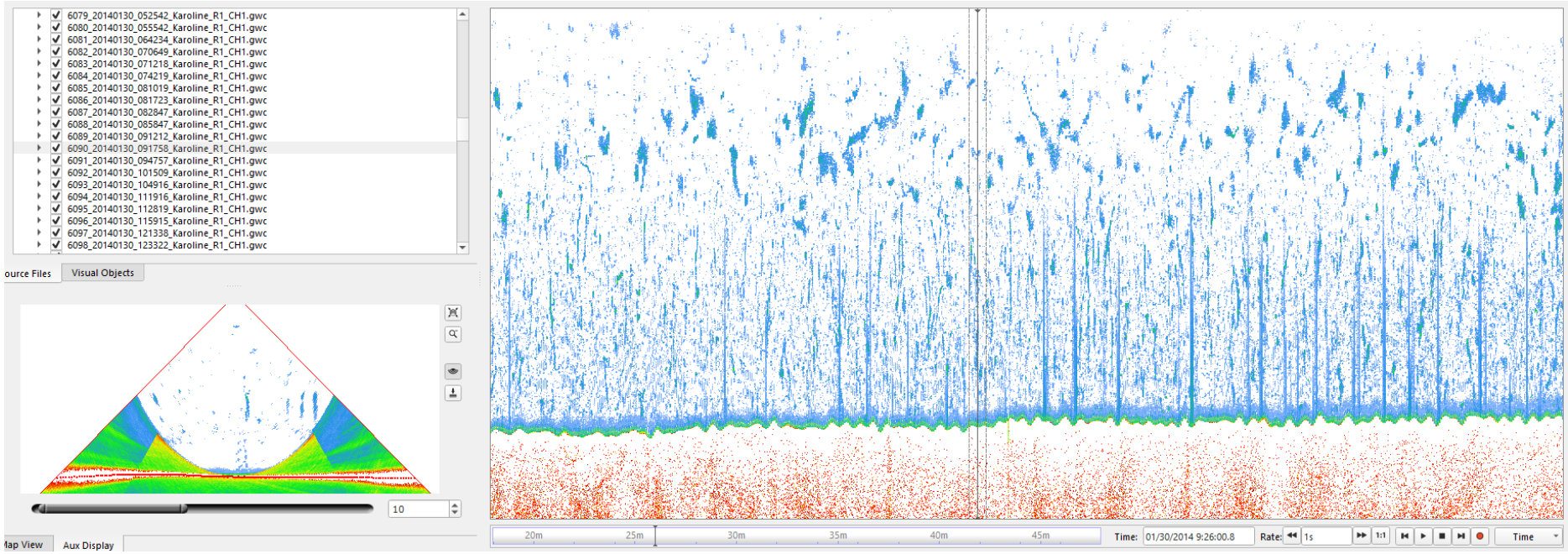

Figure 42. Possible gas flare from line 6090 showed on Fan view and stack view. Magnitude 2, Confidence 30%.

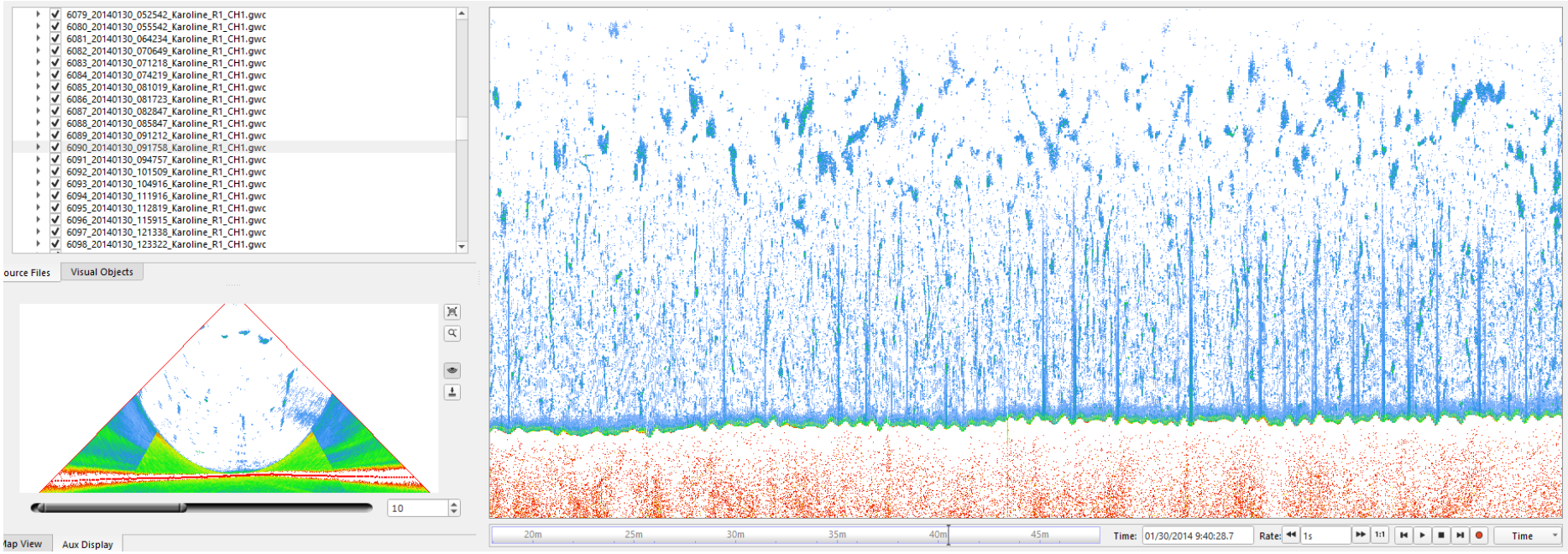

Figure 43. Possible gas flare from line 6090 showed on Fan view and stack view. Magnitude 3, Confidence 30%.

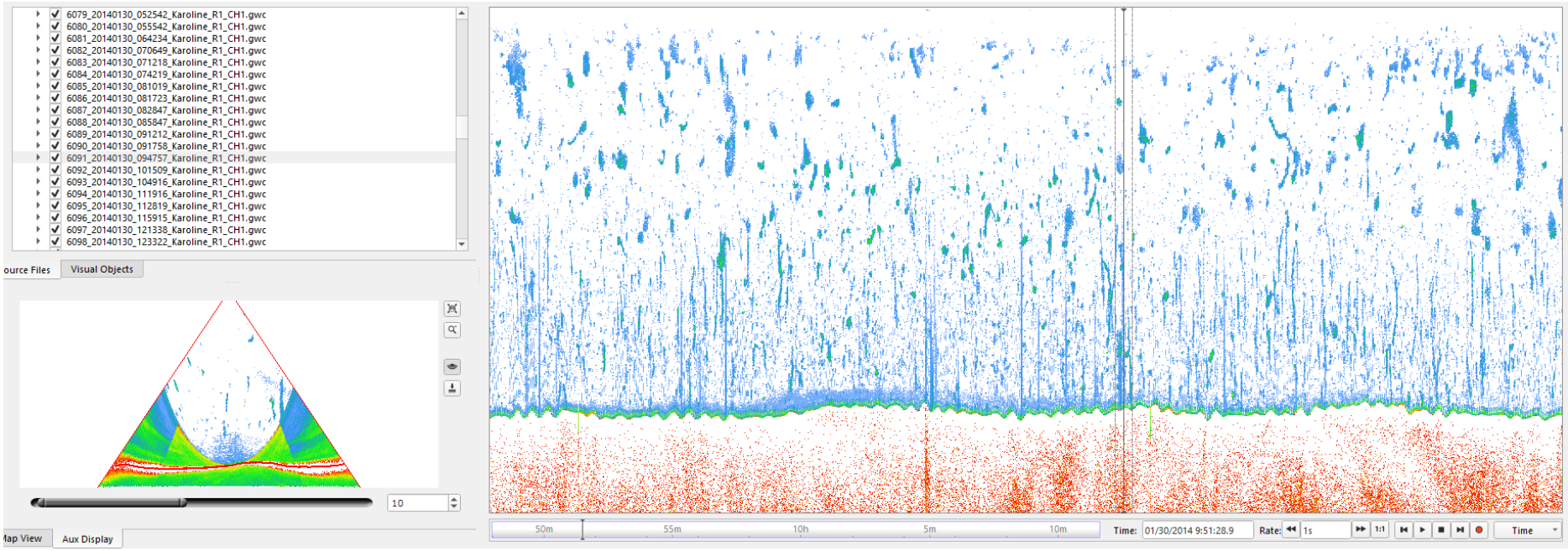

Figure 44. Possible gas flare from line 6091 showed on Fan view and stack view. Magnitude 3, Confidence 30%.

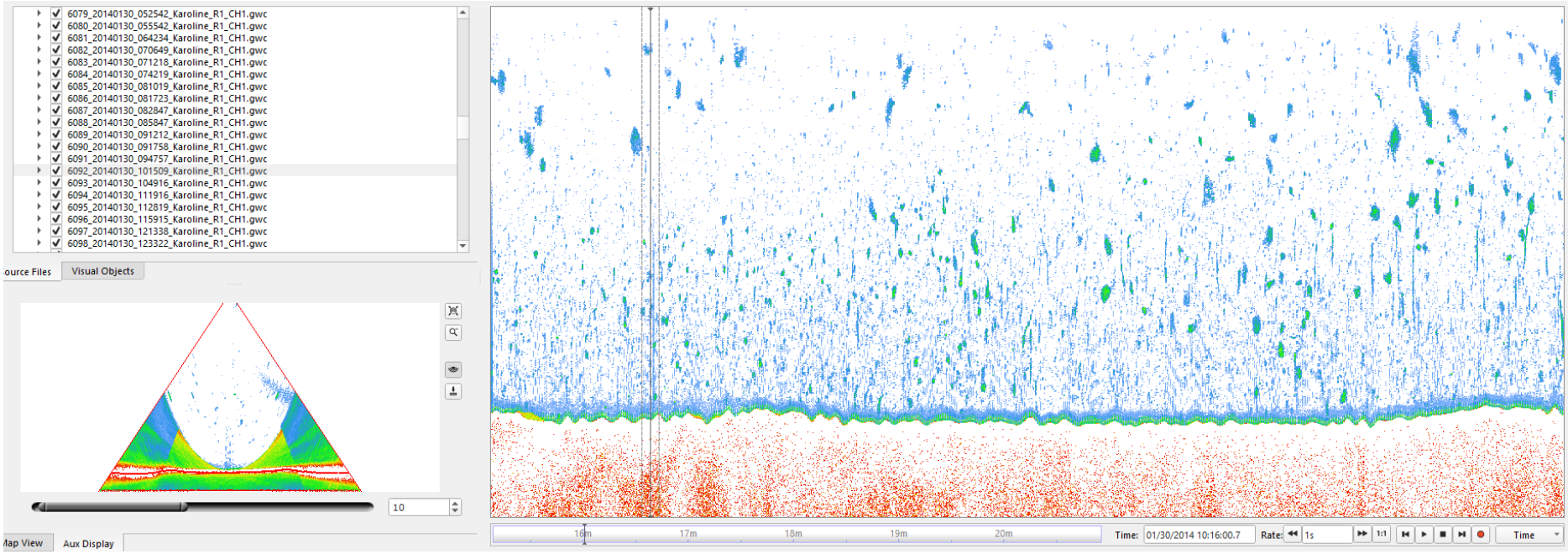

Figure 45. Possible gas flare from line 6092 showed on Fan view and stack view. Magnitude 3, Confidence 30%.

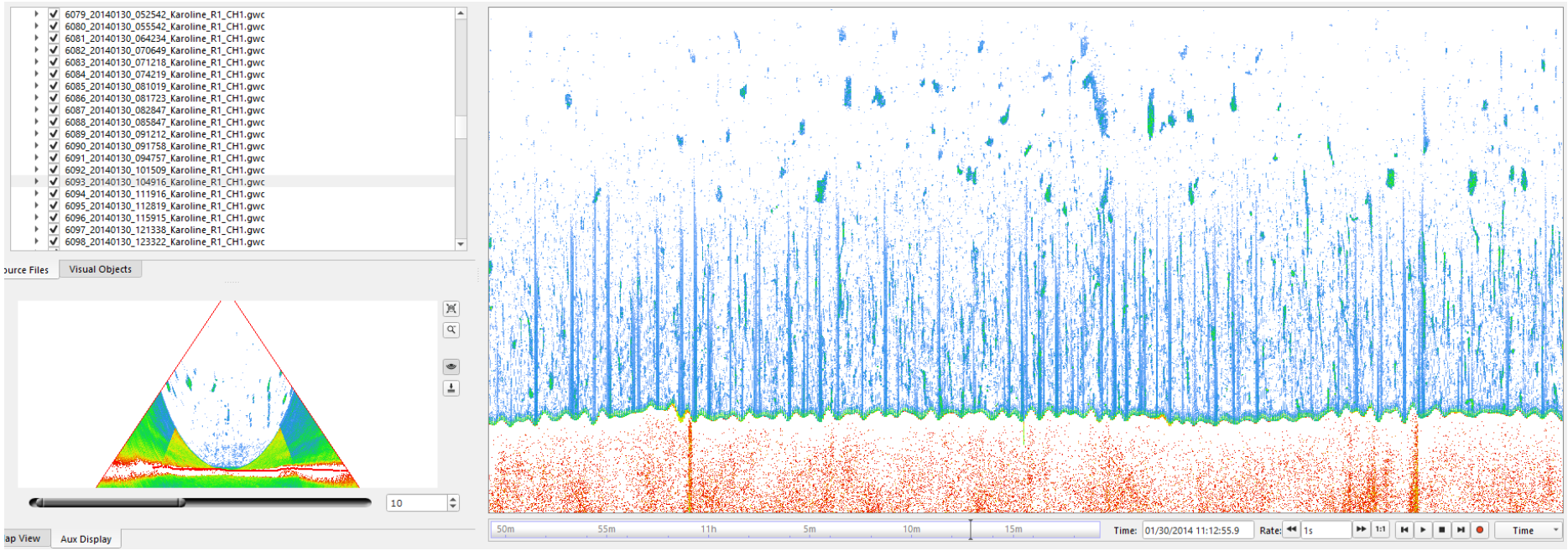

Figure 46. Possible gas flare from line 6093 showed on Fan view and stack view. Magnitude 3, Confidence 30%.

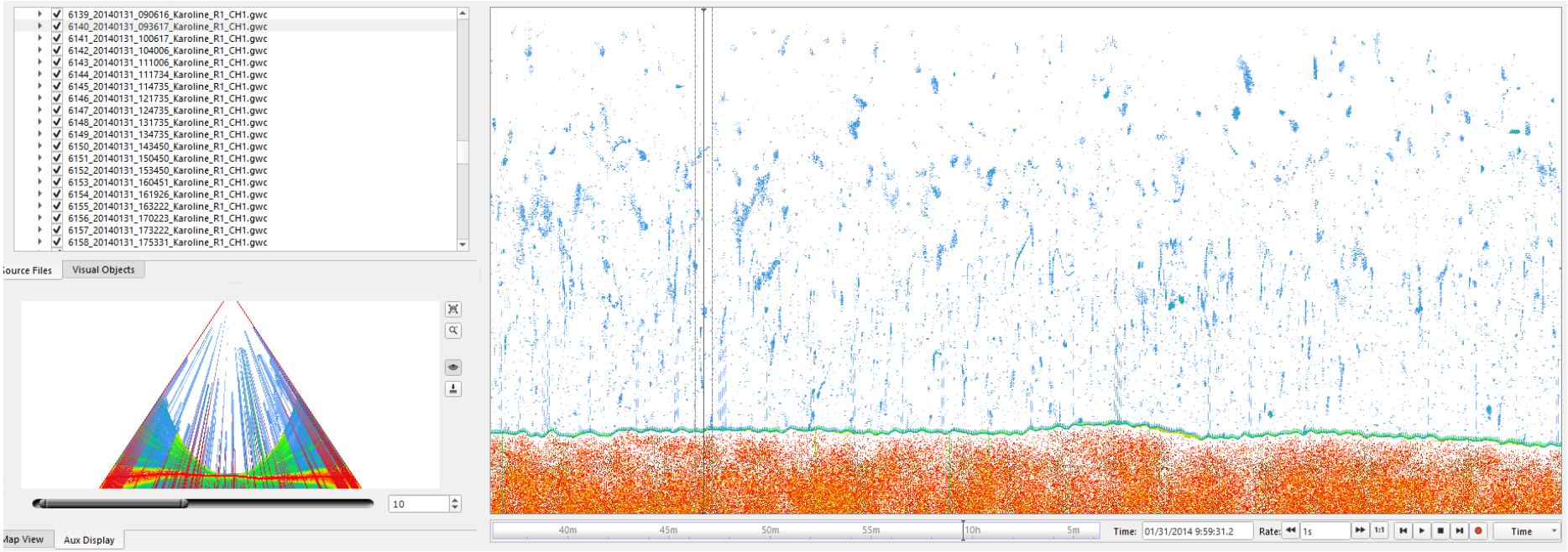

Figure 47. Possible gas flare from line 6140 showed on Fan view and stack view. Magnitude 3, Confidence 30%.

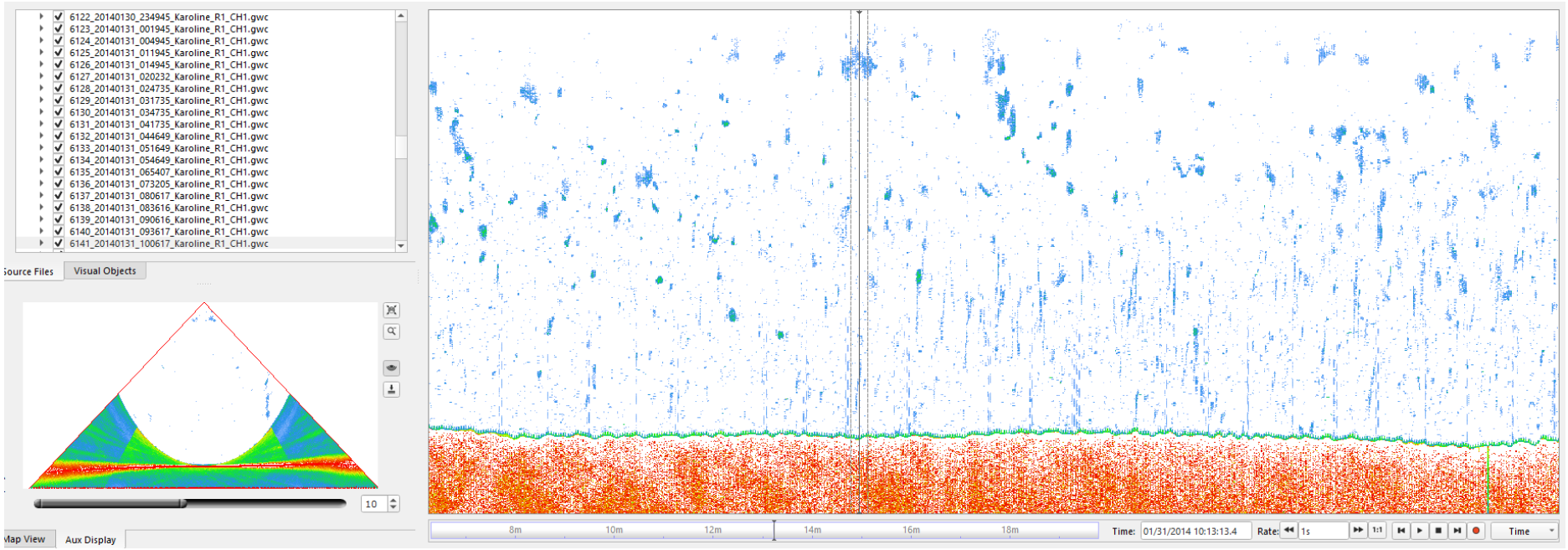

Figure 48. Possible gas flare from line 6141 showed on Fan view and stack view. Magnitude 3, Confidence 30%.

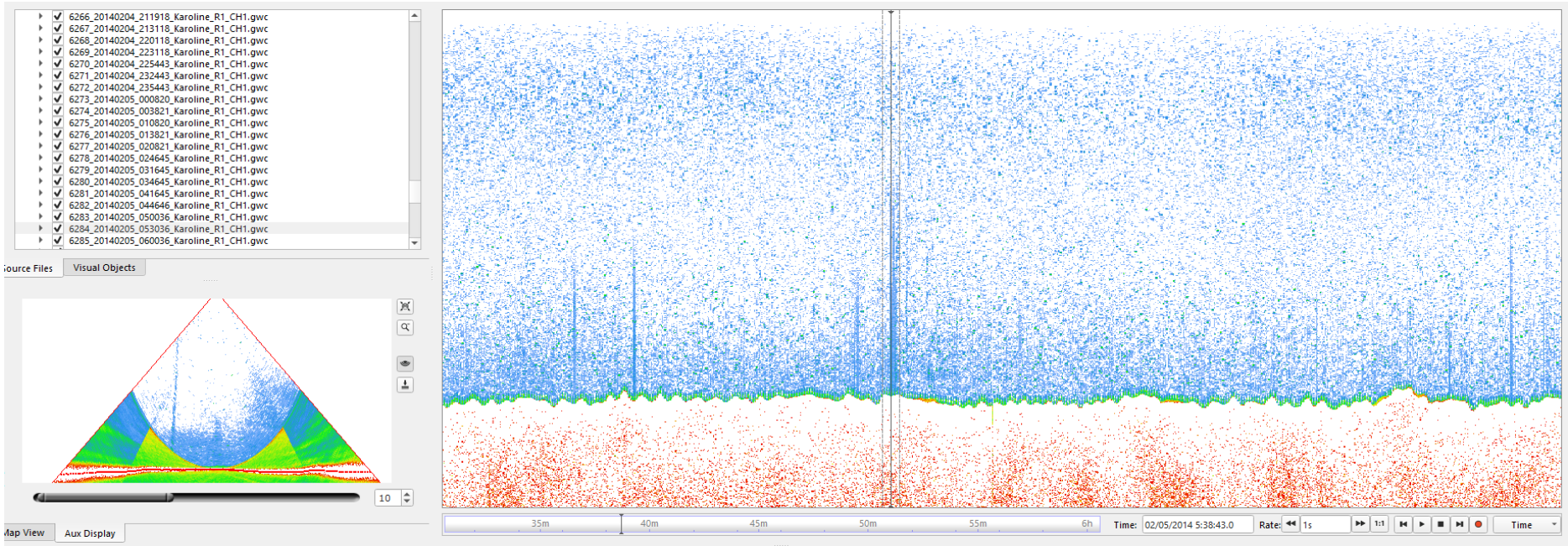

Figure 49. Gas flare from line 6284 showed on Fan view and stack view. Magnitude 3, Confidence 60%.

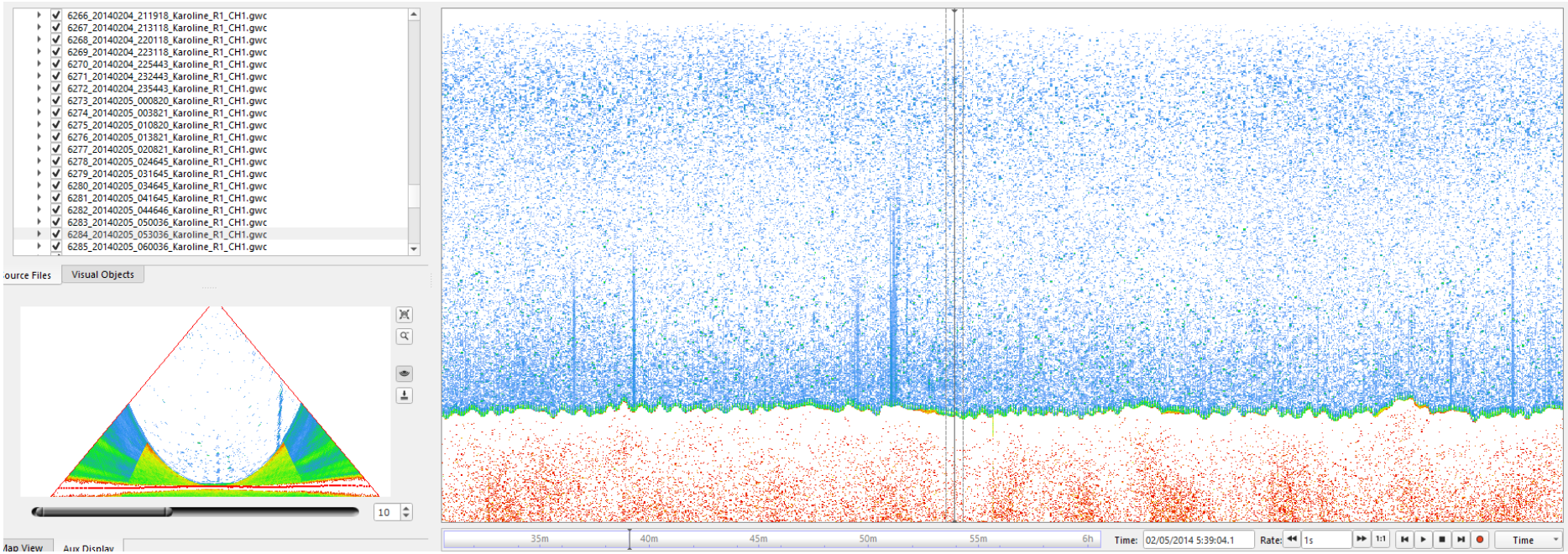

Figure 50. Gas flare from line 6284 showed on Fan view and stack view. Magnitude 3, Confidence 60%.

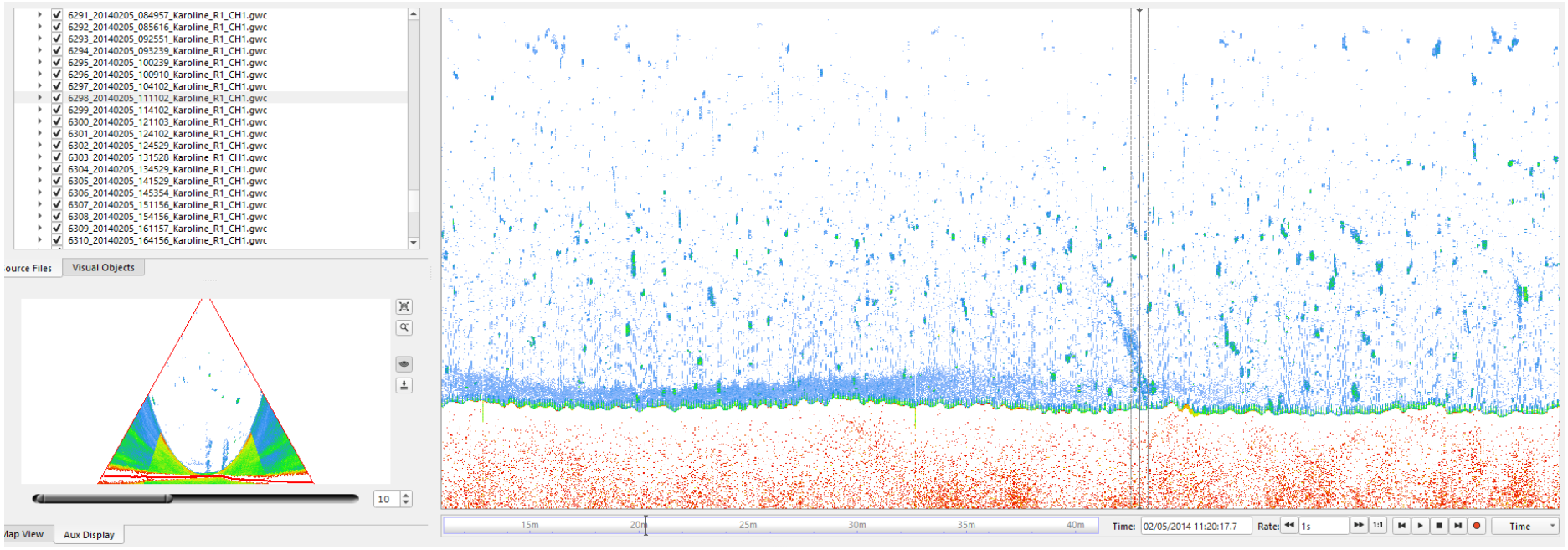

Figure 51. Gas flare from line 6298 showed on Fan view and stack view. Magnitude 3, Confidence 70%.

4.4.3 D23

The FOSAE-2013-D23 survey consists of 754 water column (*.wcd) survey lines. The data was loaded in Fledermaus Midwater along with navigation (*.all) and converted to GWC files. During conversion, it was observed that there was only 706 *.all files present. This resulted in no navigation for the 48 lines when converted to *.gwc format for analysis. The *.all file from the previous line are used to convert these *.wcd files for possible navigation loading. But only few lines were found to have navigation located in these lines. There was no flare found in the lines with missing navigation. 41 flares were found in the data of varying confidence level. The flares found are listed in Table 4. 284 lines were noisy and would have resulted in some weak flares missing. The flares identified are shown in Figs. 52 – 92.

Table 4. Details of flares identified from Survey Area D23.

Survey	LineId	Latitude	Longitude	Depth	Height	Time	Magnitude	Confidence
FOSAE-2013-D23	1665	75.62789400	37.71308300	-190.95	50.00	07/23/2013 20:01:28.7	2	40
FOSAE-2013-D23	1679	75.62117800	37.43606000	-178.11	50.00	07/24/2013 2:27:21.9	3	30
FOSAE-2013-D23	1679	75.62399500	37.42259900	-180.99	60.00	07/24/2013 2:25:30.9	3	30
FOSAE-2013-D23	1681	75.62061300	37.23962800	-176.89	50.00	07/24/2013 3:39:35.0	3	30
FOSAE-2013-D23	1681	75.62343300	37.20130300	-176.34	50.00	07/24/2013 3:45:22.5	3	30
FOSAE-2013-D23	1683	75.62364900	36.98807400	-197.56	60.00	07/24/2013 4:20:26.8	3	30
FOSAE-2013-D23	3144	75.62649300	36.93815900	-188.05	75.00	08/22/2013 17:42:06.7	2	30
FOSAE-2013-D23	3599	75.61810700	37.62763300	-186.62	45.00	07:20.5	2	30
FOSAE-2013-D23	3606	75.61955300	37.23262100	-178.40	40.00	37:32.2	3	30
FOSAE-2013-D23	3662	75.60901700	36.95689700	-201.52	45.00	09/15/2013 5:31:43.3	3	30
FOSAE-2013-D23	3679	75.60631200	37.06072900	-185.30	60.00	09/16/2013 2:19:14.5	3	30
FOSAE-2013-D23	3684	75.60671700	36.31882500	-157.51	55.00	09/16/2013 5:01:26.2	4	30

FOSAE-2013-D23	3691	75.60071400	37.31527900	-179.27	50.00	09/16/2013 8:34:30.8	4	30
FOSAE-2013-D23	3695	75.60470500	36.36720200	-160.76	45.00	09/16/2013 10:20:13.0	4	30
FOSAE-2013-D23	3706	75.59067000	37.65196500	-183.99	40.00	09/16/2013 15:01:19	3	30
FOSAE-2013-D23	3732	75.59704300	36.54998900	-174.03	60.00	09/17/2013 1:54:56	2	30
FOSAE-2013-D23	3737	75.59774100	36.37563700	-159.37	50.00	09/17/2013 3:09:59	3	30
FOSAE-2013-D23	3740	75.59815300	36.18053700	-156.43	40.00	09/17/2013 4:23:33	4	30
FOSAE-2013-D23	3748	75.59480700	37.39820200	-186.10	50.00	09/17/2013 7:28:19	3	30
FOSAE-2013-D23	3767	75.58813400	36.88681900	-193.84	70.00	09/17/2013 16:30:35	2	30
FOSAE-2013-D23	3803	75.59100600	36.73469700	-73.20	70.00	09/18/2013 14:15:55	3	30
FOSAE-2013-D23	3826	75.57217900	37.51076100	-170.95	70.00	09/18/2013 22:32:17	4	80
FOSAE-2013-D23	3826	75.57246200	37.51395700	-172.06	100.00	09/18/2013 22:32:37	3	80
FOSAE-2013-D23	3826	75.57308600	37.52131800	-175.41	100.00	09/18/2013 22:33:23	2	70
FOSAE-2013-D23	3826	75.57348400	37.52553700	-173.42	100.00	09/18/2013 22:33:49	2	60
FOSAE-2013-D23	3861	75.56760000	36.64154900	-189.56	60.00	09/19/2013 14:47:41	4	30
FOSAE-2013-D23	3863	75.56382200	37.35832300	-171.09	45.00	09/19/2013 16:33:51	2	30
FOSAE-2013-D23	3865	75.56217100	37.35307300	-172.46	65.00	09/19/2013 17:32:17	3	60
FOSAE-2013-D23	3876	75.56082100	37.34085600	-169.89	95.00	09/19/2013 22:50:29.7	2	60
FOSAE-2013-D23	3900	75.55661200	37.32716400	-168.18	60.00	09/20/2013 9:38:11.7	2	60
FOSAE-2013-D23	3904	75.55292800	36.75266400	-178.42	50.00	09/20/2013 11:24:40.2	4	40
FOSAE-2013-D23	3912	75.54933800	37.11934100	-176.71	65.00	09/20/2013 15:40:38.3	4	40
FOSAE-2013-D23	3913	75.54860500	37.20606000	-166.93	80.00	09/20/2013 16:16:21.8	4	30
FOSAE-2013-D23	3992	75.53155800	36.87243600	-193.96	60.00	09/24/2013 14:52:20.7	3	30
FOSAE-2013-D23	4027	75.52170300	36.97690800	-183.47	40.00	09/25/2013 5:30:28.6	3	30
FOSAE-2013-D23	4043	75.51991600	36.14925900	-166.22	50.00	09/25/2013 13:53:08.6	4	30
FOSAE-2013-D23	4095	75.50654500	36.22829300	-166.47	50.00	09/26/2013 13:00:37.8	4	40
FOSAE-2013-D23	4095	75.50675000	36.17980600	-164.14	55.00	09/26/2013 13:05:55.2	4	30
FOSAE-2013-D23	4155	75.49709000	36.43704600	-177.06	65.00	09/27/2013 14:57:41.0	3	30
FOSAE-2013-D23	4220	75.48431400	36.19642700	-166.23	50.00	09/28/2013 20:37:23.3	3	60
FOSAE-2013-D23	4259	75.46745100	37.09405100	-169.02	70.00	09/29/2013 14:06:25.0	4	40

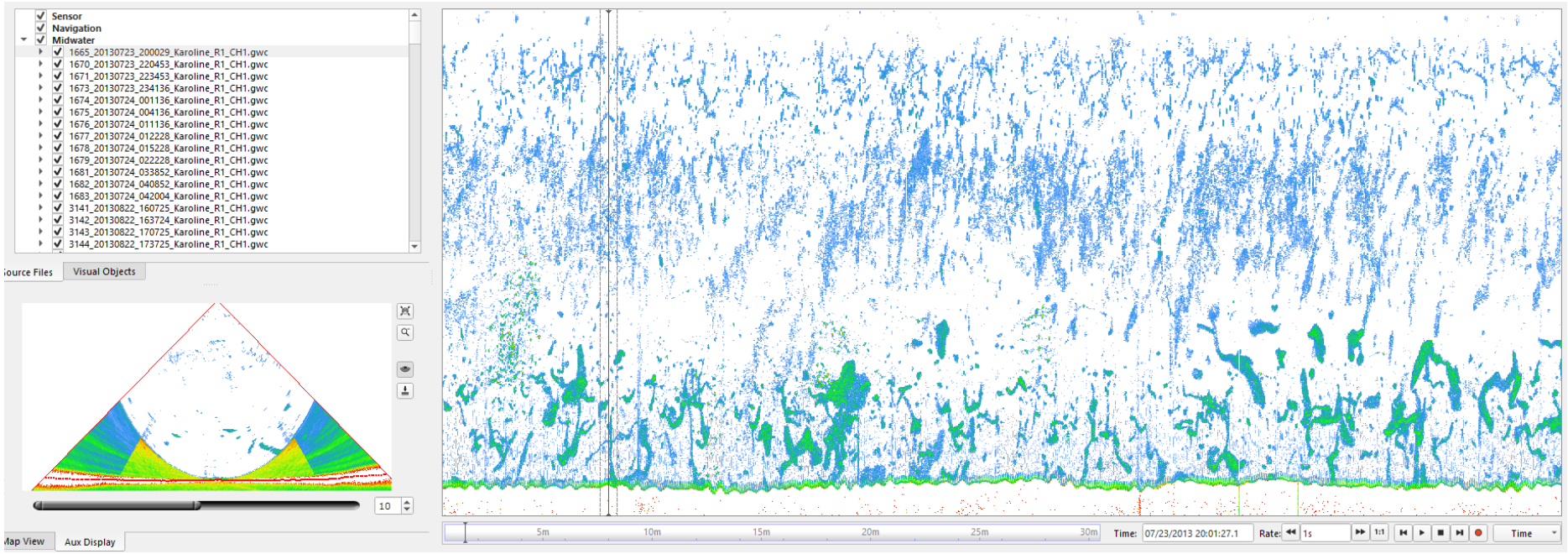

Figure 52. Possible gas flare from line 1665 showed on Fan view and stack view. Magnitude 2, Confidence 40%.

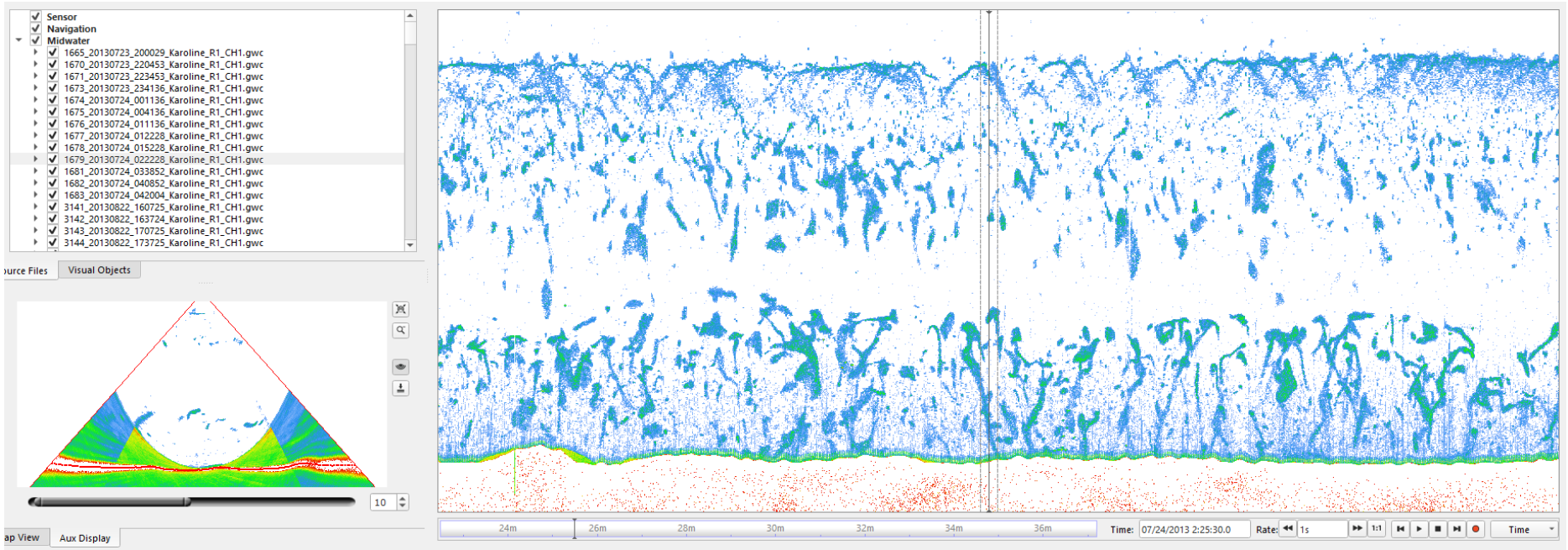

Figure 53. Possible gas flare from line 1679 showed on Fan view and stack view. Magnitude 3, Confidence 30%.

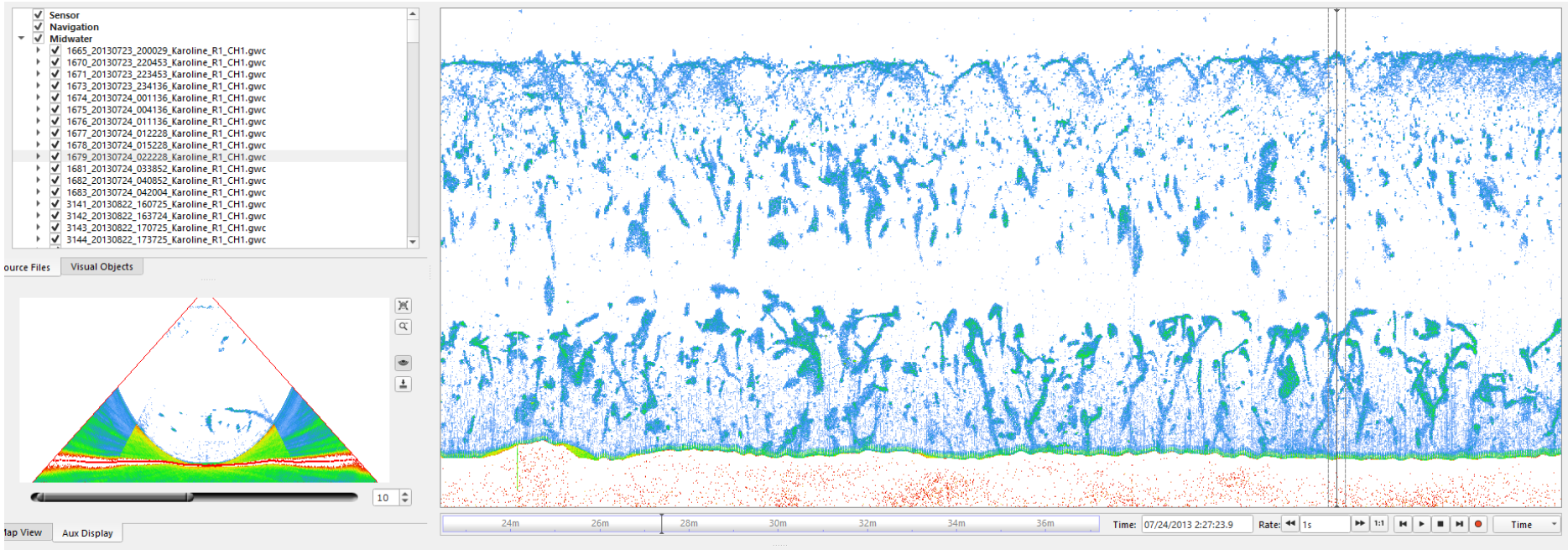

Figure 54. Possible gas flare from line 1679 showed on Fan view and stack view. Magnitude 3, Confidence 30%.

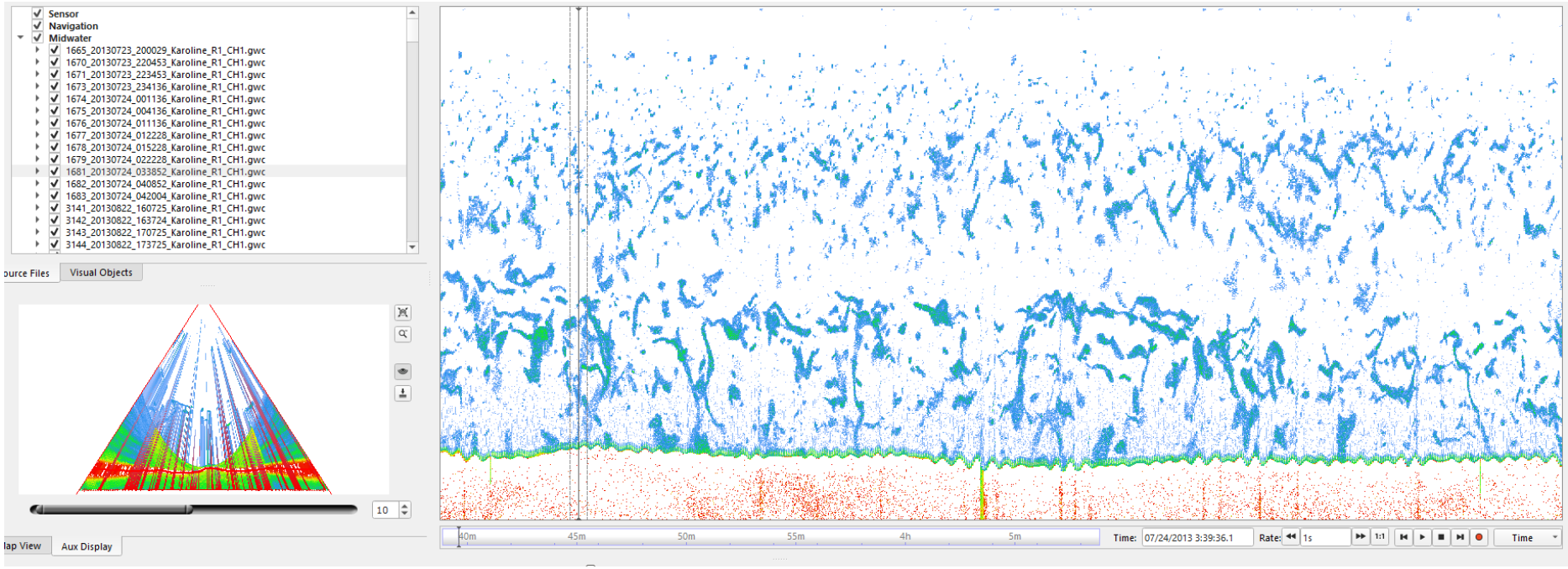

Figure 55. Possible gas flare from line 1681 showed on Fan view and stack view. Magnitude 3, Confidence 30%.

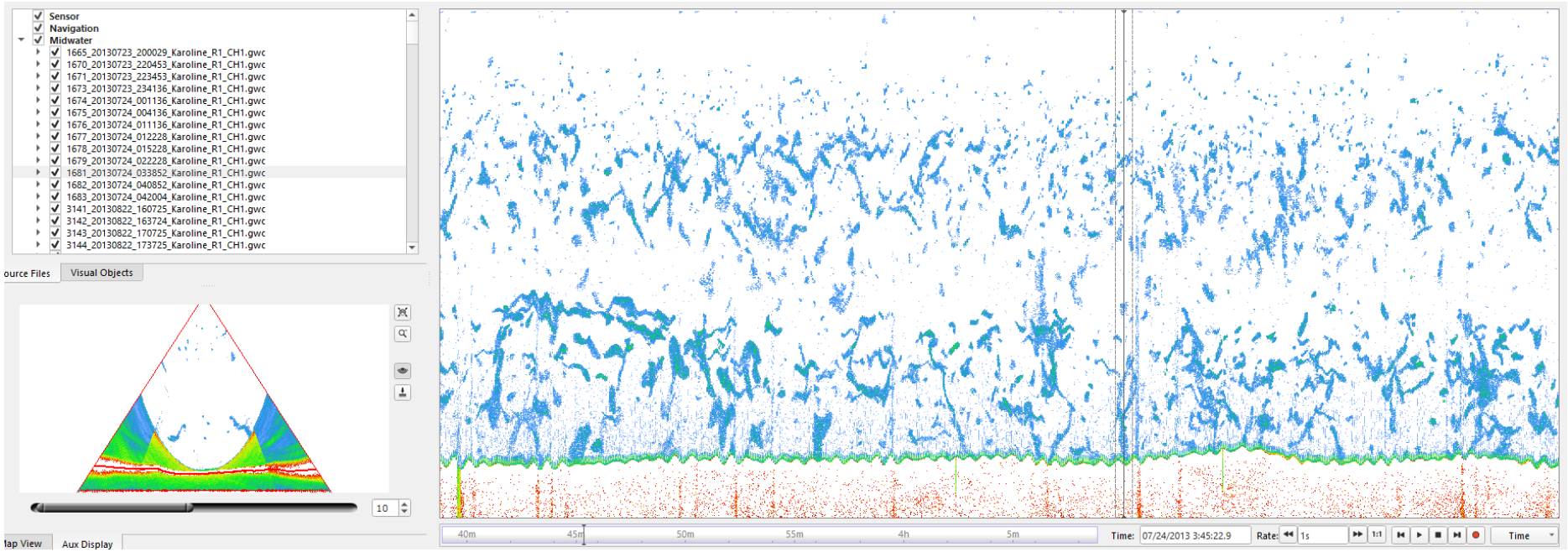

Figure 56. Possible gas flare from line 1681 showed on Fan view and stack view. Magnitude 3, Confidence 30%.

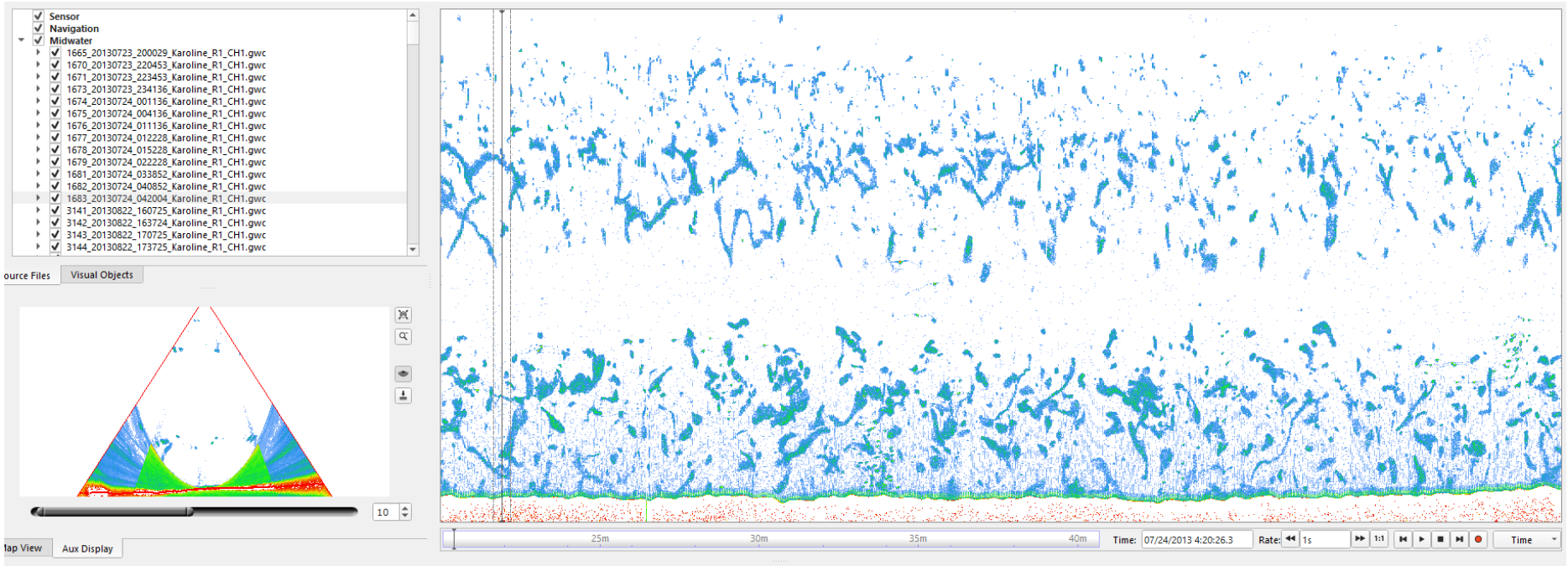

Figure 57. Possible gas flare from line 1683 showed on Fan view and stack view. Magnitude 3, Confidence 30%.

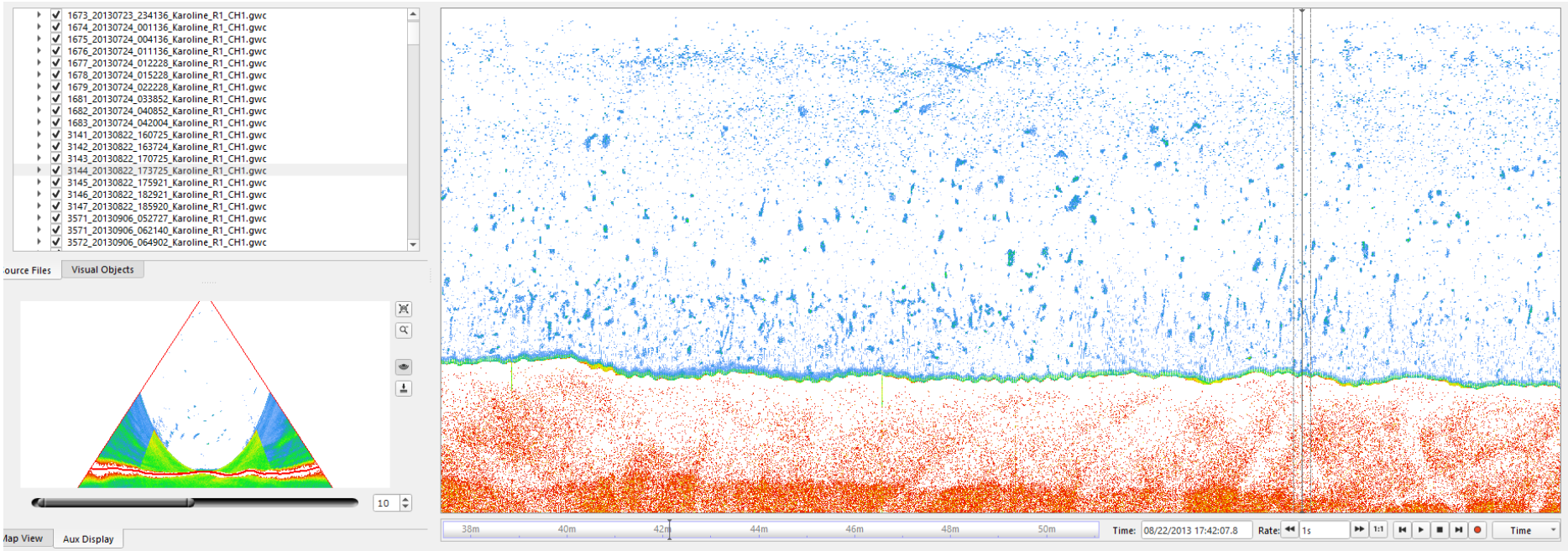

Figure. 58. Possible gas flare from line 3144 showed on Fan view and stack view. Magnitude 2, Confidence 30%.

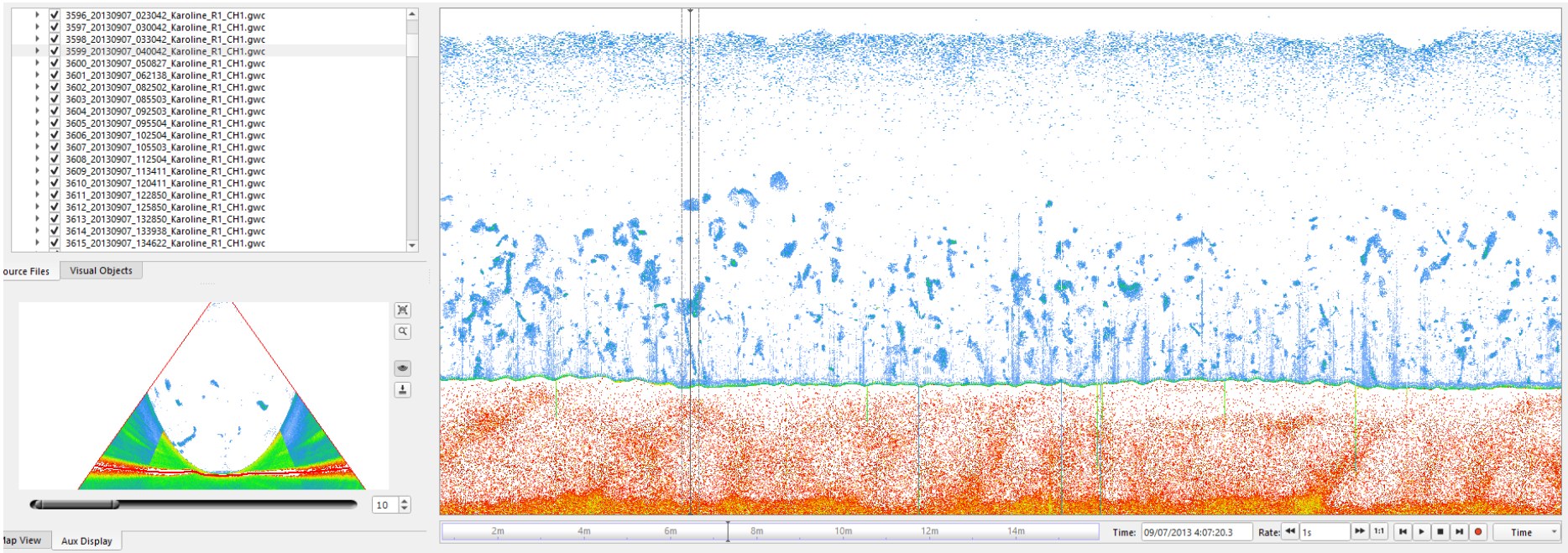

Figure 59. Possible gas flare from line 3599 showed on Fan view and stack view. Magnitude 2, Confidence 30%.

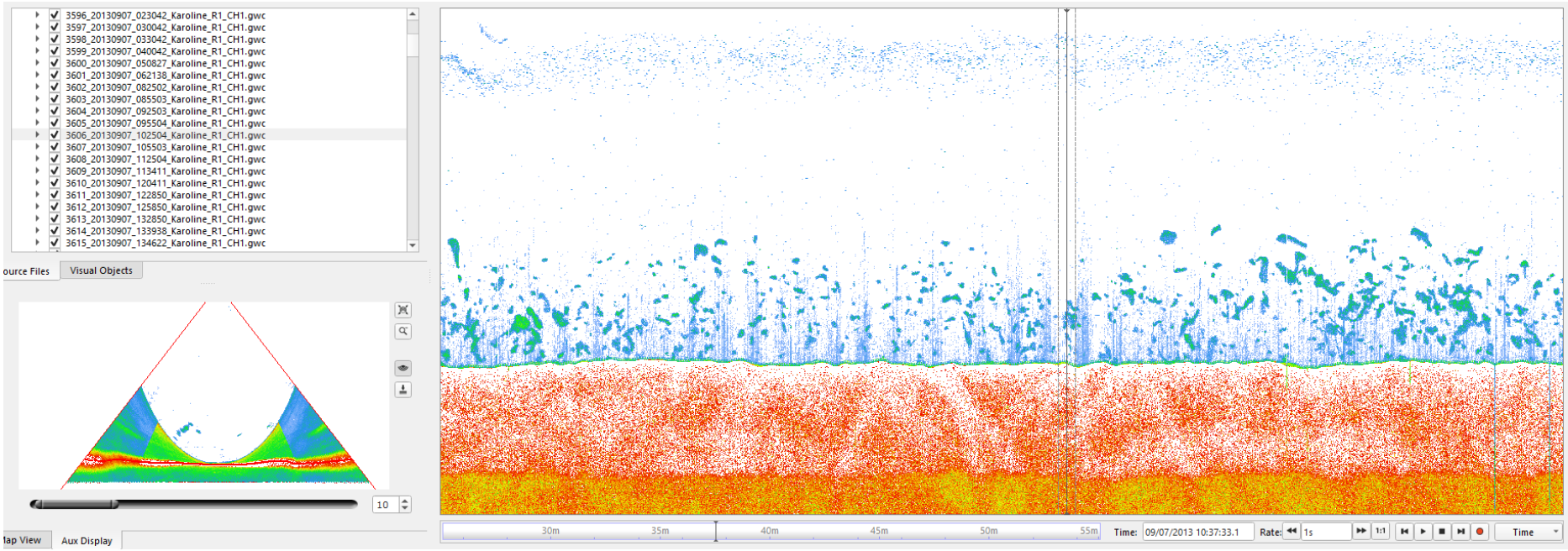

Figure 60. Possible gas flare from line 3606 showed on Fan view and stack view. Magnitude 3, Confidence 30%.

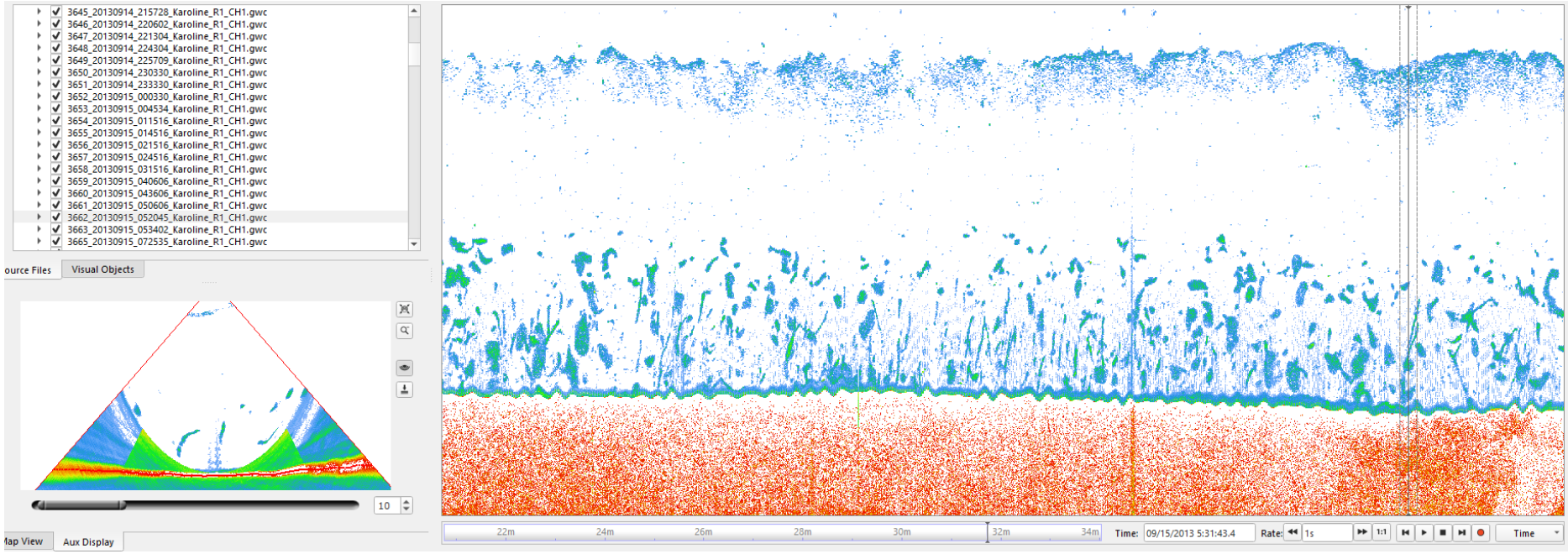

Figure 61. Possible gas flare from line 3662 showed on Fan view and stack view. Magnitude 3, Confidence 30%.

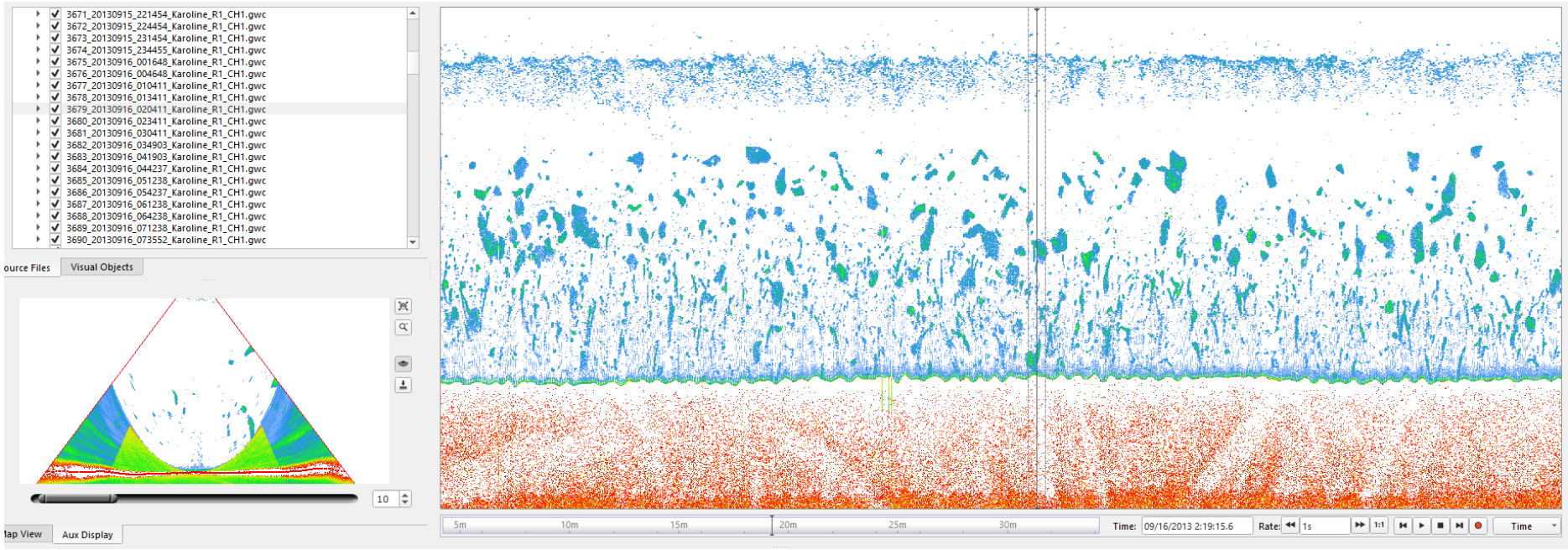

Figure 62. Possible gas flare from line 3679 showed on Fan view and stack view. Magnitude 3, Confidence 30%.

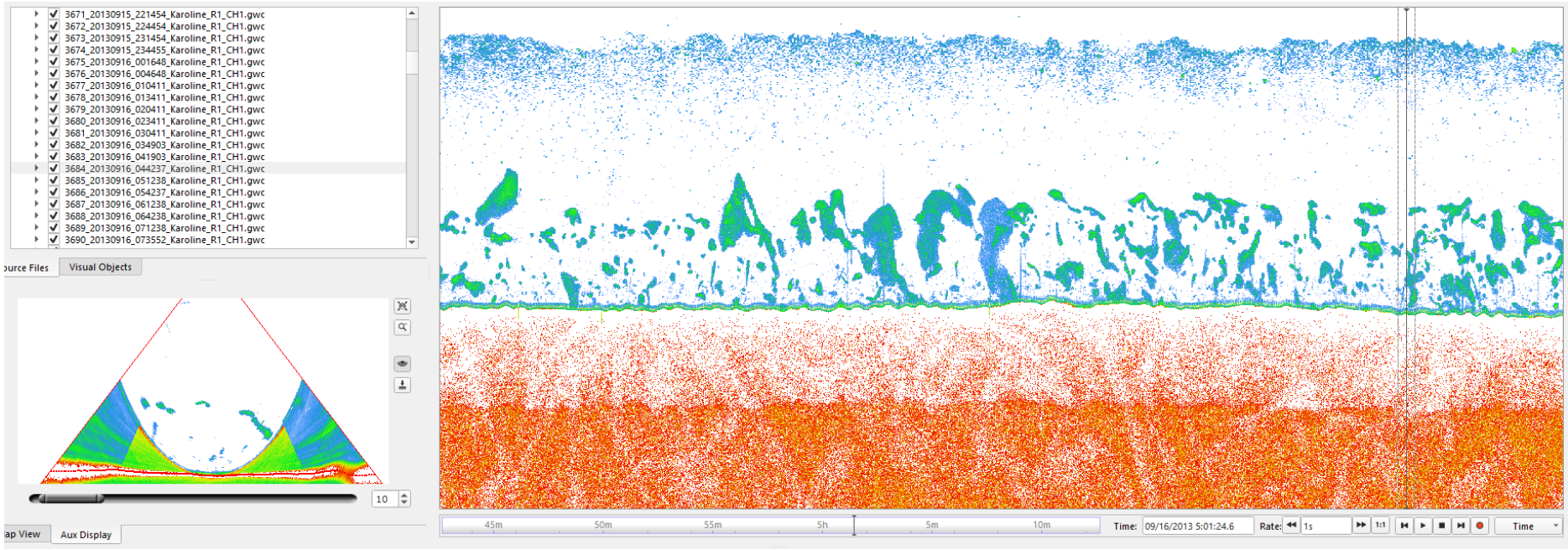

Figure 63. Possible gas flare from line 3684 showed on Fan view and stack view. Magnitude 4, Confidence 30%.

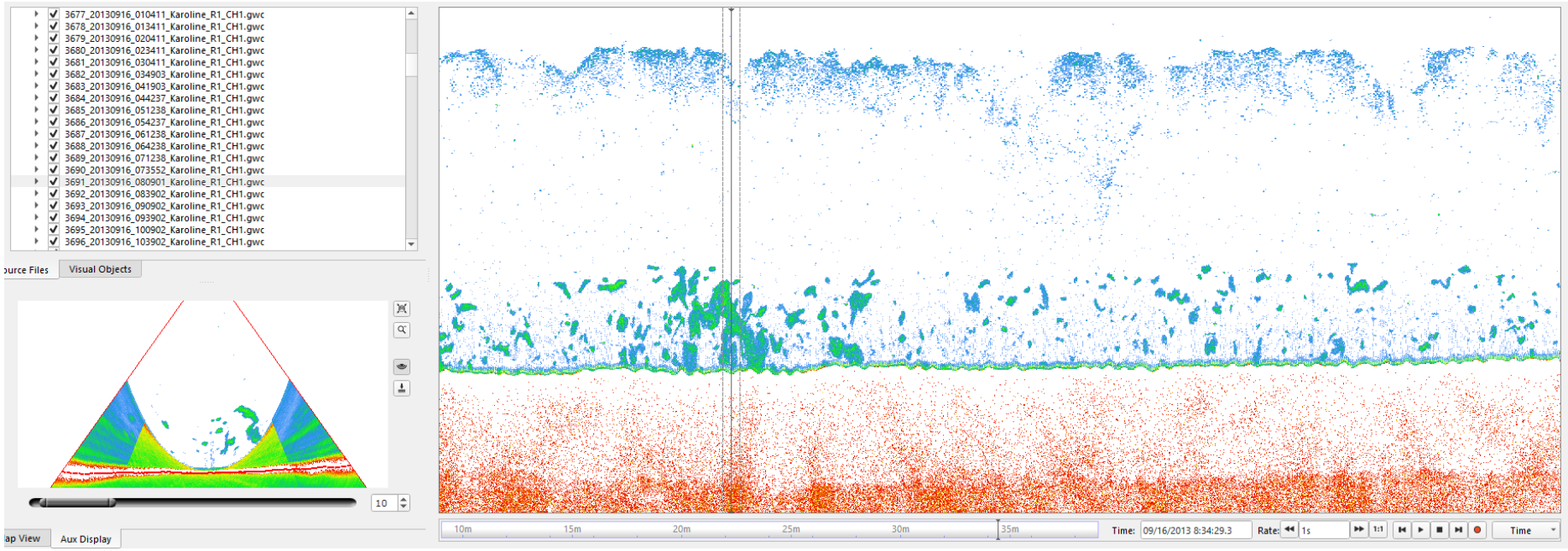

Figure 64. Possible gas flare from line 3691 showed on Fan view and stack view. Magnitude 4, Confidence 30%.

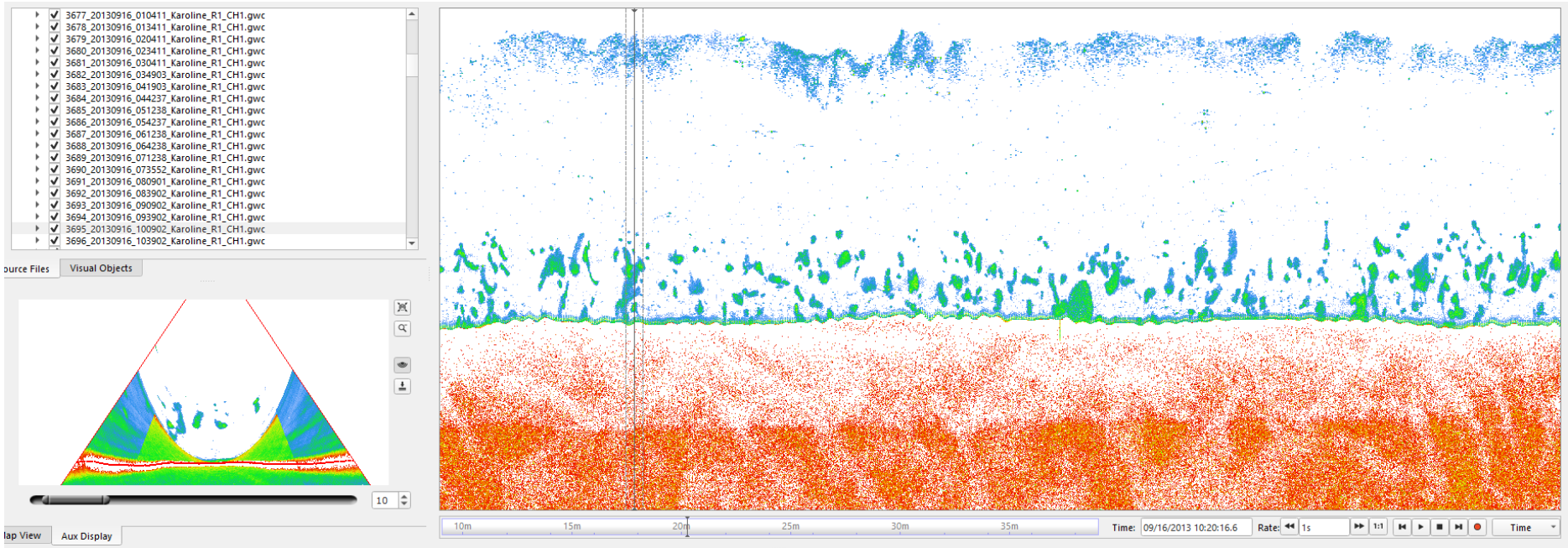

Figure 65. Possible gas flare from line 3695 showed on Fan view and stack view. Magnitude 4, Confidence 30%.

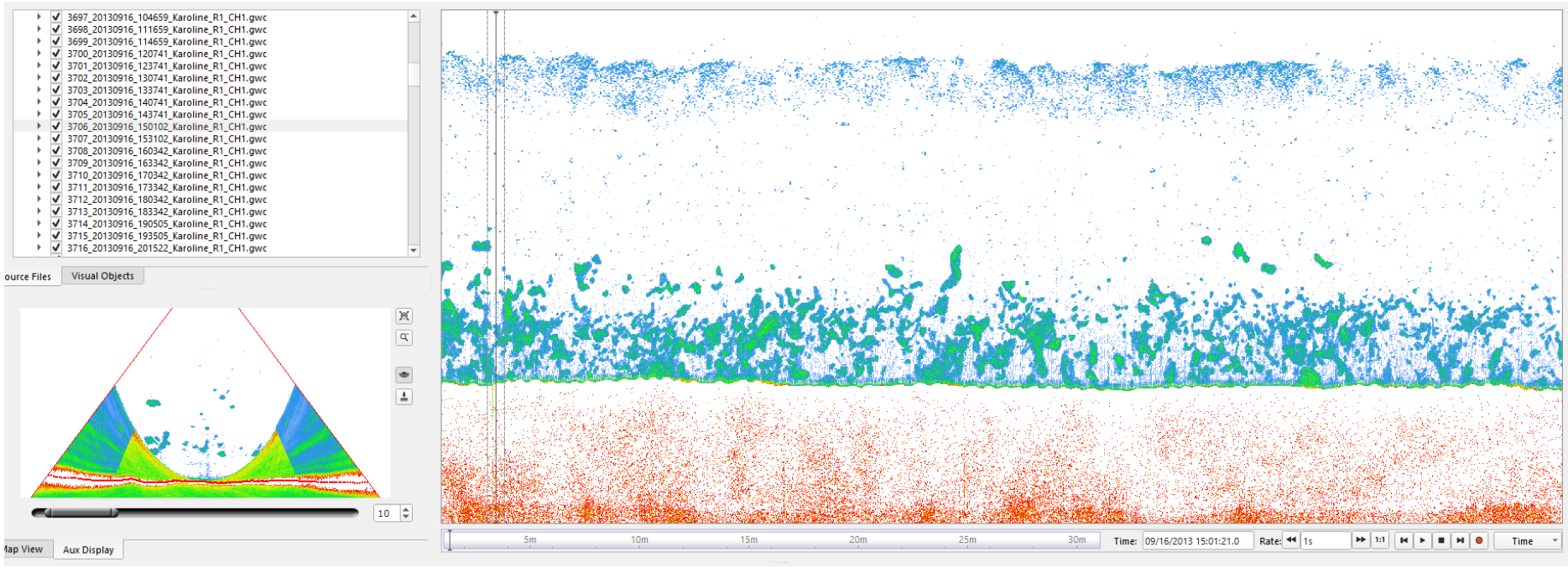

Figure 66. Possible gas flare from line 3706 showed on Fan view and stack view. Magnitude 3, Confidence 30%.

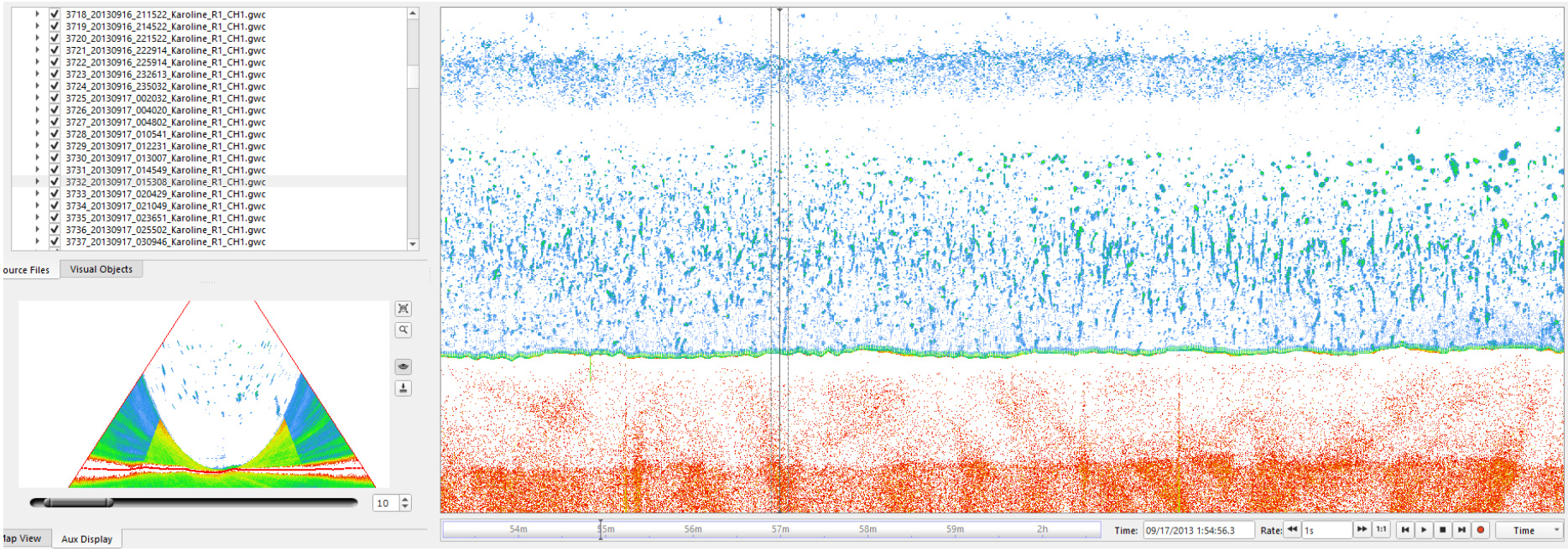

Figure 67. Possible gas flare from line 3732 showed on Fan view and stack view. Magnitude 2, Confidence 30%.

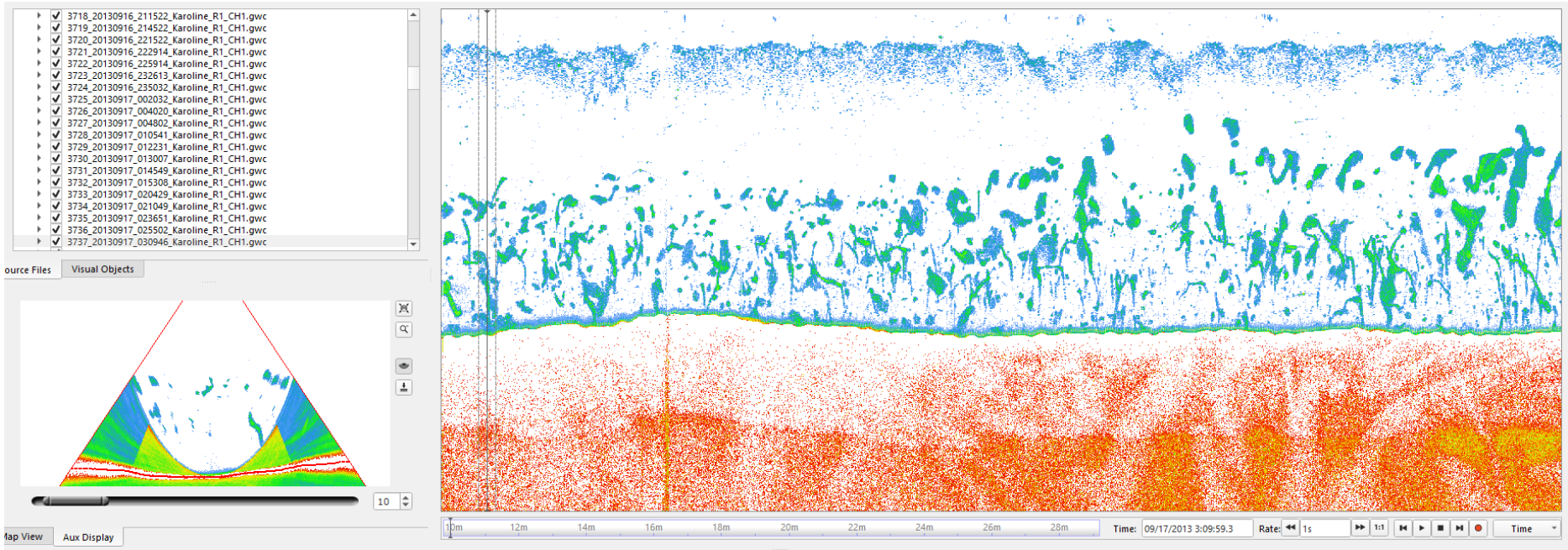

Figure 68. Possible gas flare from line 3737 showed on Fan view and stack view. Magnitude 3, Confidence 30%.

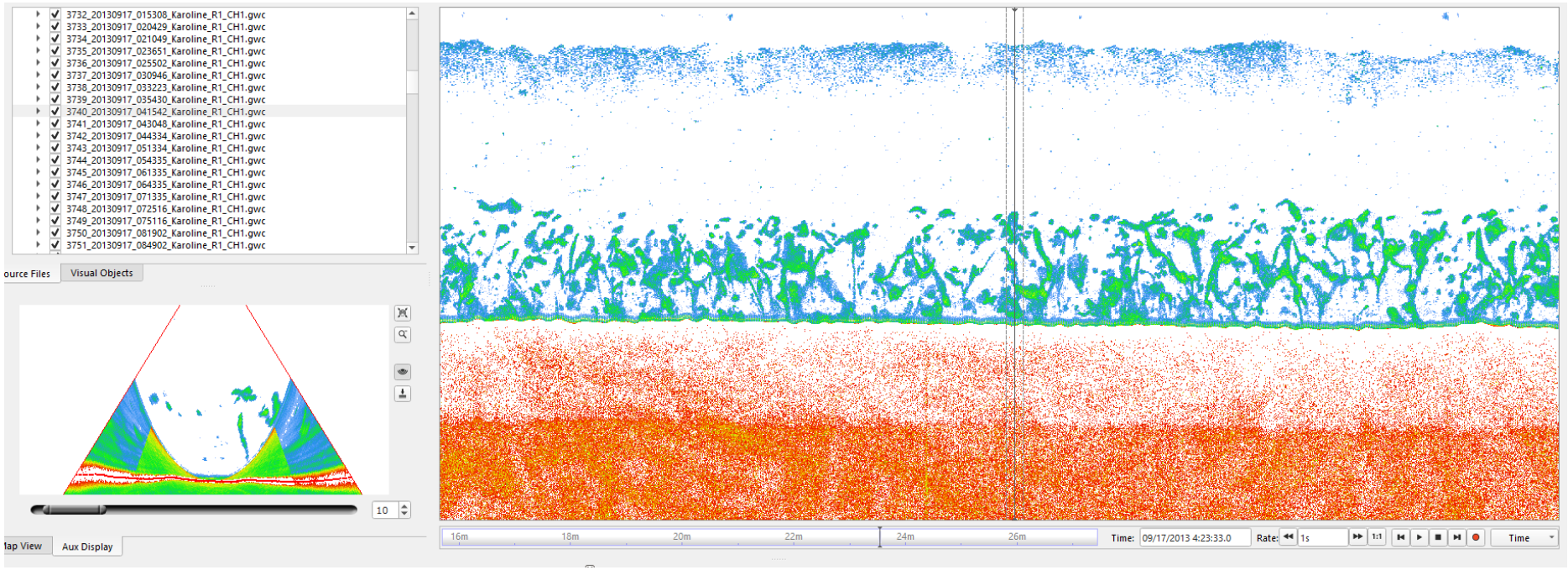

Figure 69. Possible gas flare from line 3740 showed on Fan view and stack view. Magnitude 4, Confidence 30%.

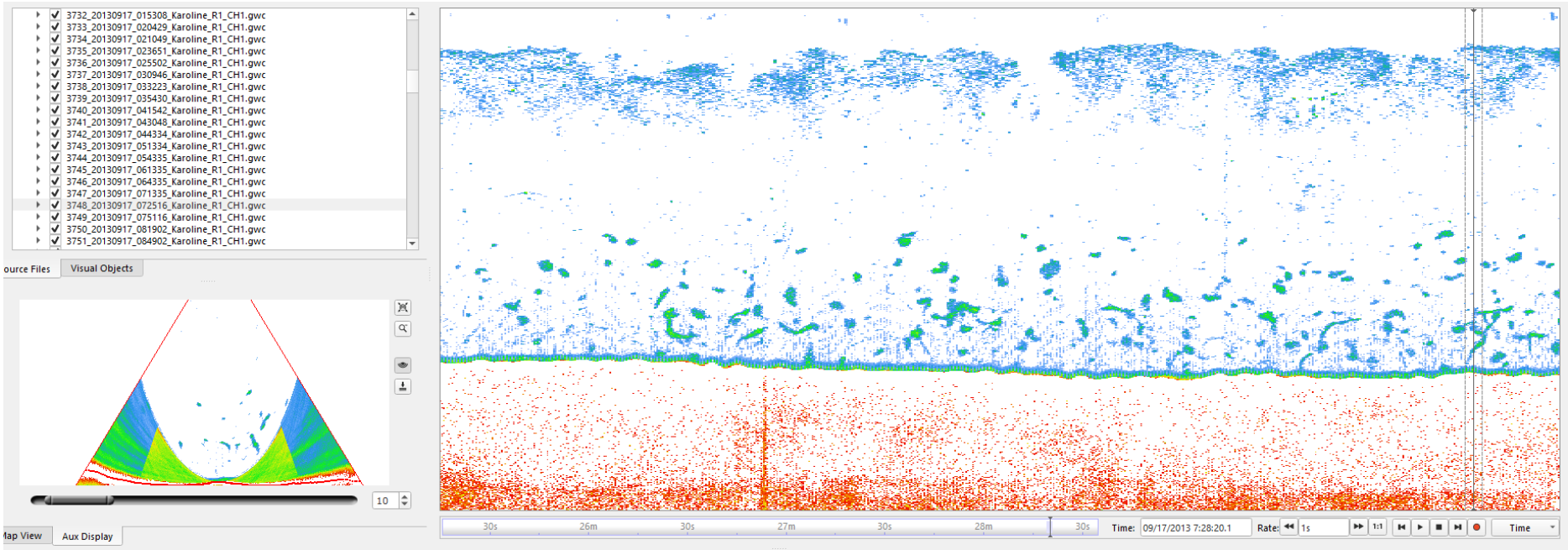

Figure 70. Possible gas flare from line 3748 showed on Fan view and stack view. Magnitude 3, Confidence 30%.

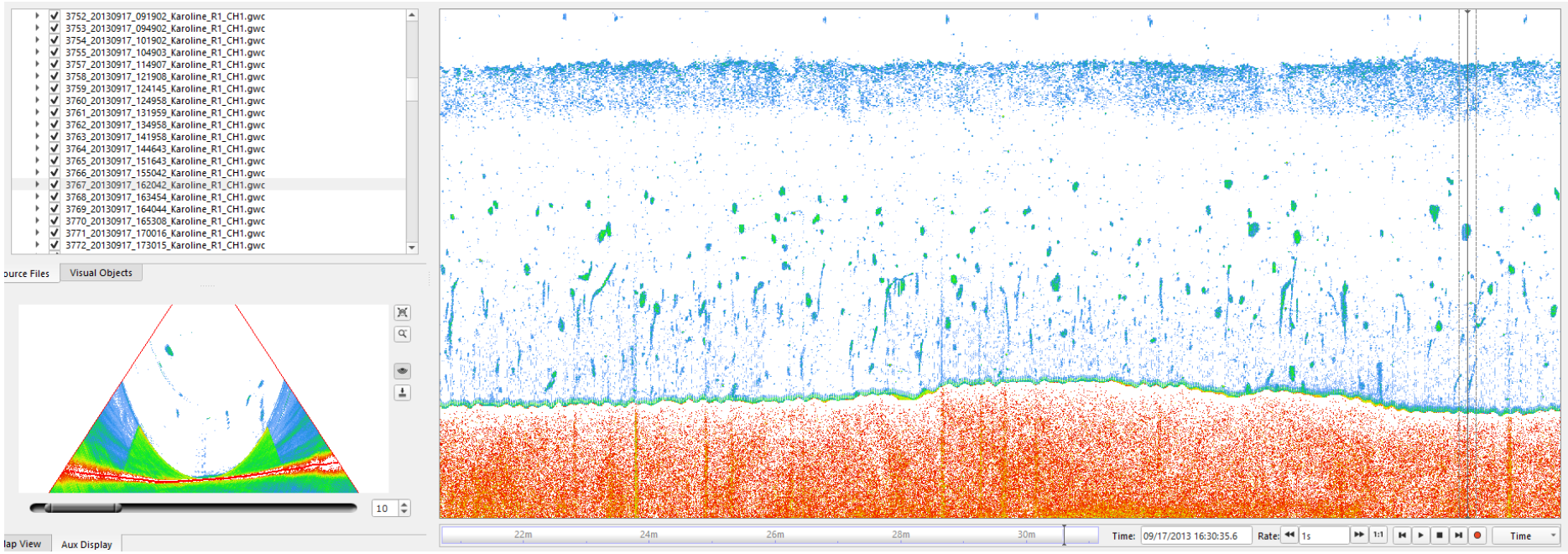

Figure 71. Possible gas flare from line 3767 showed on Fan view and stack view. Magnitude 2, Confidence 30%.

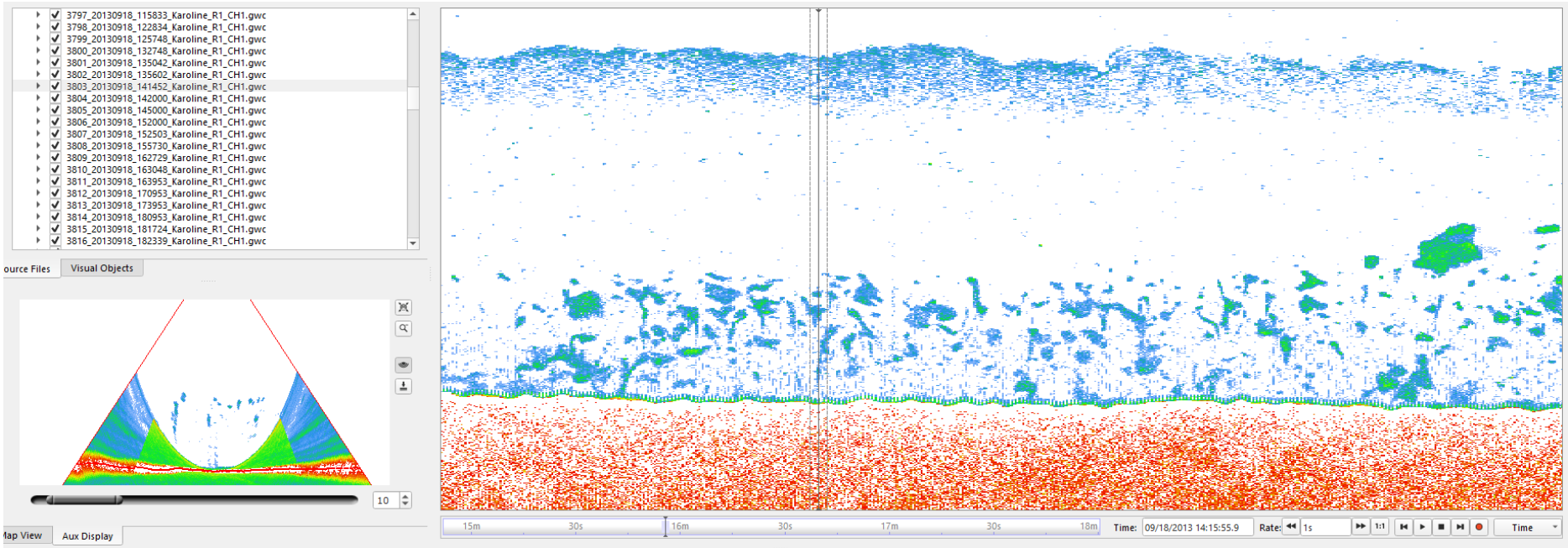

Figure 72. Possible gas flare from line 3803 showed on Fan view and stack view. Magnitude 3, Confidence 30%.

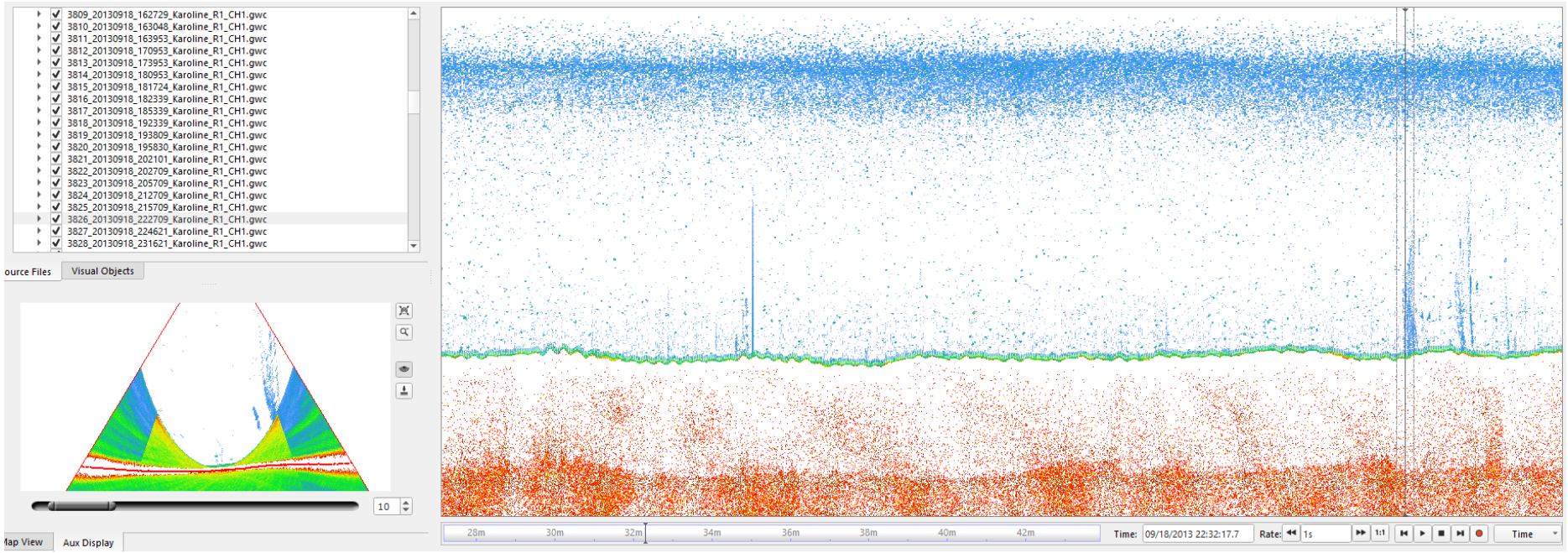

Figure 73. Possible gas flare from line 3826 showed on Fan view and stack view. Magnitude 4, Confidence 80%.

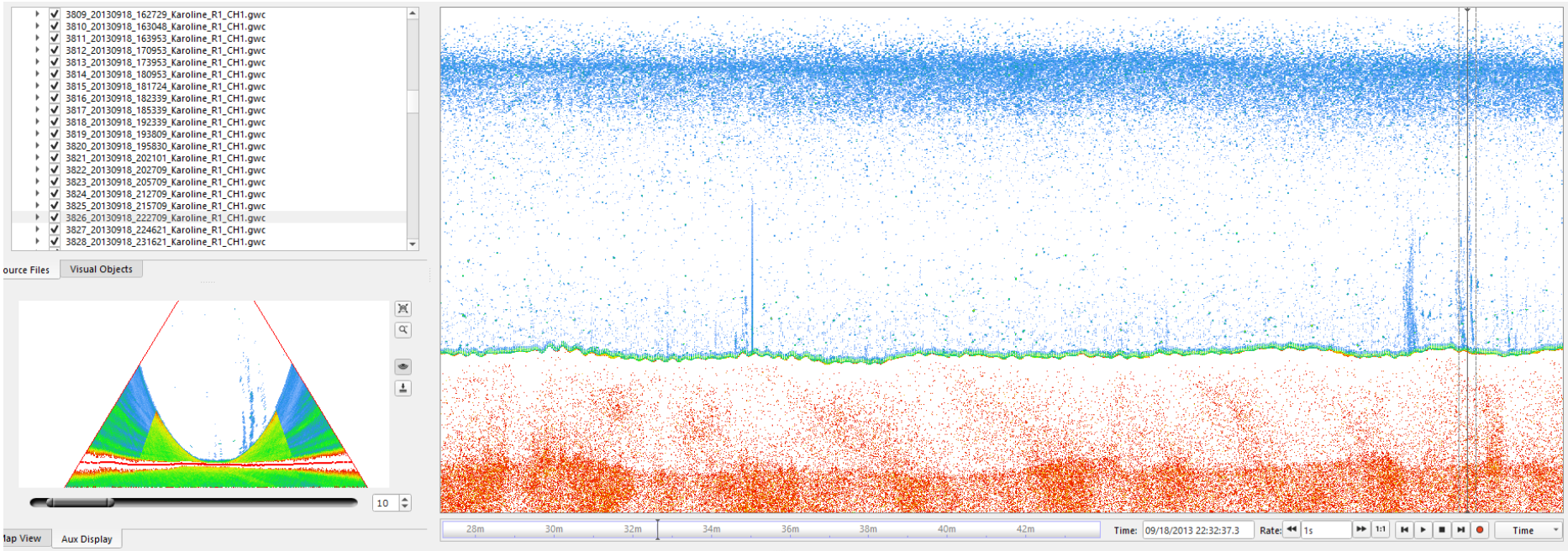

Figure 74. Gas flare from line 3826 showed on Fan view and stack view. Magnitude 3, Confidence 80%.

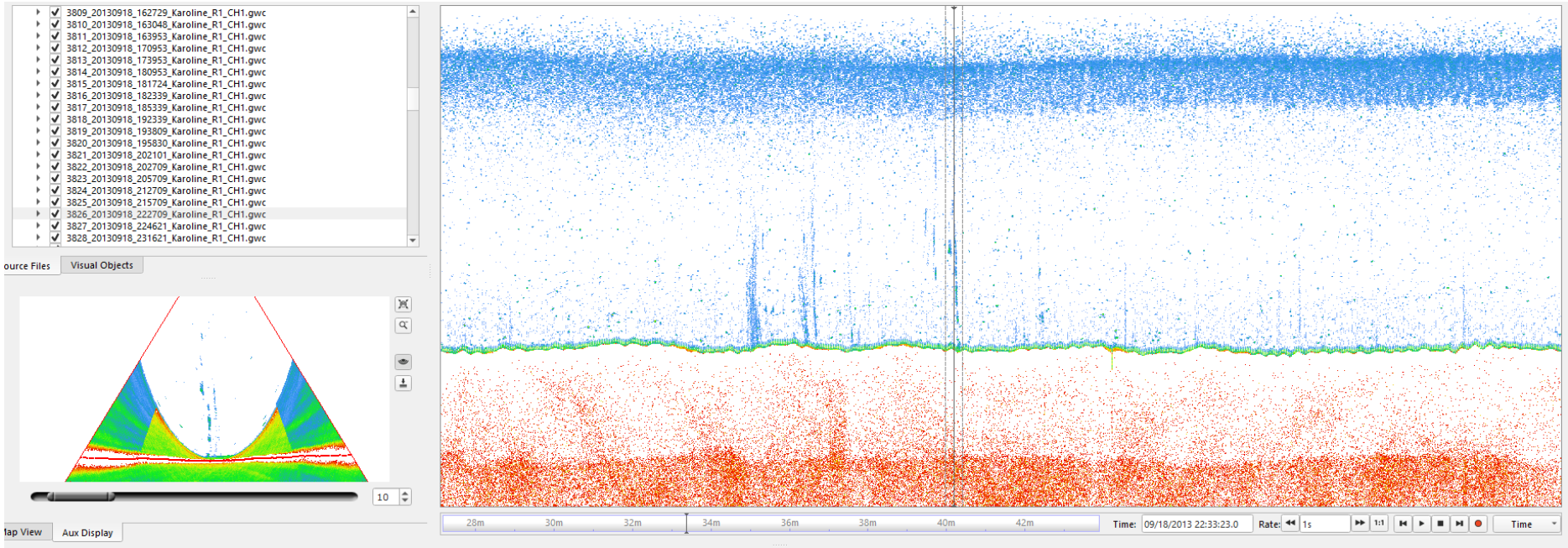

Figure 75. Gas flare from line 3826 showed on Fan view and stack view. Magnitude 2, Confidence 70%.

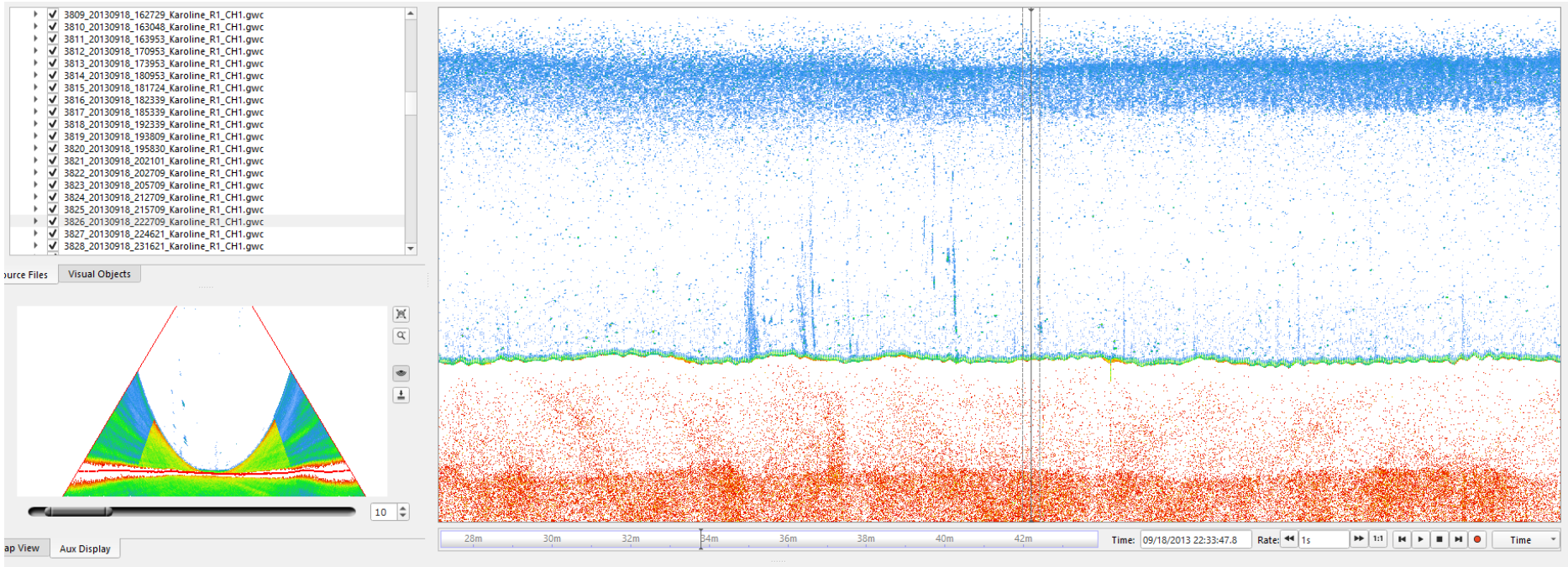

Figure 76. Gas flare from line 3826 showed on Fan view and stack view. Magnitude 2, Confidence 60%.

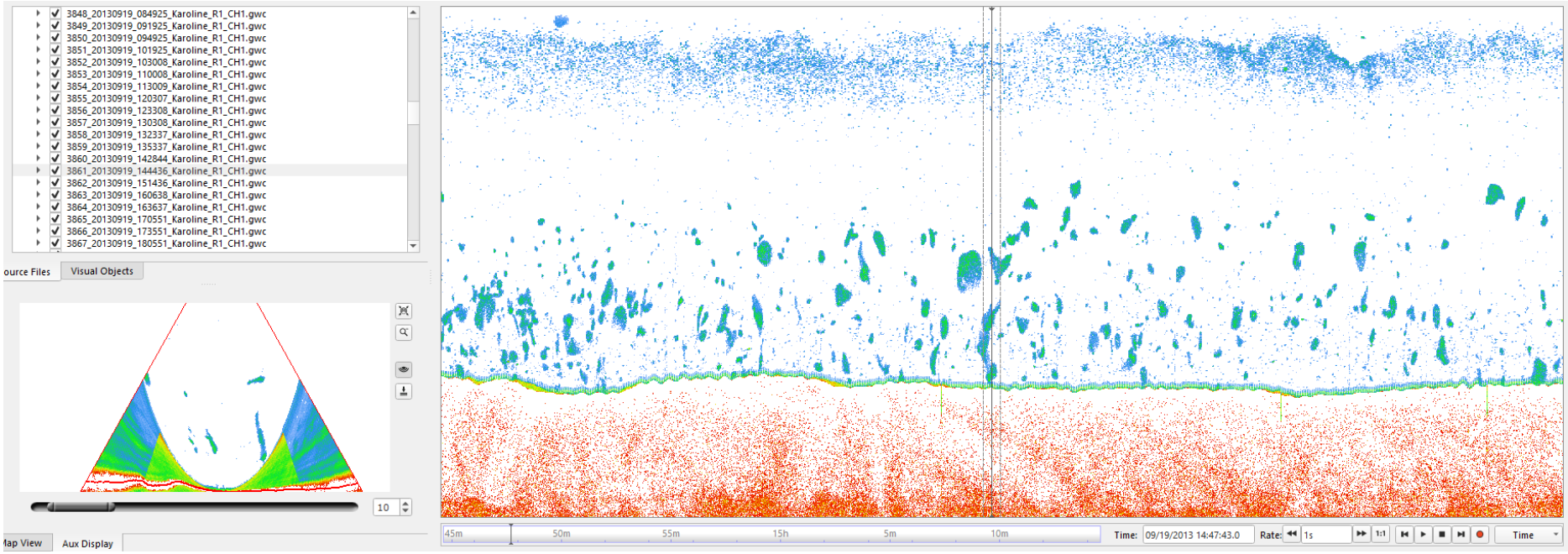

Figure 77. Possible gas flare from line 3861 showed on Fan view and stack view. Magnitude 4, Confidence 30%.

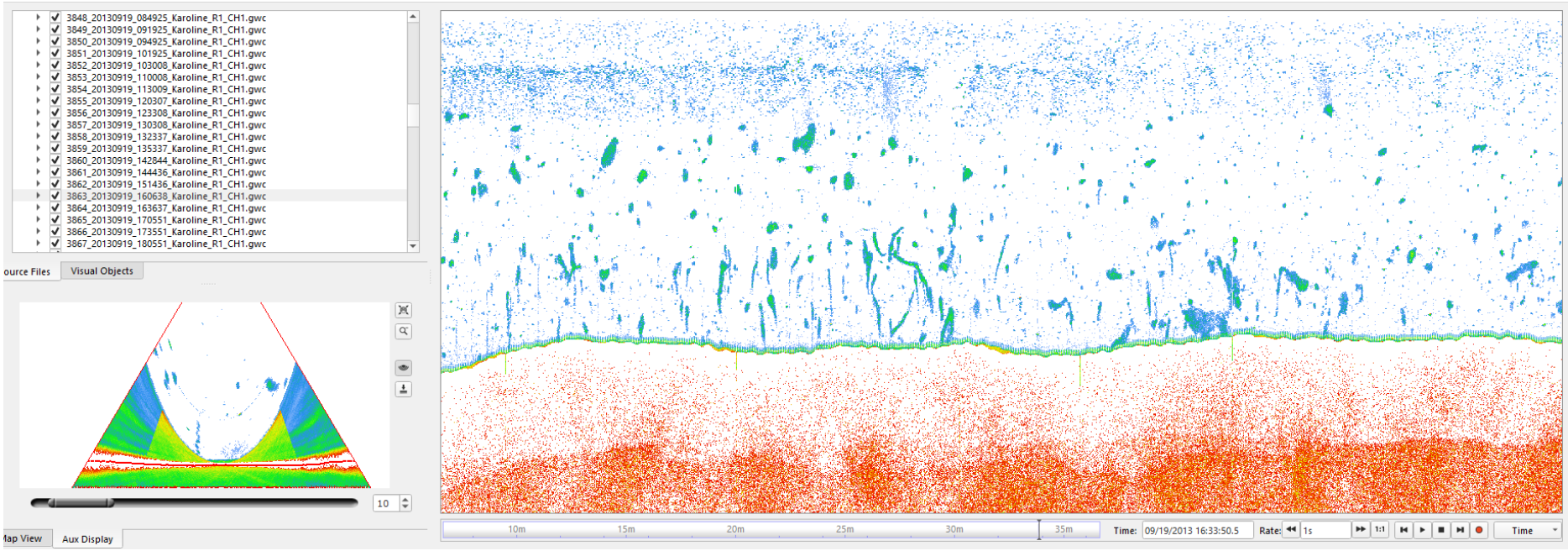

Figure 78. Possible gas flare from line 3863 showed on Fan view and stack view. Magnitude 2, Confidence 30%.

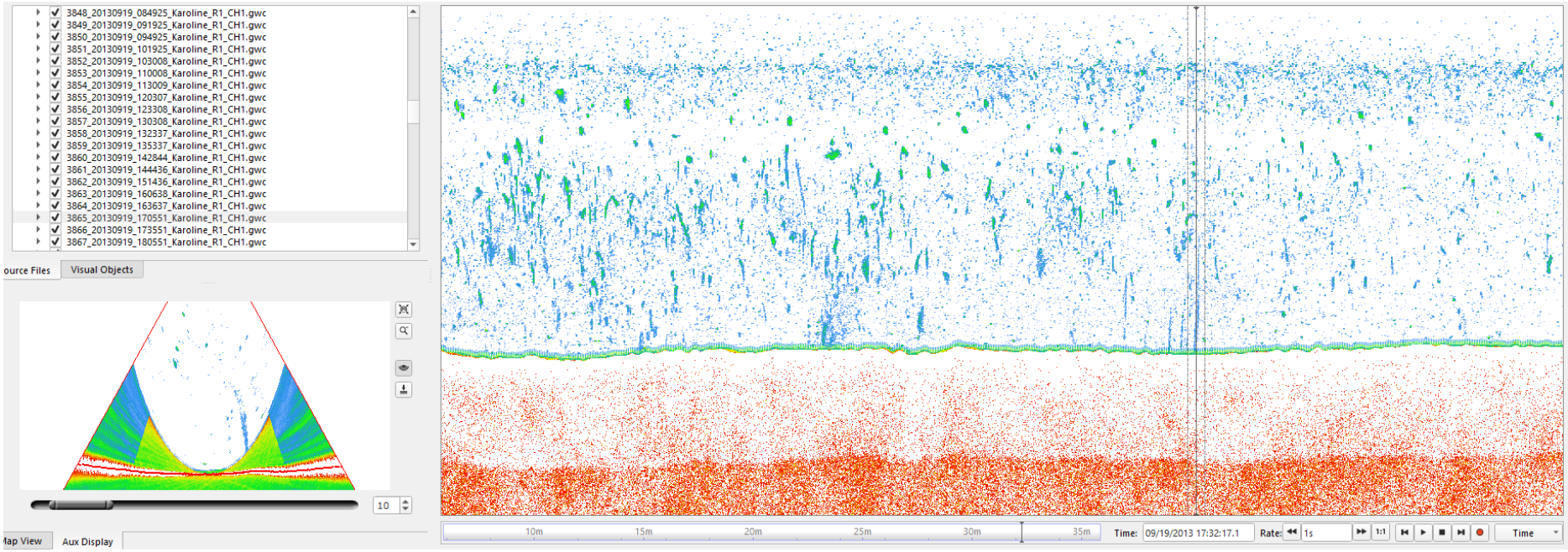

Figure 79. Gas flare from line 3865 showed on Fan view and stack view. Magnitude 3, Confidence 60%.

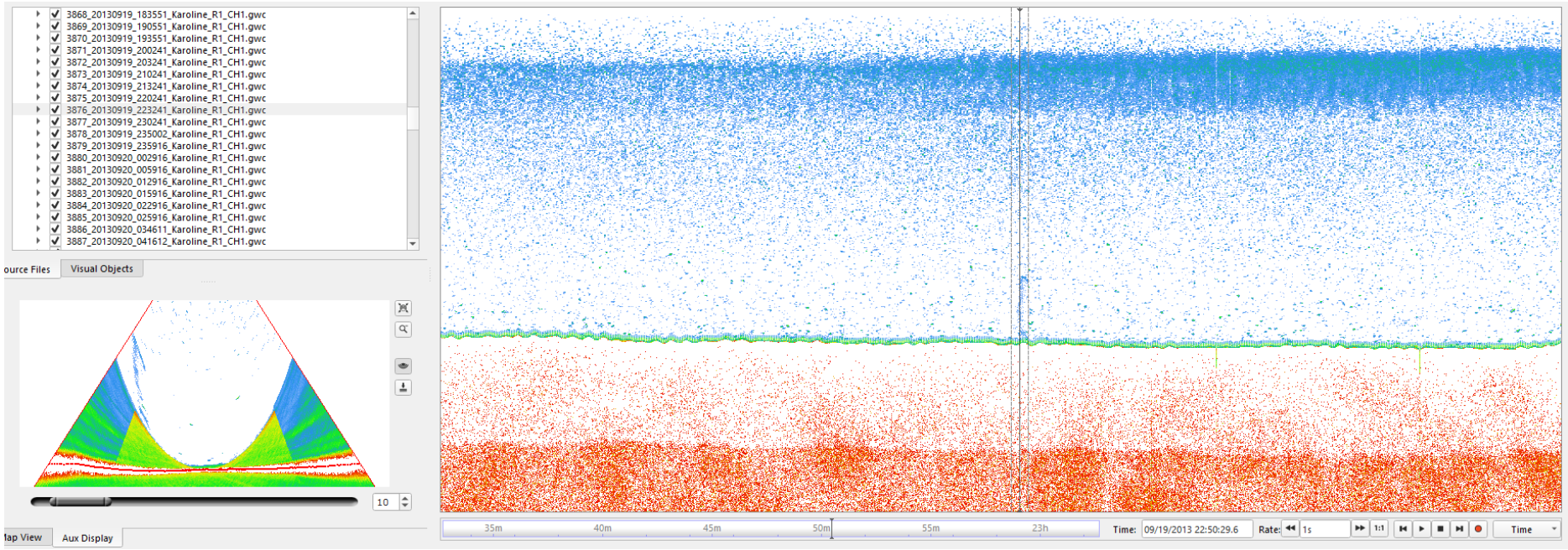

Figure 80. Gas flare from line 3876 showed on Fan view and stack view. Magnitude 3, Confidence 60%.

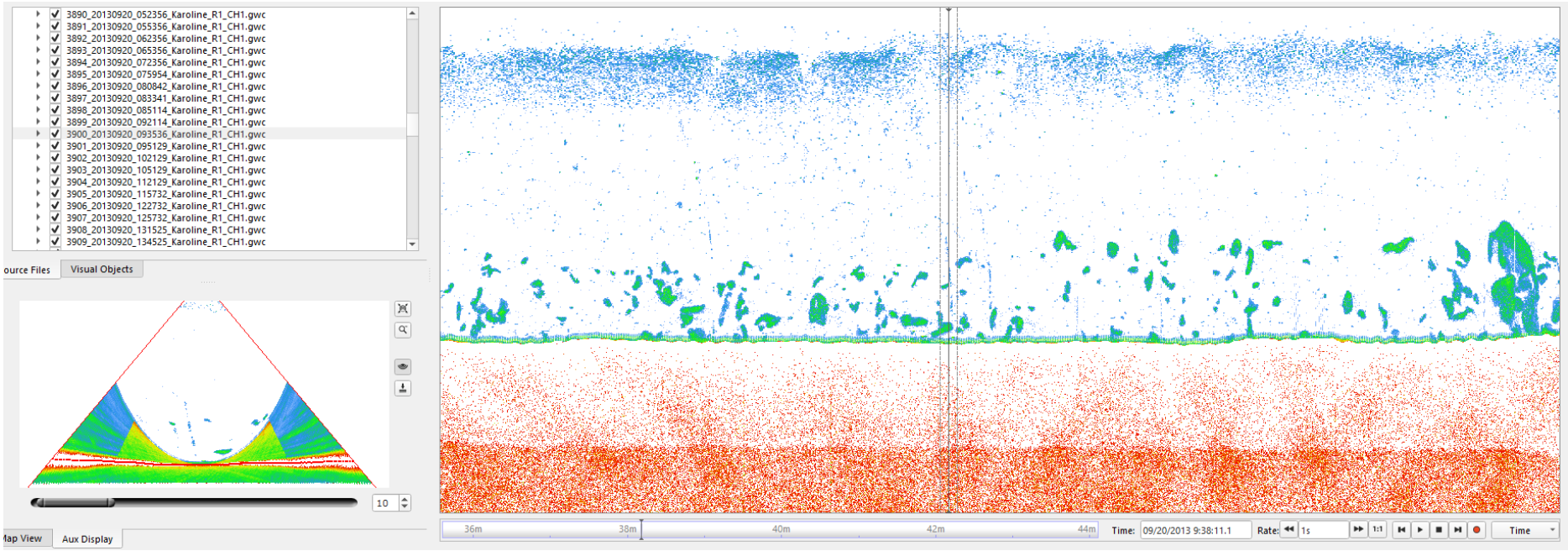

Figure 81. Gas flare from line 3900 showed on Fan view and stack view. Magnitude 2, Confidence 60%.

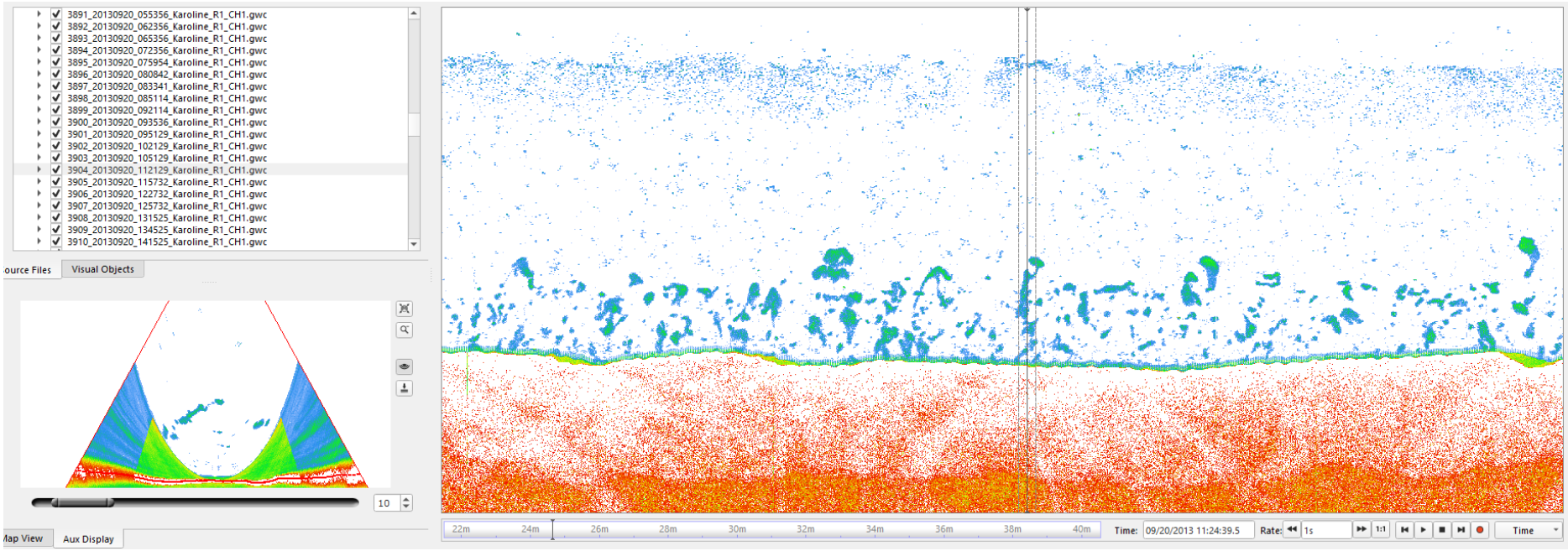

Figure 82. Possible gas flare from line 3904 showed on Fan view and stack view. Magnitude 4, Confidence 40%.

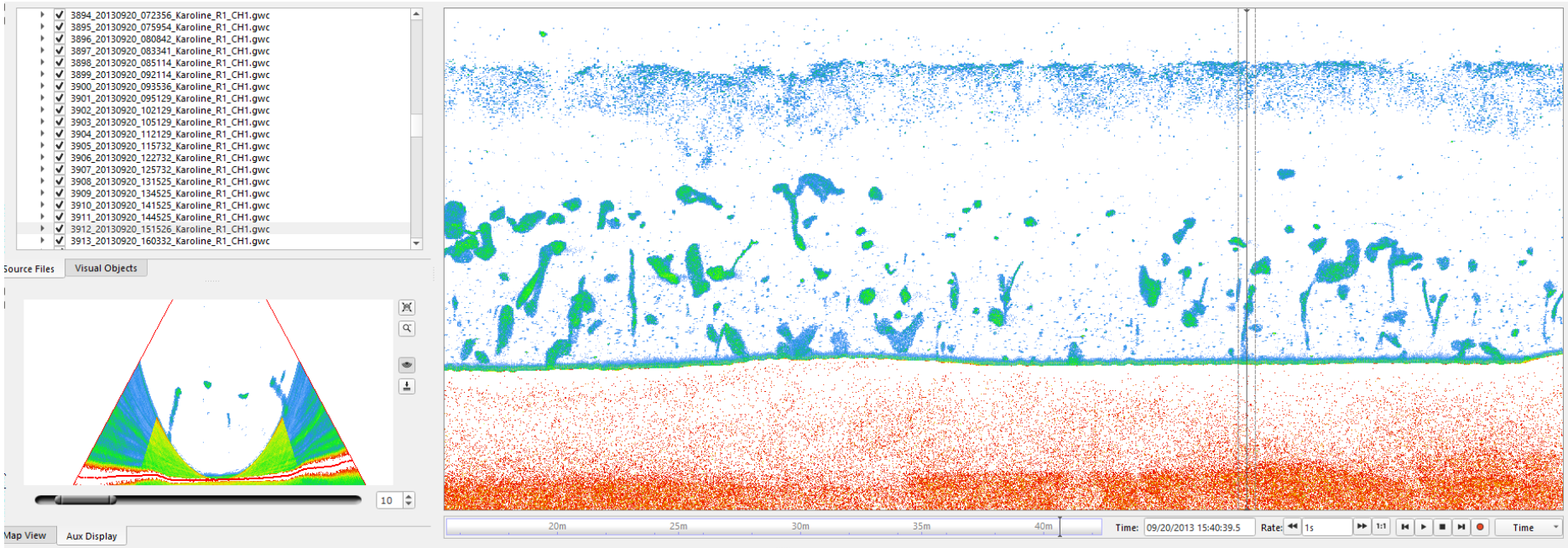

Figure 83. Possible gas flare from line 3912 showed on Fan view and stack view. Magnitude 4, Confidence 40%.

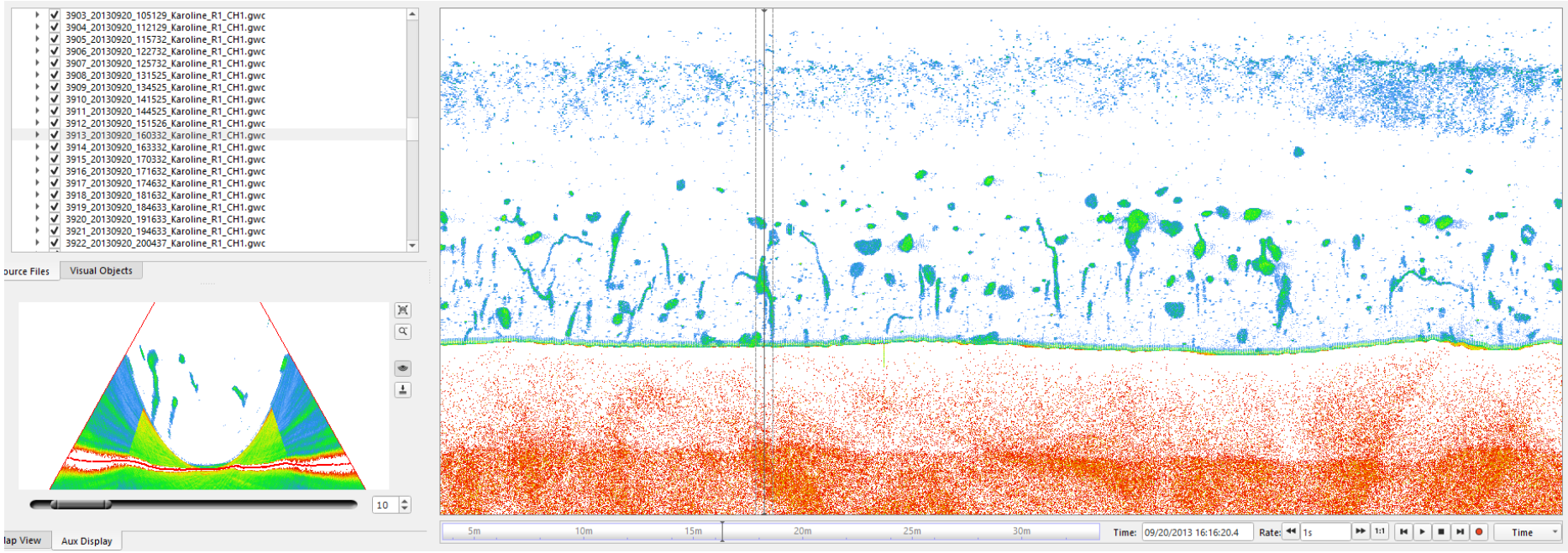

Figure 84. Possible gas flare from line 3913 showed on Fan view and stack view. Magnitude 4, Confidence 30%.

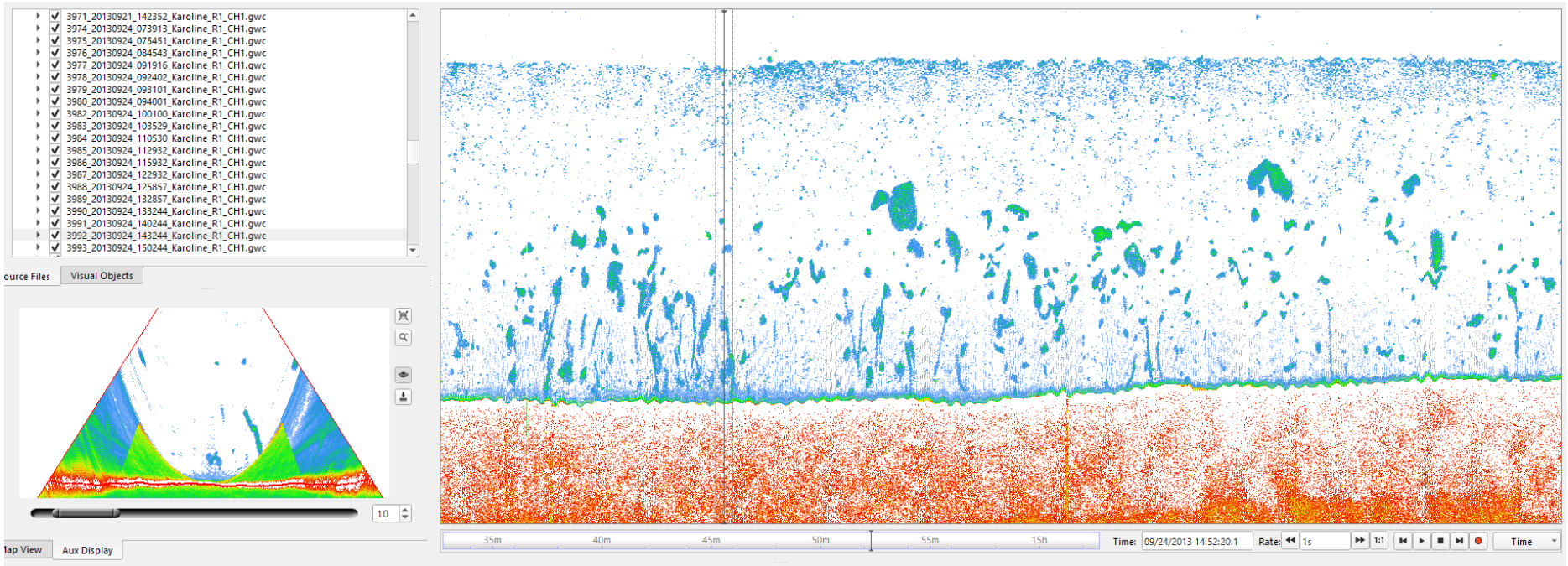

Figure 85. Possible gas flare from line 3992 showed on Fan view and stack view. Magnitude 3, Confidence 30%.

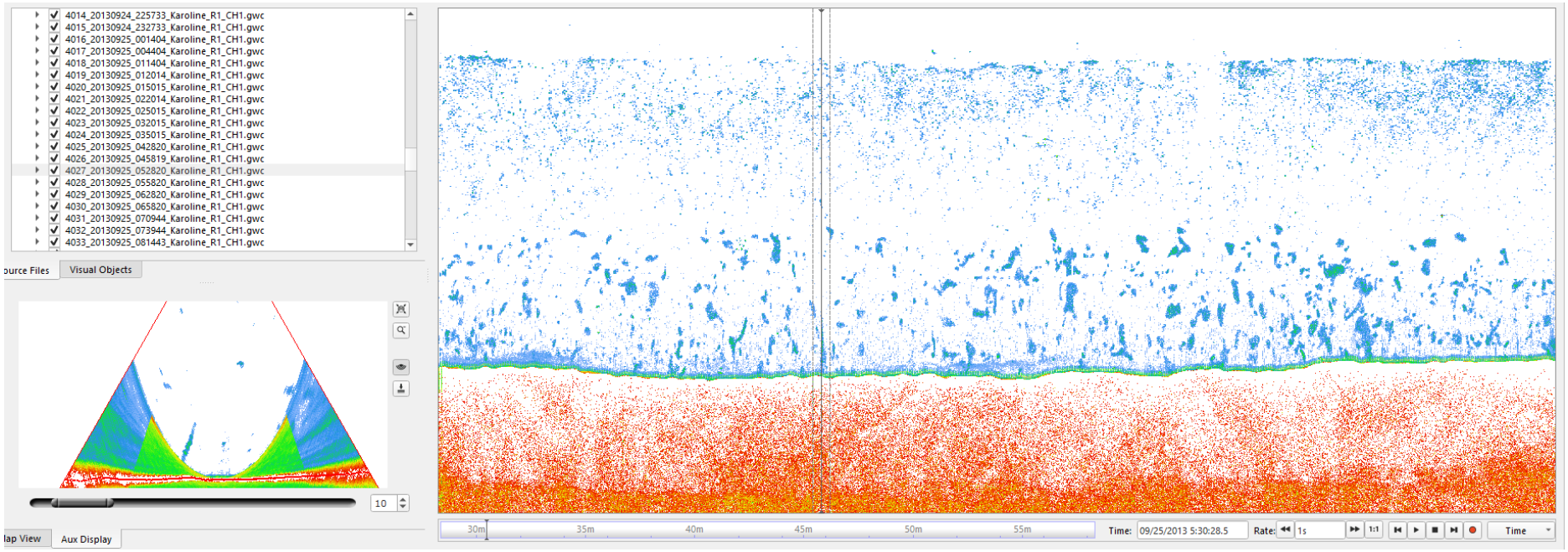

Figure 86. Possible gas flare from line 4027 showed on Fan view and stack view. Magnitude 3, Confidence 30%.

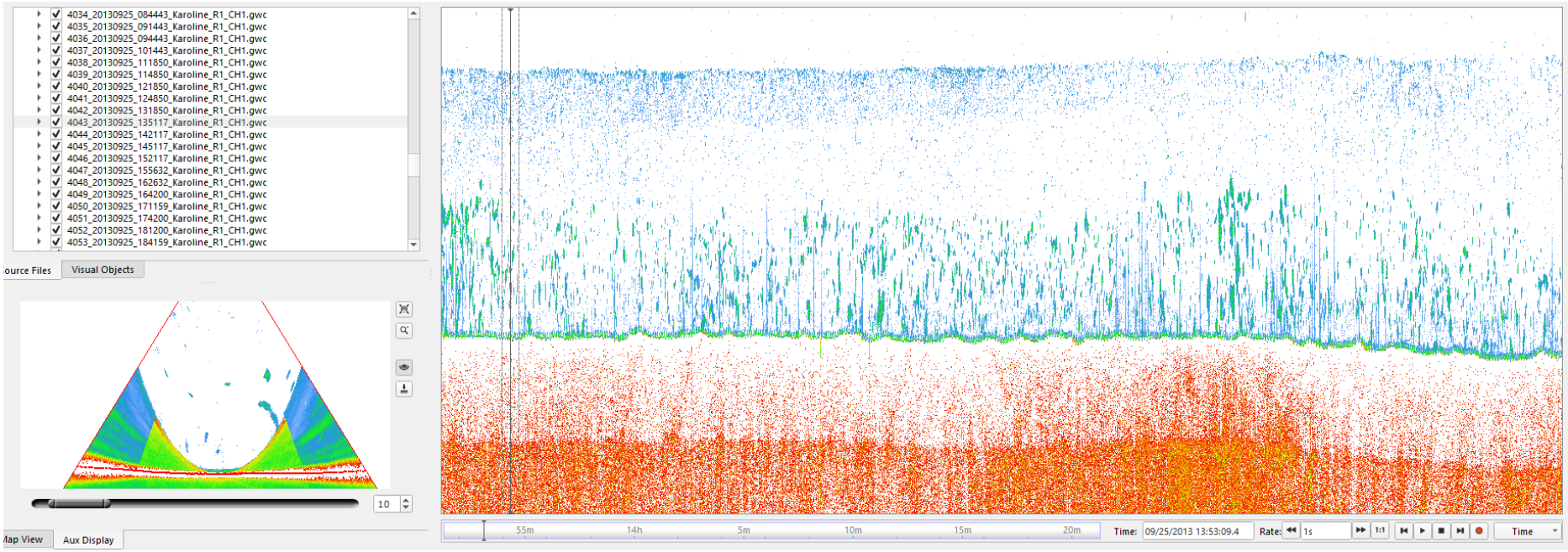

Figure 87. Possible gas flare from line 4043 showed on Fan view and stack view. Magnitude 4, Confidence 30%.

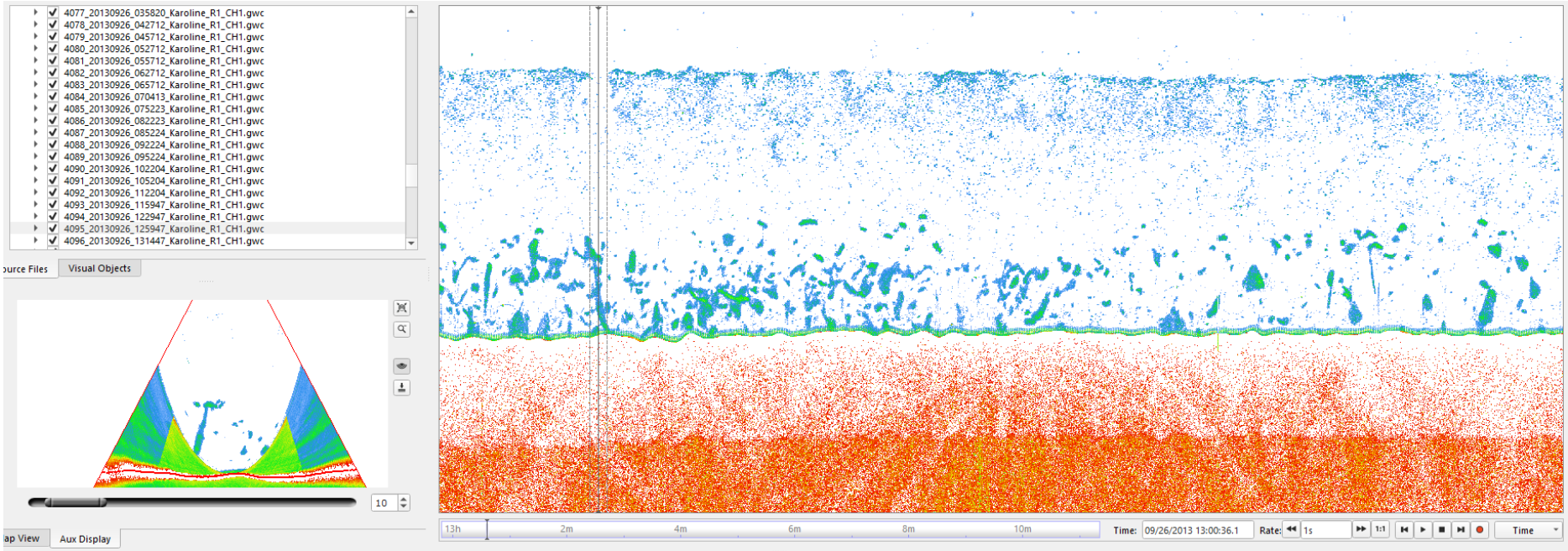

Figure 88. Possible gas flare from line 4095 showed on Fan view and stack view. Magnitude 4, Confidence 40%.

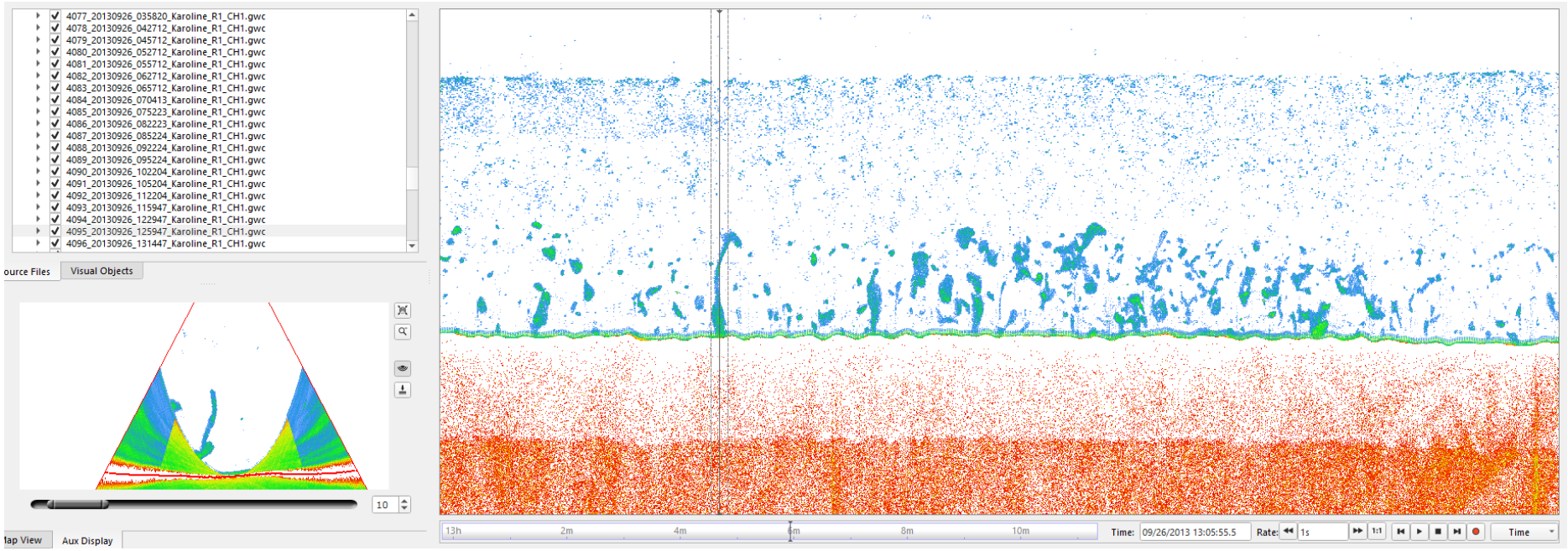

Figure 89. Possible gas flare from line 4095 showed on Fan view and stack view. Magnitude 4, Confidence 30%.

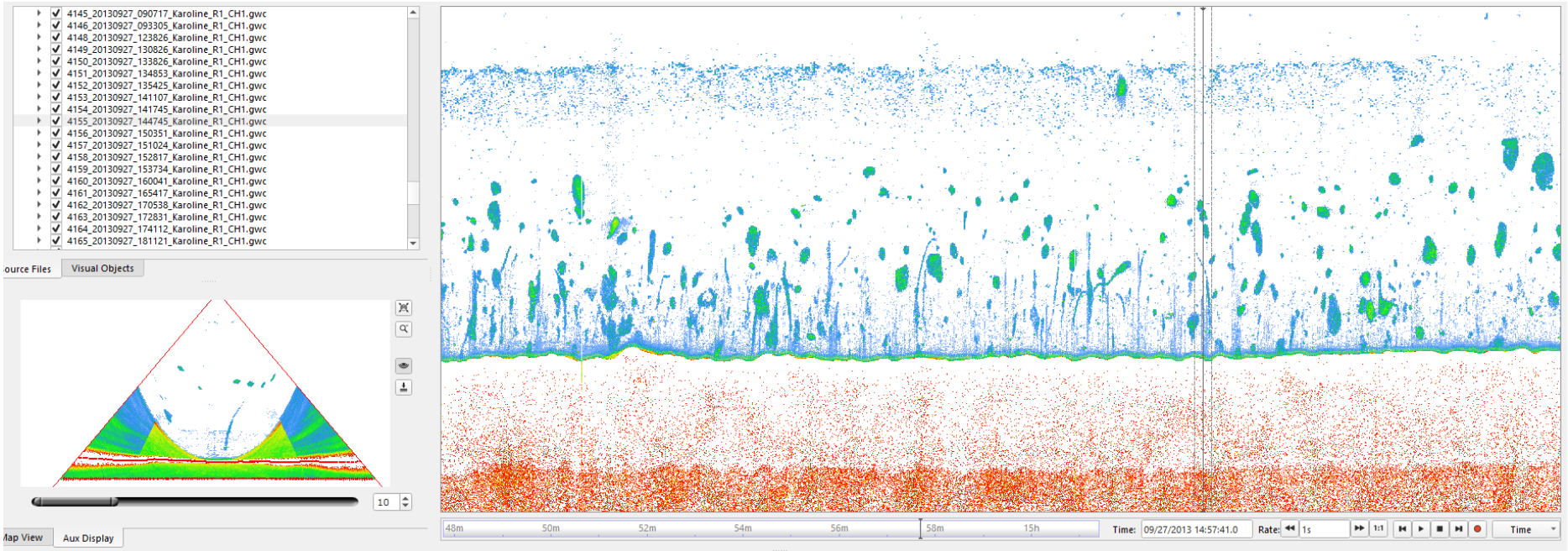

Figure 90. Possible gas flare from line 4155 showed on Fan view and stack view. Magnitude 3, Confidence 30%.

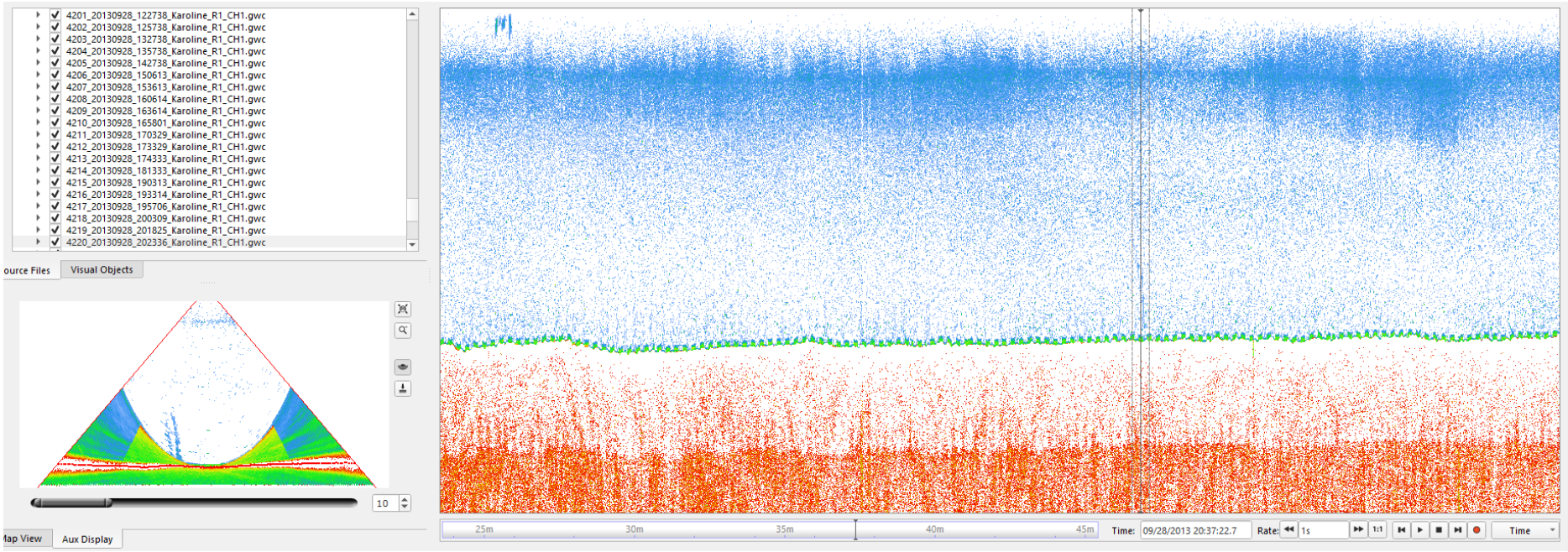

Figure 91. Gas flare from line 4220 showed on Fan view and stack view. Magnitude 3, Confidence 60%.

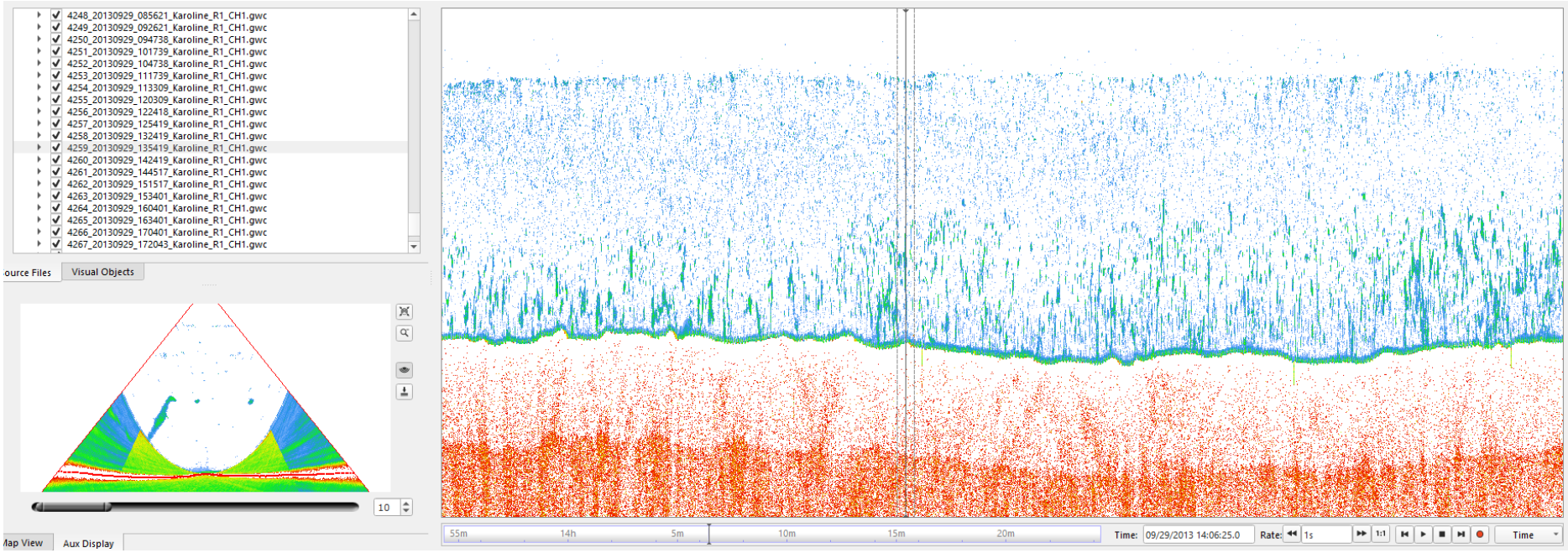

Figure 92. Possible gas flare from line 4259 showed on Fan view and stack view. Magnitude 4, Confidence 40%.

4.4.4 D26

The FOSAE-2013-D26 survey consists of 457 water column (.wcd) survey lines. The data was loaded in Fledermaus Midwater along with navigation (.all) and converted to GWC files. During conversion, it was observed that there was only 402 .all files present thereby missing navigation for 55 lines. The .all file from the previous file to the .wcd file was loaded as a test and found that some lines have navigation in located in the .all file with previous line number. All the lines were converted with this method giving 426 gwc files. There were no flares found in the lines with missing navigation. 3 possible flares were found in the data of varying confidence level. The flares found are listed in Table 5. All lines had varying levels of noise (generated by other instruments or bad weather). This may have resulted in some flares missing. Special care was taken to go through these noisy lines to avoid any missing flares. Only weak flares could have been missed through this process. Many of the lines have irregular objects, with varying acoustic reflectivity (Figs. 93-94). These have been interpreted as indications of biological material, probably ranging from plankton to fish. Some indications are seen for larger objects which may be mammals. If gas flares are present on these lines, there is a significant risk that the acoustic signals from the biological material mask the presence of gas flares. Only three possible gas flares were identified from this survey. These are shown in Figs. 95-97.

Table 5. Details of flares identified from Survey Area D26.

Survey	LineId	Latitude	Longitude	Depth	Height	Time	Magnitude	Confidence
FOSAE-2013-D26	1557	75.69685000	37.79819400	-207.00	30.00	18:00:59.6	2	30
FOSAE-2013-D26	1558	75.69493889	37.83758889	-213.00	20.00	18:09:22.1	2	30
FOSAE-2013-D26	1564	75.69773333	37.31928333	-199.00	20.00	20:56:21.4	2	30

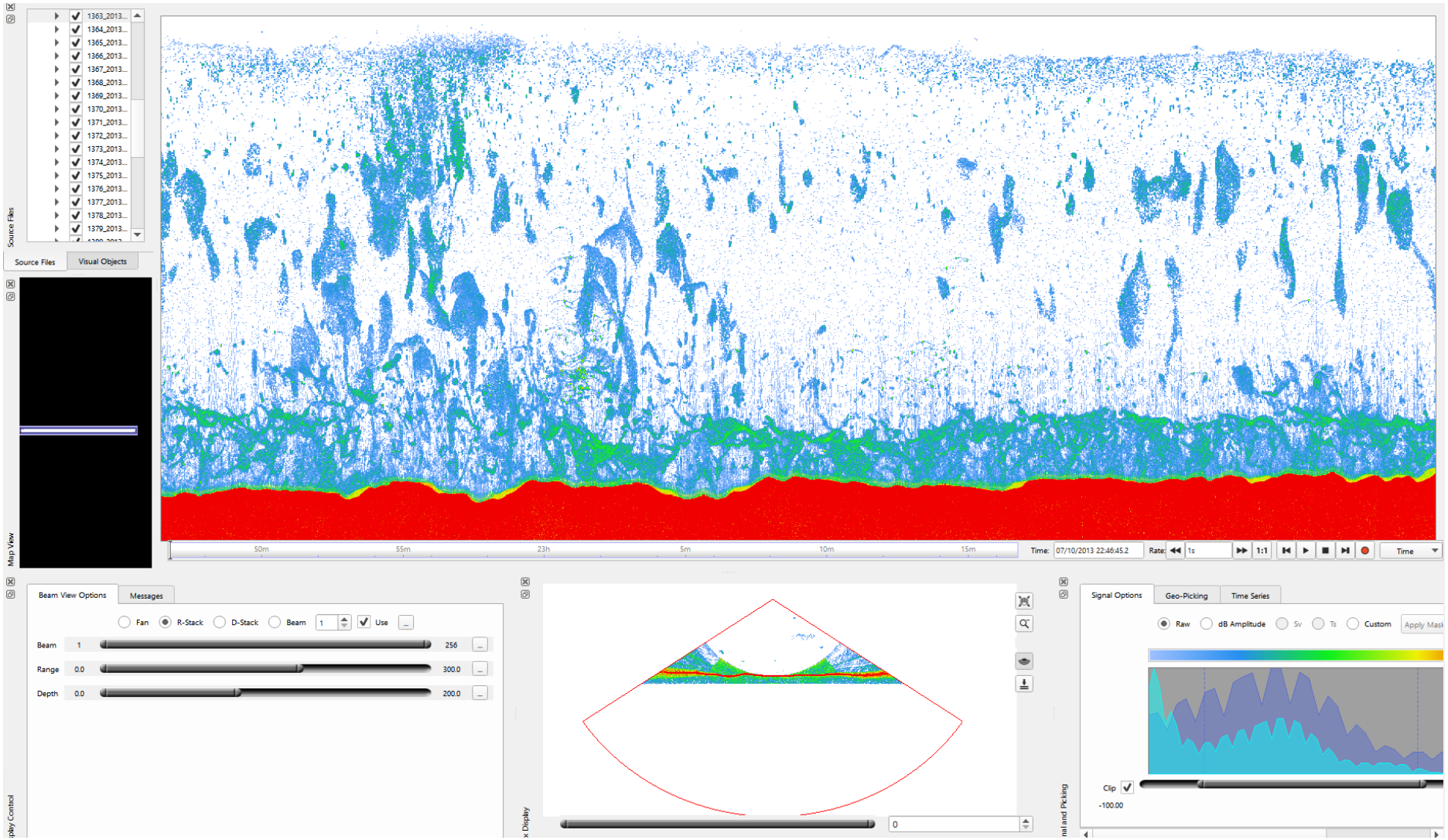

Figure 93. Irregular acoustic objects interpreted as plankton and fish. Note that the objects may mask gas flares.

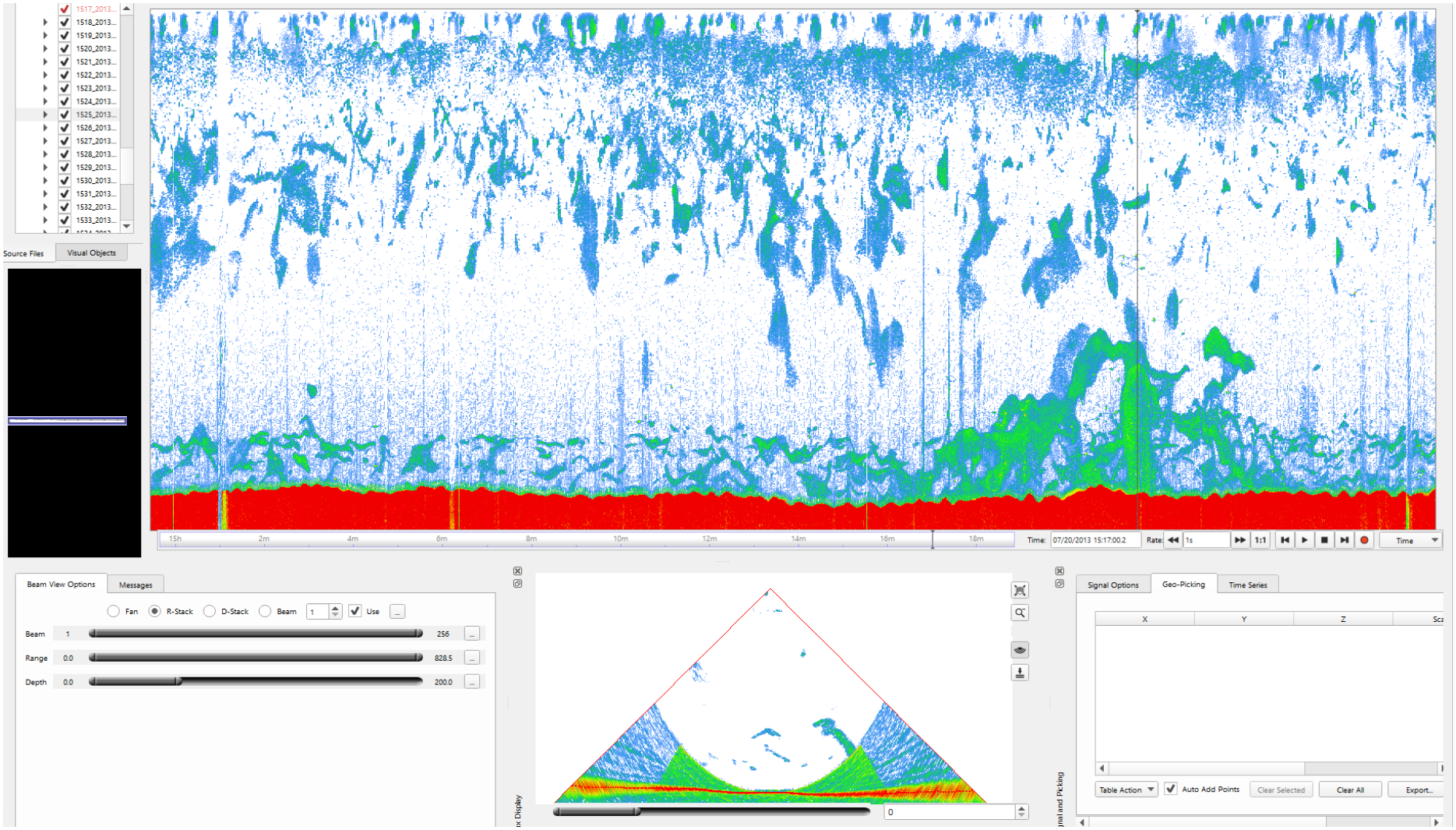

Figure 94. Irregular acoustic objects interpreted as plankton and fish. Note that such objects may be misidentified as gas flares.

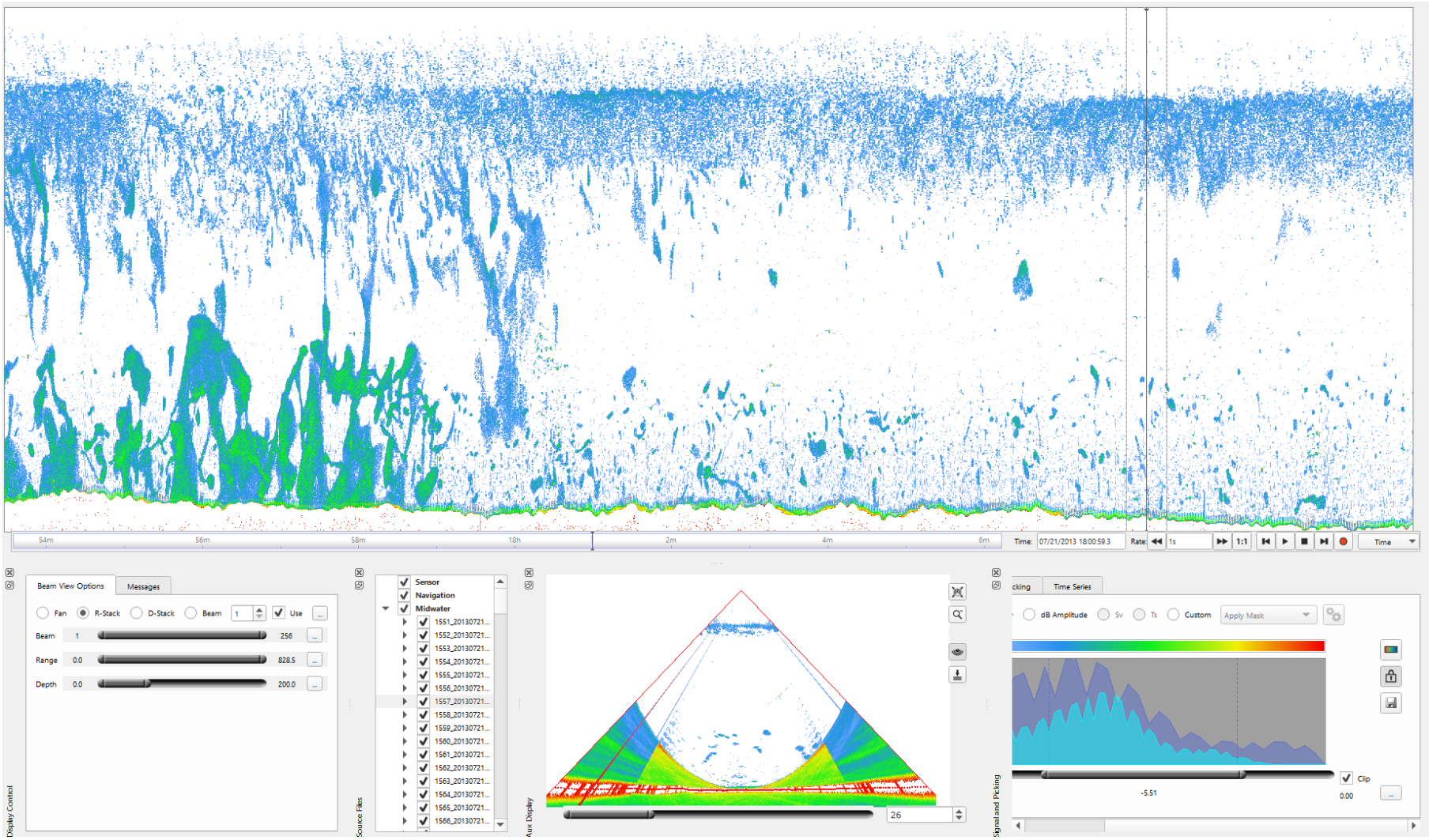

Figure 95. Possible gas flare from line 1557 showed on fan view and stack view. Magnitude 2, Confidence 30%

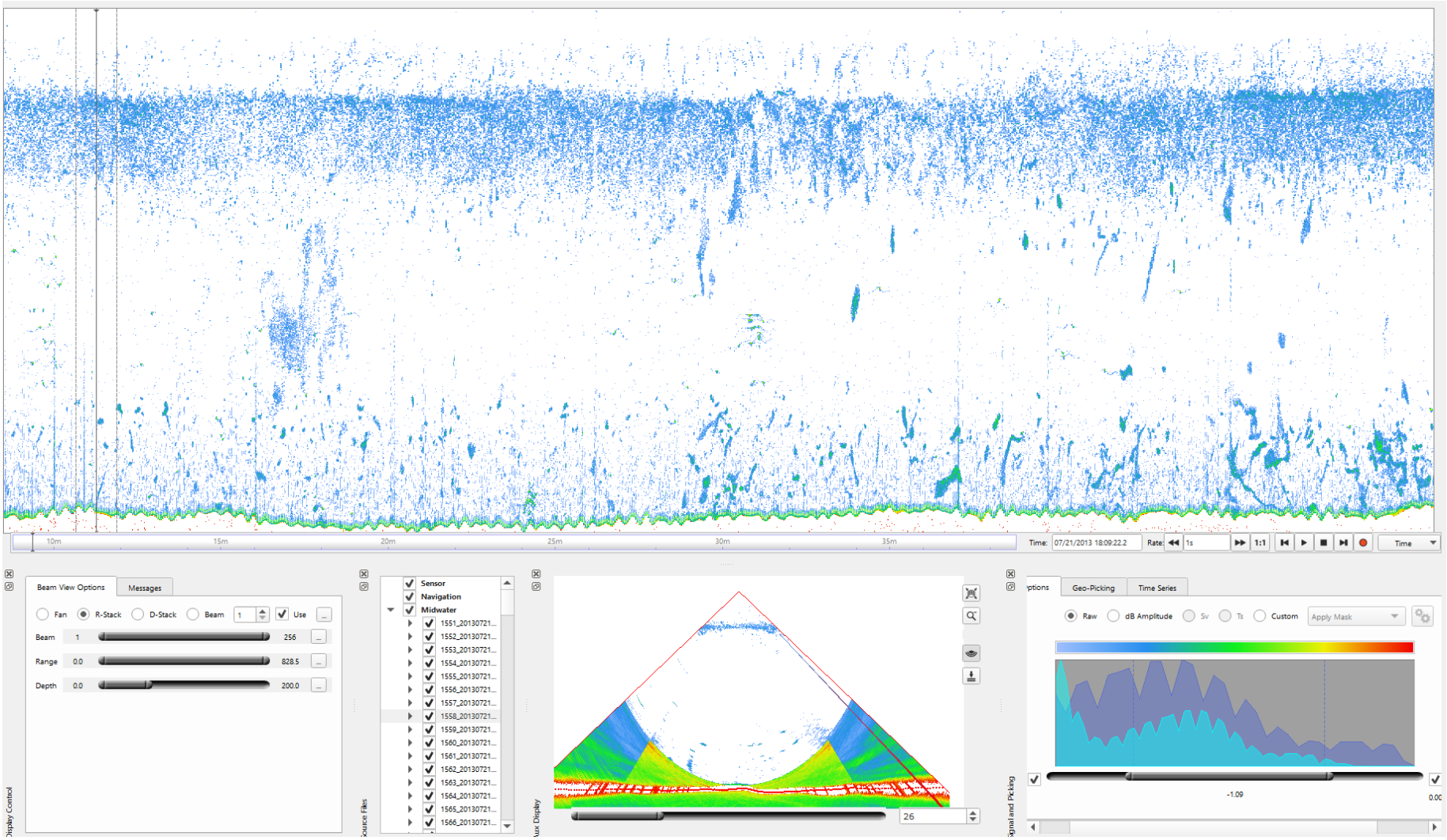

Figure 96. Possible gas flare from line 1558 showed on fan view and stack view. Magnitude 2, Confidence 30%

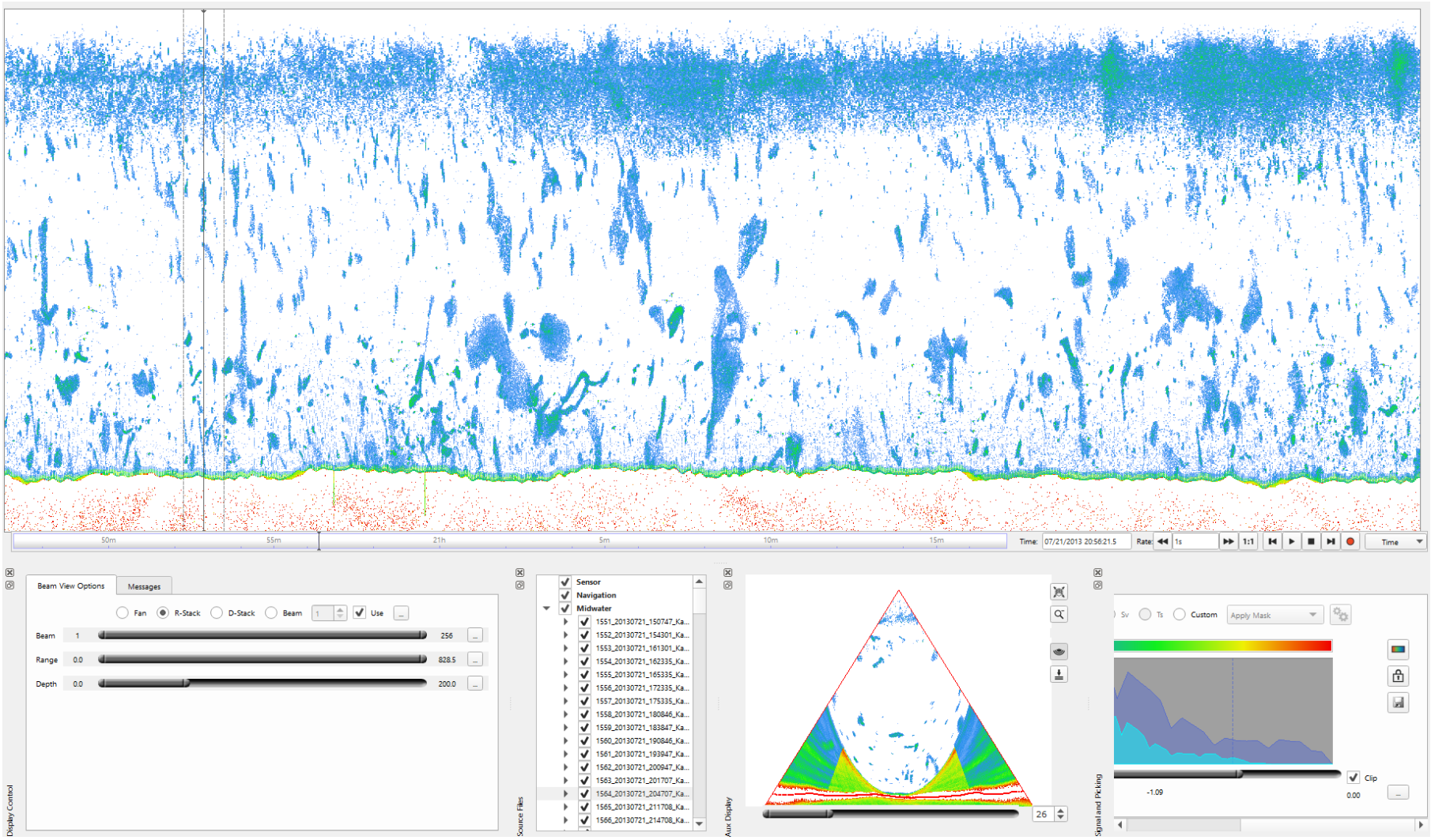

Figure 97. Possible gas flare from line 1564 showed on fan view and stack view. Magnitude 2, Confidence 30%

5. **SUMMARY**

Flares are observed with high confidence in the first three survey areas of the study area. They are distributed evenly and do not correlate with any features observed on bathymetry or backscatter data.

Details of water column acoustic gas flares found including both certain and uncertain gas flares indicate a total of 98 flares.

38 flares were identified, with a confidence level higher than 50% thus representing 40% of total flares.

6. **REFERENCES**

Chand, S., Cremiere, A., Lepland, A., Thorsnes, T., Brunstad, H., Stoddart, D. 2016: Long-term fluid expulsion revealed by carbonate crusts and pockmarks connected to subsurface gas anomalies and palaeo-channels in the central North Sea. Geo Marine Letters, doi.10.1007/s00367-016-0487-x.

Chand, S., Thorsnes, T., Rise, L., Bøe, R. 2012a: Pockmarks, gas flares, tectonic features and processes leading to their formation, south western Barents Sea. NGU Report 2012.017.

Chand, S., Thorsnes, T., Brunstad, H., Stoddart, D., Bøe, R., Lågstad, P., Svolsbru, T. 2012b: Huge gas flares, pockmarks and gas accumulation along the Loppa High, SW Barents Sea indicate multiple episodes of formation and fault controlled focused fluid flow. Earth and Planetary Science Letters, 331-332, 305-314.

Milkov, A.V., Sassen, R. 2003: Two-dimensional modeling of gas hydrate decomposition in the northwestern Gulf of Mexico: significance to global change assessment. Global and planetary Change 36, 31-46.

Nixon, F. C., Chand, S., Thorsnes, T., Bjarnadottir, L.R. 2019: A modified gas hydrate-geomorphological model for a new discovery of enigmatic craters and seabed mounds in the Central Barents Sea, Norway. Geo Marine Letters, doi.org/10.1007/s00367-019-00567-1.

Sheriff, R. 1980: Nomogram for Fresnel zone calculation. Geophysics 45, 968-972.

Skarke, A., Ruppel, C., Kodis, M., Brothers, D., Lobecker, E. 2014: Widespread methane leakage from the sea floor on the northern US Atlantic margin: Nature Geoscience. doi.10.1038/NGEO2232

Urban, P., Koser, K., Greinert, J. 2017: Processing of multibeam water column image data for automated bubble/seep detection and repeated mapping. Limnology Oceanography: Methods 15, 1-21. Doi.10.1002/lom3.10138.

GEOLOGICAL
SURVEY OF
NORWAY

· NGU ·

Geological Survey of Norway
PO Box 6315, Sluppen
N-7491 Trondheim, Norway

Visitor address
Leiv Eirikssons vei 39
7040 Trondheim

Tel (+ 47) 73 90 40 00
E-mail ngu@ngu.no
Web www.ngu.no/en-gb/